PARTITIONING AND MOLECULAR RECOGNITION IN TEFLON AF / FC-72 AND DETERMINATION OF BARBITURATES WITH CAPILLARY ELECTROPHORESIS

by

Hong Zhao

BS, Xiamen University, P. R. China, 1992

MS, Xiamen University, P. R. China, 1995

Submitted to the Graduate Faculty of

Art and Science in partial fulfillment

of the requirements for the degree of

Doctor of Philosophy

University of Pittsburgh

2005

UNIVERSITY OF PITTSBURGH

FACULTY OF ARTS AND SCIENCES

This dissertation was presented

by

Hong Zhao

It was defended on

Aug. 22, 2005

and approved by

Prof. Eric Beckman

Prof. Dennis Curran

Prof. Adrian Michael

Prof. Stephen Weber

Dissertation Director

PARTITIONING AND MOLECULAR RECOGNITION IN TEFLON AF / FC-72 AND DETERMINATION OF BARBITURATES WITH CAPILLARY ELECTROPHORESIS

Hong Zhao, PhD

University of Pittsburgh, 2005

The unique nature of fluorocarbon solvents makes them significant in selective extraction. The poor solubility of hydrocarbons in fluorous phases has been useful in separation of fluorous compounds from hydrocarbon compounds. Molecular recognition based on intermolecular associations between a receptor (host) and a substrate (guest) has been widely used to enhance extraction selectivity. We therefore studied noncovalent intermolecular associations in fluorous media (fluorous solvents/polymers), and extraction with a fluorous solvent, FC-72, and a fluorous polymer, Teflon AF 2400, as the extracting solvents. The association through hydrogen bonding and electrostatic interactions between fluorinated carboxylic acids and 3-hydroxypyridine improves the extraction of 3-hydroxypyridine into FC-72 and the films prepared from Teflon AF 2400. The association is found to be substantially stronger in FC-72 than in chloroform; however, it is weaker in the fluorous films due to the specific properties of the polymer and sorption of solvents in the films.

Dimensionally stable and chemically inert fluorous polymer films have advantages in fluorous separations. Films of an amorphous fluorous polymer, Teflon AF 2400, were cast from solution. Transport measurements on a series of solutes with different polarity and functional groups reveal that the selectivity of the films with and without a

perfluoropolyether plasticizer. The films show selectivity for small nonpolar solutes compared to solutes with larger molecular weight or high polarity. The films also favor the transport of fluorinated solutes in comparison to the hydrogen-containing control. Transport rates are dependent on the solvent making up the source and receiving phases. Solvents are sorbed to a substantial amount in the films, producing great changes of the diffusion coefficient of a solute; however, only slight changes of the partition coefficient. Various solvents, including organic solvents and the nonvolatile perfluoropolyether plasticizer, were investigated and compared.

To study the selectivity of extraction and membrane transport, an important part of the work is analysis of mixtures of solutes. Capillary electrophoresis (CE) is a powerful analytical technique for separation of diverse samples. The disadvantage of low concentration sensitivity with absorbance detectors can be overcome by applying sample stacking techniques. We investigated the optimal stacking conditions for separation of barbiturates and analogs with capillary zone electrophoresis (CZE), and micellar electrokinetic chromatography (MEKC). Investigations have shown that high pH sample matrices are essential for stacking in MEKC by ionizing the analytes, thus decreasing their affinity for the SDS micelles. Consequently, stacking similar to that in CZE can be achieved for all the investigated analytes with a wide distribution of retention factors, while without any effects on MEKC separation. Both normal stacking and transient ITP stacking are involved, depending on the sample matrix.

TABLE OF CONTENTS

LIST OF FIGURES

LIST OF TABLES

CHAPTER 1

INTRODUCTION

1.1 MOLECULAR RECOGNITION AND SELECTIVITY

1.1.1 Molecular recognition and selectivity in extraction

Molecular recognition is based on the intermolecular associations between a receptor (host) and a substrate (guest).[1] The binding interactions between a receptor and a substrate include noncovalent intermolecular forces such as hydrogen bonding, electrostatic attraction, π-π stacking interactions, and van der Waals attractions. Effective intermolecular association depends on the compatibility between the receptor and the substrate in their size, shape, and charge density. Also important is the precise alignment of the binding groups of the receptor with the complementary regions on the substrate to provide both proper orientation and selective complexation.[2] Among all the noncovalent interactions, hydrogen bonding plays an important role in biological systems such as peptides and proteins. Although a single hydrogen bond is weak (5 - 10 kcal·mol^{-1}) compared to electrostatic interactions (about 20 kcal·mol^{-1}), multiple hydrogen bonds produce strong interactions,[3] as demonstrated by the attraction between antigens and antibodies. Schneider showed that the free energy of association increased almost linearly with an increase of the number of hydrogen bonds.[4] In recent years, hydrogen bond based-molecular recognition has gained a great deal of attention, resulting in rapid development and wide-spread use in extractions for enhanced selectivity.[5-10]

Extraction selectivity can be described as the ratio of the relative concentration of the target analyte and interference species in the two phases.[11] The goal of extraction is to selectively extract target species from their matrix to another phase. Simple partitioning of solutes, with or without the aid of synthetic receptors, has been of great value in chemistry. Selective partitioning, with synthetic receptors binding to specific types of compounds, is particularly reliable because artificial receptors are robust and predictable [2, 12-16] Artificial receptor based-molecular recognition can greatly enhance the selectivity of extraction, while minimizing the consumption of solvents.[13, 15, 17] In one example, the use of a synthetic molecular receptor[2] increases the extraction of phenobarbital into chloroform up to 40-fold with the same amount of solvent.[13]

For extraction of an aqueous solution with an organic solvent in absence of receptors, the fraction of the substrate left in the aqueous phase after extraction, q, is defined by the distribution coefficient D_c, and the phase ratio ϕ ($\phi = V_{organic}/V_{aqueous}$):

$$q = 1/(D_c\phi + 1) \qquad (1\text{-}1)$$

Equation 1-1 shows that a large distribution coefficient and a large volume of the organic solvent result in a small q, thus a high extraction yield. In receptor-enhanced extraction, the equilibrium between the substrate (S), the receptor (R), and their complex (RS) needs to be taken into consideration in assessing the distribution coefficient.

$$R + S \rightleftharpoons RS$$

$$K_f = [RS]/([R][S]) \qquad (1\text{-}2)$$

The fraction of the substrate left in the aqueous phase is then defined as:

$$q = 1/[(D_c\phi(1 + K_f[R_t]_{org}) + 1] \qquad (1\text{-}3)$$

where K_f is the formation constant of the substrate-receptor complex, and $[R_t]_{org}$ is the total concentration of the receptor present in the organic phase. The equation is deduced with the assumption: $[R_t]_{org} >> [S]$. Equation 1-3 takes into account the dependence of the extraction on the solvent type, phase volume, receptor concentration, and formation constant of the complex. The factor $1+K_f[R_t]_{org}$ is considered as an extraction enhancement factor due to application of the receptor. A large formation constant and a high receptor concentration in the organic phase enhance the extraction.

To achieve high selectivity, a suitable solvent should have the maximum partitioning of the interested substrate while inhibiting the partitioning of interference species. Meanwhile, the solvent should have good solubility of both the receptor and the complex. Unfortunately, it is difficult to meet all the above criteria simultaneously. The extraction selectivity can be increased to certain degree by careful choices of the organic solvent according to the properties of the target analyte.

The effects of solvents on extraction selectivity was demonstrated by Sun in an extraction of phenobarbital from aqueous solution with a good solvent ($CHCl_3$) and a poor solvent (0.01% $CHCl_3$ mixed in cyclohexane) in presence/absence of a synthetic receptor **1** (Fig. 1.1).[18] The extracted solutes were analyzed by capillary electrophoresis, and the results are shown in Fig. 1.2. When $CHCl_3$ was used as the extracting solvent, all the nine solutes were extracted with large distribution coefficients; addition of the receptor in $CHCl_3$ did not significantly increase the selectivity for phenobarbital. On the other hand, when a hydrophobic solvent mixture, 0.01% (v/v) $CHCl_3$ in cyclohexane, was used, less amount of all nine solutes were extracted by the solvent in absence of the receptor. With addition of the receptor at the same concentration as in the case of $CHCl_3$, only the

extraction of phenobarbital (PB) was greatly enhanced, while the extraction of other interferences remained about the same. Consequently, a more selective extraction was obtained. Unfortunately, the receptor does not dissolve in pure cyclohexane, which prevents the investigation of the extraction selectivity in an even “poorer” solvent.

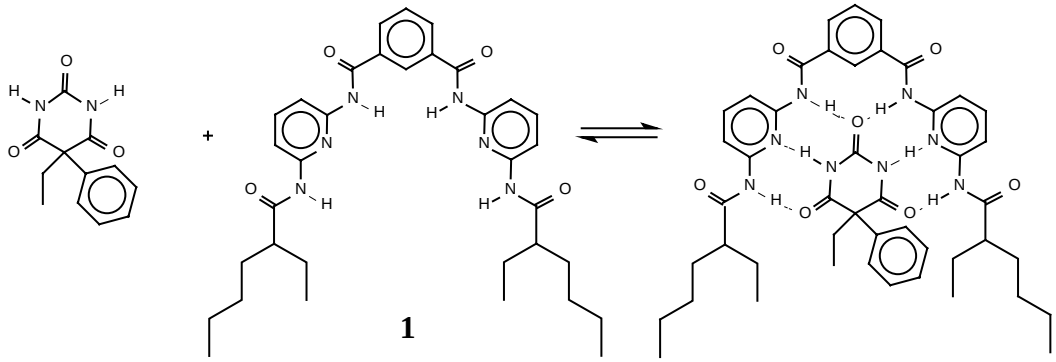

Figure 1.1. Synthetic receptor **1** and the complex with phenobarbital.

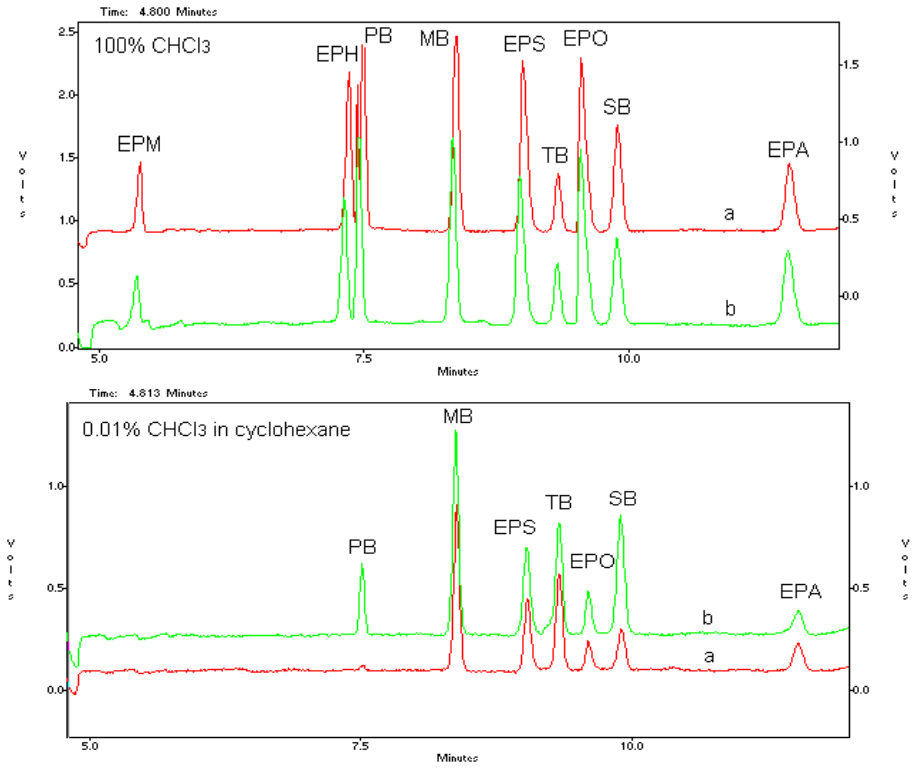

Figure 1.2. The dependence of extraction of barbiturates on the organic solvents. Top: 100% $CHCl_3$, bottom: 0.01% $CHCl_3$ in cyclohexane. Electropherograms: a (red line), without receptor **1**; b (green line), with 0.1 mM receptor **1**. EPM: 2-ethyl-2-phenyl-malonamide, EPH: DL-5-ethyl-5-phenyl-hydantion, PB: phenobarbital, MB: mephobarbital, EPS: 2-ethyl-2-phenyl-succinimide, TB: thiopental, EPO: 5-ethyl-5-phenyl-oxazolidinedione, SB: secobarbital, and EPA: ethyl phenyl-acetylurea.

Solvents influence not only the partitioning of solutes, but also the association between receptors and substrates. Studies of the impact of solvents on hydrogen bond-based molecular recognition of phenobarbital[13,19-21] have revealed that solvent properties (hydrogen bonding acidity α, basicity β, dipolarity π^*, and solvent cohesive energy density δ_H^2)[22] affect the equilibria relevant to analyte distribution (partitioning, association with the receptor, as well as the solubility of the receptor) differently. PVC

(poly(vinyl chloride)) plasticizers have been investigated in our lab as substitute solvents to achieve extractions free from volatile solvents. Plasticizers were found to affect the formation constant of the phenobarbital-artificial receptor complex.[14, 21] Large formation constants are obtained with plasticizers that are poor hydrogen bond donors and acceptors. Earlier work of Adrian and Wilcox regarding the influence of water addition in $CDCl_3$ on the association constants of a 2-aminopyridine complex reveals that water acts as a competitive inhibitor and interferes with the complex formation by taking up the receptor bonding sites.[23]

In general, partitioning is much less selective as compared to the highly selective molecular recognition process. We postulate that extraction selectivity can be improved by a judicious choice of solvents to minimize the nonspecific extraction and encourage specific molecular recognition-based association. However, it is not a trivial task to investigate a series of solvents for each receptor. It becomes important to have a general way to encourage the desired association and inhibit the nonspecific extraction of interfering species. As we have shown that a "poor" solvent could satisfy both requirements. Fluorous solvents (highly fluorinated solvents) are extremely poor solvents for organic compounds. This property has been useful in fluorous biphasic synthesis by simplifying the post-reaction purification process.[24-30] Fluorous biphasic synthesis is based upon tagging an organic substrate (catalyst, reagent, or reactant) with a fluorinated moiety; fluorinated compounds can be easily separated from nonfluorinated compounds according to their solubility in fluorous solvents at the end of the reaction. The rapid development of fluorous chemistry in recent years has not only introduced a wide variety of fluorinated compounds, it has also enriched the understanding of fluorous synthesis

and separation (solubility, partitioning, etc.).[31-35] Fluorous solvents are unique in selective extraction since they provide a universal matrix to suppress the partitioning of sample matrices. One of our objectives is to explore the potential of using fluorinated solvents in combination with artificial receptors in selective extractions. Knowledge of fluorous chemistry provides useful guidance in the choice of fluorous receptors and in understanding of the molecular recognition process in fluorous media.

1.2 MEMBRANE TRANSPORT

1.2.1 General Introduction

Membrane transport is an attractive alternative to liquid-liquid and solid-phase extraction. It decreases solvent consumption, and lowers the cost due to membrane reusability. In this separation scheme, a membrane acts as a barrier between the source (feed) phase and the receiving (product) phase. Separation occurs when one component of a mixture moves through the membrane faster than other components, either by differences of diffusion coefficients or partition ratios. Membrane separation is a rate process; the driving forces come from the chemical potential gradient caused by differences in concentration, pressure, or other forces.[36] Bulk liquid membranes (BLM), supported liquid membranes (SLM), and polymeric membranes are the most common ones used in membrane transport. In BLM transport mode, a relatively thick layer of immiscible liquid is used to separate the source phase and the receiving phase. The flux through bulk liquid membranes is fast, but the liquid membranes are usually not stable. In SLM transport, the solvent is impregnated into the pore structure of a microporous solid support such as silica or polymers so the membranes can be prepared thinly and are more stable

compared to BLM. The polymeric membrane provides good mechanic strength and usually has a longer lifetime than BLM and SLM. Diffusion in polymeric membranes is generally slow, therefore thin membranes are used in practical applications.

Selectivity enhancement in membrane transport can be achieved through molecular recognition[12, 37, 38] or template polymers.[17, 39] In the first case, receptors are impregnated into the membrane and used as selective "carriers" in carrier-facilitated membrane transport. Fig. 1.3 illustrates the concept of carrier-facilitated membrane transport. Carrier-facilitated membrane transport has been successfully applied in the separation of alkali metal ions with crown ethers or their analogues as the carriers.[12, 36, 40] In comparison, the applications for neutral organic substrates are fewer, probably due to the lack of receptors for organic molecules and suitable support materials. Facilitated transport of dopamine and catecholamine through BLM and SLM was achieved in Reinhoudt's group by using polypropylene-supported 2-nitrophenyl octyl ether (NPOE) that contained crown boronic acids as the carriers.[37] Our group has reported selective transport of phenobarbital with a synthetic receptor impregnated in plasticized PVC membranes.[21, 38] Functionalized polymeric membranes are able to enhance the membrane selectivity. A well-known example is perfluorosulfonic acid ionomers (Nafion). Separation of olefins from paraffins through the Ag^+-Nafion film has been reported.[36, 41]

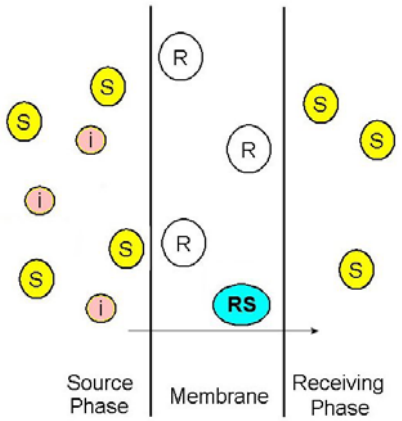

Figure 1.3. A scheme of receptor facilitated membrane transport.

The substrate (S) transports through the membrane with the assistance of the receptor (R), while interference species (i) does not bind with the receptor and has a much smaller flux than the substrate.

Although supported liquid membranes have been widely used, the instability of these membranes has hindered their applications. The instability mainly comes from solvent or carrier loss from the microporous support materials through evaporation or exclusion.[42] For transport carried out in aqueous solutions, increase of lipophilicity of the solvent will enhance the membrane stability; one such example is 2-nitrophenyl octyl ether (NPOE). Using solvents with high boiling points is another effective approach to decrease the loss of solvents during transport process, such as the PVC plasticizers used in our group.[38, 43] An alternative approach is to covalently link the carrier to the polymer so thin, stable membranes can be prepared and high flux is possible.[44] In all the cases, suitable polymers that provide high flux, chemical stability, and desired solubility to carriers are required. Currently, the widely used support polymers are polypropylene, polyethylene, polytetrafluoroethylene, polysulfone, PVC, cellulose triacetate, and polyimide.[42]

1.2.2 Transport through Teflon AF films

Highly permeable fluoropolymers such as Teflon AF polymers could be alternative polymer supports in membrane transport. Teflon AF is a copolymer of tetrafluoroethylene (TFE) and 2,2-bistrifluoromethyl-4,5-difluoro-1,3-dioxole (PDD) (Fig. 1.4). The obvious advantages are its excellent chemical stability and high permeability for small molecules. Transport of gas phase species (penetrants) through Teflon AF films has shown that the films have extremely high permeability coefficients for gases.[45,46] Studies have been carried on in gas separation[47-52] and pervaporation of volatile organic solvents with films prepared from these polymers.[53, 54] Teflon AF films have size-sieving characteristics and show certain selectivity according to the molecular size of the gases. A recent study by Merkel and coworkers demonstrated an enhancement of permeability for comparatively larger molecules by physically dispersing silica nanoparticles in the Teflon AF polymer films.[55,56] Another application of the highly permeable Teflon AF polymers is in the preparation of composite membranes where the Teflon AF films are utilized as a thin protecting coating on top of other selective membranes. Jones reported of composite membranes prepared by coating carbon molecular sieving membranes with Teflon AF film.[57] The Teflon coating was shown to increase the lifetime of the membranes, and the performance of the carbon molecular sieving membranes under exposure to water vapor.

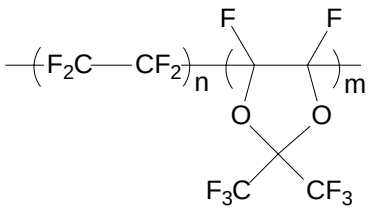

Figure 1.4. Teflon AF

With Teflon films, the transport can be conducted in gas phase, aqueous phase, or organic solvents. Using organic solvents in membrane transport tremendously increases the choice of suitable solvents for optimal selectivity and transport speeds. We are the first to study the transport of organic solutes through Teflon AF films to explore the potential of this material in selective transport.[58,59] The transport was conducted in chloroform solutions. Much larger (2-3 orders) permeabilities for small neutral solutes such as benzene were obtained compared to gas phase permeation. The films show selectivity according to molecular size, polarity, as well as selectivity for fluorinated solutes in comparison to the hydrogen-containing control.[59] The selectivity for fluorinated solutes suggests promising applications of these films in fluorous separation. The films can be plasticized by a variety of organic solvents, fluorinated solvents, and a nonvolatile perfluoropolyether oligomer (Krytox®, average molecular weight as 7500). The Krytox-plasticized films maintain the selectivity for fluorinated solutes, but shows decreases in permeabilities of neutral solutes about an order of magnitude as compared to the pure Teflon AF films. The finding of plasticization of Teflon AF polymers by fluorous plasticizers is significant. It suggests that nonvolatile fluorous solvents /plasticizers can be introduced into the films in a similar manner as that in organic polymer membranes such as PVC membranes. Modification of the solubility and fluidity of these films by

fluorous plasticizers is promising for better film selectivity. This part of work is included in Chapter 3.

1.3 CAPILLARY ELECTROPHORESIS (CE) AND IMPROVED SENSITIVITY WITH ON-LINE CONCENTRATION TECHNIQUES

1.3.1 CE separation

Capillary electrophoresis (CE) has been developed as a powerful analytical technique for separation of diverse samples. The main advantages of CE are outstanding separation efficiency, high mass sensitivity (femtomole limits can easily be reached), fast separation speeds, and minimal use of samples (a few nanoliters) and solvents.[60] It has been routinely employed in analytical separations of both small molecules and large biomolecules such as peptides, proteins, and nucleic acids.[61-64] CE separates charged compounds by their different electrophoretic speeds in an electrically conductive buffer. The electric field is generated by applying a potential across the two ends of the capillary that has been filled with a separation buffer. The potential can be as high as 30 kV, which not only enables fast separation but also increases the separation resolution. The capillary has a typical i.d. of 25 - 100 μm and a length of 50-100 cm. Recent development of "CE on a chip" uses much shorter capillaries (<10 cm) and multiple CE channels for separations. The small size of the capillary greatly improves heat dissipation and decreases the fluid convection, which are the two main factors limiting the efficiency of conventional electrophoresis techniques such as slab gel electrophoresis.

The most commonly used CE separation mode is capillary zone electrophoresis (CZE). In CZE, analytes migrate at different velocities corresponding to their mobilities and separate one from another as "zones". CZE is most useful in separation of charged species. Neutral compounds that do not have electrophoretic mobility in CE can be separated by micellar electrokinetic chromatography (MEKC).[65-69] MEKC was first introduced by Terabe et al. in 1984,[65] in which an ionic surfactant is used as a pseudostationary phase, and analytes are separated based on their differential partitioning between the aqueous phase and the micelle phase. Analytes with stronger affinity for the micelles have migration mobilities closer to that of the micelles; and *vice versa*, analytes with weaker affinity for the micelles have migration mobilities farther away from that of the micelles.

The short optical path length, due to the small inner diameter of the CE capillary, creates challenges of analysis sensitivity when absorbance detection such as UV-Vis detection is used. The lowest detectable concentration with Uv-Vis detection without preconcentration lies in 0.2-5 mg/L range for good absorbers.[70] The low concentration sensitivity brings difficulty not only to quantitative analysis, but also to qualitative identification of small peaks.[71] Detection techniques with better sensitivity are also used in CE, such as laser induced fluorescence (LIF),[72-74] electrochemical detection,[75-78] and mass spectrometric detection.[79-82] LIF and mass spectrometry can lower detection sensitivity by several orders; however they are expensive and are not widely applicable.

1.3.2 On-line concentration techniques in CE

Low detection limits and reduced band broadening can be achieved by applying on-line (on-column) concentration techniques, which allows for a large sample injection without sacrificing the separation efficiency. “Stacking” is another term commonly used for the zone sharpening effects that result in sample concentration phenomena. The simplest stacking mode is normal stacking mode, whose principle is shown in Fig. 1.5. The sample is prepared in a buffer that has a lower conductivity than the CE separation buffer (run buffer). When a voltage is applied across the capillary, a greater field is developed across the sample plug compared to the separation buffer, which causes the sample ions to migrate faster within the sample plug than in the CE run buffer. Upon reaching the boundary between the sample plug and the run buffer, the higher conductivity of the separation buffer induces a decrease in the velocity of the sample ions. Consequently, the analytes are stacked into a narrow zone at the boundary. The degree of stacking and enhancement of concentration is proportional to the ratio of the conductivity of the sample solution to the run buffer. However, laminar flow induced by the different rates of electroosmotic flow (EOF) in the two areas results in band broadening. Calculations indicate that the best stacking result is obtained when the concentration of the sample buffer is about one tenth of the run buffer.[83] Normal stacking mode has been widely applied in enhancing the CE sensitivity.[84, 85]

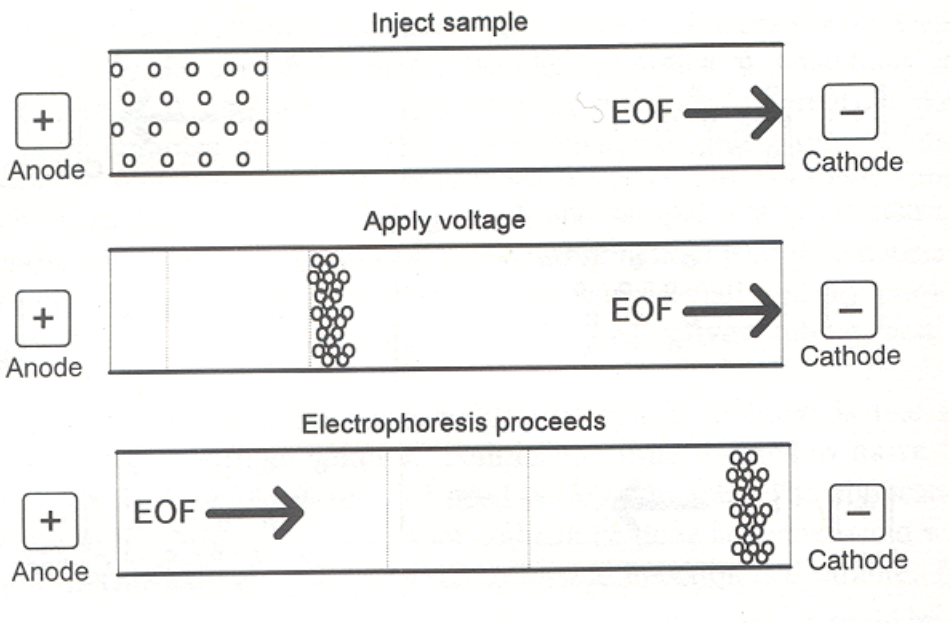

Figure 1.5. The principle of CZE normal stacking mode

The circles represent an example of a cationic solute. Top: A long sample plug is injected. Middle: A high voltage is applied and the cationic solute gets stacked at the boundary between the sample plug and the CE run buffer. Bottom: the stacked ions migrate through the capillary as a zone narrower than the injection sample plug and are separated in the CE run buffer (Baker, Capillary Electrophoresis).[61]

Normal stacking mode can be included in a larger class called “field amplified sample stacking”, in which conductivity differences in the sample zone and the CE separation buffer result in analytes stacked at the boundary. Another widely used mode in this class is field-amplified polarity switching injection. It can reduce the dispersion caused by the nonhomogeneous electroosmotic flow in the system by pumping the sample buffer out of the capillary. In this mode, a large volume of sample dissolved in a low-conductivity matrix is introduced hydrodynamically into the capillary. A negative voltage is applied, resulting an EOF directed to the injection inlet (cathode inlet). The anionic analytes move

fast through the low-conductivity sample zone and are sacked at the sample zone boundary on the detector side; at the same time the strong cathodic EOF pushes the sample matrix out of the capillary inlet. At the moment when the majority of the sample matrix is removed from the capillary and the zone of stacked analytes approaches the capillary inlet, the electrode polarity is reversed for CE separation. Field-amplified polarity switching injection can increase the sensitivity up to 100 times.[83, 84, 86]

Another stacking approach is to incorporate transient isotachophoresis (ITP) into the separation process.[87-90] ITP is a CE separation mode in which samples are inserted between a leading ion (the ion with the highest mobility) and a terminating ion (the ion with the lowest mobility). A steady-state configuration is ultimately reached according to the moving boundary principle, and all the analytes move adjacent to each other at the same speed determined by the leading ion. The concentration of an analyte in its zone is adjusted to the concentration of the leading ion, thus is greatly increased due to the high concentration of the leading ion used in ITP. Transient ITP stacking in CZE is obtained by selecting a proper composition of the sample buffer and the separation buffer so that there is a leading ion and a terminating ion existing in the system. For example, addition of sodium chloride in the sample matrix can introduce a chloride-leading ion for anionic analyses, or sodium-leading ion for cationic analyses, as long as there is a terminating component present in the separation buffer.[88]

Stacking in MEKC is different from that in CZE, because neutral analytes do not respond to the electric field. MEKC stacking is obtained through control of the mobility of the charged analyte/micelle complex. Nice reviews have been published about on-line concentration in MEKC.[68,88,91-93] Among all the on-line concentration techniques, normal

stacking mode,[84, 85, 94, 95] field amplified sample stacking,[94, 96] high salt stacking,[97-99] and sweeping[100-102] are most widely used.

In 1994, Liu and coworkers published the first paper about on-column concentration of neutral molecules in MEKC by means of field-amplified sample stacking.[94] The idea was similar to field-amplified sample stacking in CZE. The sample buffer used to dissolve the neutral analytes had a lower conductivity than that of the separation buffer, and contained SDS with a concentration above the critical micelle concentration (CMC) of SDS. When a positive voltage is applied, micelles from the separation buffer migrate towards the anode, enter the sample buffer, gain a higher velocity in this zone, and focused at the sample zone boundary at the injection side where their velocity becomes slower. During this process, the analytes in the sample zone associate with the micelles and are stacked. The concentration of SDS in the sample matrix is critical; the best stacking efficiency occurs when the concentration is slightly above the CMC. They examined both normal stacking mode and polarity switching injection; with the latter one producing a higher increase in sensitivity (up to 75-80 fold).

Later, Quirino and Terabe studied a similar mechanism with analytes dissolved only in water or a sample buffer with a low conductivity and no surfactants.[95] They calculated the concentration of the micelles in the sample zone ($[mc]_s$) during the stacking process:

$$[mc]_s = [mc]_{BGS}/\gamma \qquad (1\text{-}4)$$

where $[mc]_{BGS}$ is the concentration of the micelles in the separation buffer, γ is the ratio of the field strength in the sample zone to the separation buffer. They reported that $[mc]_s$ should be higher than the micelle CMC to achieve an effective stacking.

Electrokinetic injection has been reported for zone sharpening of neutral analytes in MEKC by field-amplified polarity switching injection.[103] Acidic phosphate buffers containing SDS were utilized in both the sample solvent and the separation buffer. A water plug was hydrodynamically injected to achieve field amplification at the injection end of the capillary during electrokinetic injection, while a negative voltage was applied during sample injection. The acidic buffer reduced the EOF below the electrophoretic mobility of the analyte/micelle complex. As a result, the water matrix was gradually pushed out of the capillary, and the analyte/micelle complex migrated toward the detector and was stacked at the injection inlet.

"Sweeping" on-line sample concentration was introduced by Quirino and Terabe in late nineties.[100, 102, 104] Sweeping is not dependent on field amplification. It is achieved in such an arrangement that micelles from the sample reservoir can move into the sample zone and "sweep" neutral analytes. In sweeping mode, the sample is prepared in a matrix without micelles, and the conductivity is about the same as that of the CE separation buffer. Low pH separation buffer was used to suppress the EOF. The anionic micelles (such as SDS) move into the sample zone from the cathodic reservoir following the voltage application, "picking up" and accumulating the analytes in the sample zone. Once the micelles sweep through the sample zone, the separation process begins as in normal MEKC. The sweeping efficiency of an analyte is proportional to its affinity towards the micelles; thus very high sweeping efficiency can be obtained (for example, 5000 for quinine as using SDS micelles[100]) for an analyte having a strong affinity for the micelles. Sweeping mode can be combined with other stacking modes such as field amplified stacking to achieve an even higher stacking efficiency.[102]

A very different approach developed by Palma et al. utilizes high conductivity sample matrices to stack neutral analytes.[97] The sample matrix contains inorganic salts such as NaCl to achieve a higher conductivity than that of the separation buffer. Field amplification is transferred from the sample zone to the separation buffer. The micelles in the separation buffer migrate with a higher velocity from the separation buffer to the sample zone interface on the detector side, where they slow down and are accumulated at the interface. Neutral analytes moving out of the sample zone with EOF are efficiently concentrated at the stacked micelle front. The stacking efficiency in the high-salt stacking mode is decided by the affinity of the analyte for the micelles, the salt concentration (usually 2-3 folds of the conductivity of the separation buffer), and the sampling volume relative to the capillary volume. Quirino et al. explained high-salt stacking as sweeping in a reduced electric field. Their model comprises the stacking of micelles, the sweeping of analyte zone, and the destacking of micelles.[101]

It is clear that all the stacking/sweeping modes in MEKC are strongly dependent on the affinity of analytes toward micelles. Generally, higher affinity results in better stacking efficiency. Our study of molecule recognition for barbitals requires separation of barbitals and barbital analogs that have quite different affinity for the SDS micelles (retention factors are from 0.1 to 2.5 for the eight investigated compounds). Under the MEKC conditions, the analytes with very low retention factors show electrophoretic characteristics similar as in CZE. Therefore it is challenging to achieve effective stacking for all analytes. We first investigated the optimal stacking conditions of four barbitals in CZE, then stacking of a more complicate mixture that contains eight analytes in MEKC. The MEKC separation buffer is similar as that used in CZE, and contains 24 mM SDS.

To achieve efficient stacking for the investigated analytes, the composition of the sample buffer and the separation buffer, the injection time etc. were investigated.

1.4 REFERENCES

(1) Hamilton, A. D. *Bioorganic Chemistry Frontiers* **1991**, *2*, 115-174.

(2) Chang, S. K.; Van Engen, D.; Fan, E.; Hamilton, A. D. Journal *of the American Chemical Society* **1991**, *113*, 7640-7645.

(3) Fessenden, R. J.; Fessenden, J. S. *Organic Chemistry*, 1979.

(4) Schneider, H. J. *Angewandte Chemie* **1991**, *103*, 1417-1436.

(5) Lehn, J. M. *Science* **1985**, *227*, 849-856.

(6) Garcia-Tellado, F.; Goswami, S.; Chang, S. K.; Geib, S. J.; Hamilton, A. D. *Journal of the American Chemical Society* **1990**, *112*, 7393-7394.

(7) Goswami, S.; Ghosh, K.; Dasgupta, S. *Tetrahedron* **1996**, *52*, 12223-12232.

(8) Ghaddar, T. H.; Castner, E. W.; Isied, S. S. *Journal of the American Chemical Society* **2000**, *122*, 1233-1234.

(9) Chou, H.-C.; Hsu, C.-H.; Cheng, Y.-M.; Cheng, C.-C.; Liu, H.-W.; Pu, S.-C.; Chou, P.-T. *Journal of the American Chemical Society* **2004**, *126*, 1650-1651.

(10) Ishizaka, S.; Kinoshita, S.; Nishijima, Y.; Kitamura, N. *Analytical Chemistry* **2003**, *75*, 6035-6042.

(11) Giddings, J. C. *Unified Separation Science*; Wiley, New York, N. Y., 1991.

(12) Visser, H. C.; Reinhoudt, D. N.; de Jong, F. *Chemical Society Reviews* **1994**, *23*, 75-81.

(13) Valenta, J. N.; Dixon, R. P.; Hamilton, A. D.; Weber, S. G. *Analytical Chemistry* **1994**, *66*, 2397-2403.

(14) Valenta, J. N.; Weber, S. G. *Journal of Chromatography, A* **1996**, *722*, 47-57.

(15) Chen, H.; Weiner, W. S.; Hamilton, A. D. *Current Opinion in Chemical Biology* **1997**, *1*, 458-466.

(16) Rebek, J., Jr. *Chemical Communications (Cambridge)* **2000**, 637-643.

(17) Joshi, V. P., Karmalkar, Rohini N., Kulkarni, Mohan G., Mashelkar, Raghunath A. *Ind. Eng. Chem. Res.* **1999**, *38*, 4417-4423.

(18) Sun, L. F. **1997**, Unpublished work about the dependence of extraction of barbiturates on the organic solvents.

(19) Sun, L.; Weber, S. G. *J. Molecular Recognition* **1998**, *11*, 28-31.

(20) Valenta, J. N.; Sun, L.; Ren, Y.; Weber, S. G. *Analytical Chemistry* **1997**, *69*, 3490-3495.

(21) Zhang, X.; Zhao, H.; Chen, Z.; Nims, R.; Weber, S. G. *Analytical Chemistry* **2003**, *75*, 4257-4264.

(22) Kamlet, M. J.; Abboud, J. L.; Taft, R. W. *Journal of the American Chemical Society* **1977**, *99*, 6027-6038.

(23) Adrian, J. C., Jr.; Wilcox, C. S. *Journal of the American Chemical Society* **1991**, *113*, 678-680.

(24) Gladysz, J. A. *Science* **1994**, *266*, 55-56.

(25) Horvath, I. T.; Rabai, J. *Science* **1994**, *266*, 72-75.

(26) Barthel-Rosa, L. P.; Gladysz, J. A. *Coordination Chemistry Reviews* **1999**, *190-192*, 587-605.

(27) Studer, A.; Hadida, S.; Ferritto, R.; Kim, S.-Y.; Jeger, P.; Wipf, P.; Curran, D. P. *Science* **1997**, *275*, 823-826.

(28) Linclau, B.; Sing, A. K.; Curran, D. P. *Journal of Organic Chemistry* **1999**, *64*, 2835-2842.

(29) Luo, Z.; Zhang, Q.; Oderaotoshi, Y.; Curran, D. P. *Science* **2001**, *291*, 1766-1769.

(30) Gladysz, J. A., Curran, Dennis P., Horvath, Istvan T. *Handbook of Fluorous Chemistry*; Wiley-VCH: Weinheim, 2004.

(31) Lepilleur, C.; Beckman, E. J.; Schonemann, H.; Krukonis, V. J. *Fluid Phase Equilibria* **1997**, *134*, 285-305.

(32) Curran, D. P.; Luo, Z. *Journal of the American Chemical Society* **1999**, *121*, 9069-9072.

(33) Palomo, C.; Aizpurua, J. M.; Loinaz, I.; Fernandez-Berridi, M. J.; Irusta, L. *Organic Letters* **2001**, *3*, 2361 -2364.

(34) Richter, B. d. W., Elwin; van Koten, Gerard; Deelman, Berth-Jan. *Journal of Organic Chemistry* **2000**, *65*, 3885-3893.

(35) De Wolf, E.; Ruelle, P.; Van den Broeke, J.; Deelman, B.-J.; Van Koten, G. *Journal of Physical Chemistry B* **2004**, *108*, 1458-1466.

(36) Bartsch, R. A.; Way, J. D. *Chemical separations with liquid membranes*; Washington, DC : American Chemical Society, 1996.

(37) Paugam, M.-F.; Bien, J. T.; Smith, B. D.; Chrisstoffels, L. A. J.; de Jong, F.; Reinhoudt, D. N. *Journal of the American Chemical Society* **1996**, *118*, 9820-9825.

(38) Zhang, X.; Zhao, H.; Weber, S. G. *Analytical Chemistry* **2002**, *74*, 2184-2189.

(39) Kempe, M.; Mosbach, K. *Tetrahedron Letters* **1995**, *36*, 3563-3566.

(40) Schow, A. J.; Peterson, R. T.; Lamb, J. D. *Journal of Membrane Science* **1996**, *111*, 291-295.

(41) Koval, C. A.; Spontarelli, T.; Thoen, P.; Noble, R. D. *Industrial & Engineering Chemistry Research* **1992**, *31*, 1116-1122.

(42) Baker, R. W. *Membrane technology and applications*; McGraw-Hill: New York, 2000.

(43) Li, S.; Weber, S. G. *Analytical Chemistry* **1997**, *69*, 1217-1222.

(44) Wienk, M. M.; Stolwijk, T. B.; Sudholter, E. J. R.; Reinhoudt, D. N. *Journal of the American Chemical Society* **1990**, *112*, 797-801.

(45) Alentiev, A. Y.; Yampolskii, Y. P.; Shantarovich, V. P.; Nemser, S. M.; Plate, N. A. *Journal of Membrane Science* **1997**, *126*, 123-132.

(46) Pinnau, I.; Toy, L. G. *Journal of Membrane Science* **1996**, *109*, 125-133.

(47) Nemser, S. M.; Roman, I. C., 1991, Pat. US5051114.

(48) Dasgupta, P. K.; Genfa, Z.; Poruthoor, S. K.; Caldwell, S.; Dong, S.; Liu, S.-Y. *Analytical Chemistry* **1998**, *70*, 4661-4669.

(49) Bondar, V. I.; Freeman, B. D.; Yampolskii, Y. P. *Macromolecules* **1999**, *32*, 6163-6171.

(50) Merkel, T. C.; Bondar, V.; Nagai, K.; Freeman, B. D. *Macromolecules* **1999**, *32*, 370-374.

(51) Alentiev, A. Y.; Shantarovich, V. P.; Merkel, T. C.; Bondar, V. I.; Freeman, B. D.; Yampolskii, Y. P. *Macromolecules* **2002**, *35*, 9513-9522.

(52) De Angelis, M. G.; Merkel, T. C.; Bondar, V. I.; Freeman, B. D.; Doghieri, F.; Sarti, G. C. *Macromolecules* **2002**, *35*, 1276-1288.

(53) Polyakov, A. M.; Starannikova, L. E.; Yampolskii, Y. P. *Journal of Membrane Science* **2003**, *216*, 241-256.

(54) Polyakov, A. M.; Starannikova, L. E.; Yampolskii, Y. P. *Journal of Membrane Science* **2004**, *238*, 21-32.

(55) Merkel, T. C.; He, Z.; Pinnau, I.; Freeman, B. D.; Meakin, P.; Hill, A. J. *Macromolecules* **2003**, *36*, 8406-8414.

(56) Merkel, T. C.; Freeman, B. D.; Spontak, R. J.; He, Z.; Pinnau, I.; Meakin, P.; Hill, A. J. *Science* **2002**, *296*, 519-522.

(57) Jones, C. W.; Koros, W. J. *Ind. Eng. Chem. Res.* **1995**, *34*, 164-167.

(58) Zhao, H.; Ismail, K.; Weber, S. G. *Journal of the American Chemical Society* **2004**, *126*, 13184-13185.

(59) Zhao, H., Wu, N, Zhang, J., Zhang, X., Crowley, K., Weber, S. G. *Journal of the American Chemical Society* **2005**, Accepted.

(60) Tellez, S.; Forges, N.; Roussin, A.; Hernandez, L. *Journal of Chromatography* **1992**, *581*, 257-266.

(61) Baker, D. R. *Capillary Electrophoresis*; Wiley, New York, N. Y., 1995.

(62) Landers, J. P.; Editor *Handbook of Capillary Electrophoresis, Second Edition*; CRC, Boca Raton, Fla., 1997.

(63) Shintani, H.; Polonsky, J.; Editors *Handbook of Capillary Electrophoresis Applications*; Blackie Avademic & Professional: London, UK, 1997.

(64) Wehr, T.; Rodriguez-Diaz, R.; Liu, C.-M. *Capillary electrophoresis of proteins*; Marcel Dekker, Inc.: New York, NY, 1999.

(65) Terabe, S.; Otsuka, K.; Ichikawa, K.; Tsuchiya, A.; Ando, T. *Analytical Chemistry* **1984**, *56*, 111-113.

(66) Issaq, H. J. *Electrophoresis* **1999**, *20*, 3190-3202.

(67) Mitchelson, K. R.; Cheng, J. E. *Capillary electrophoresis of natural products*; Humana Press: Totowa, NJ, 2001.

(68) Pyell, U. *Fresenius' Journal of Analytical Chemistry* **2001**, *371*, 691-703.

(69) Molina, M.; Silva, M. *Electrophoresis* **2002**, *23*, 3907-3921.

(70) Boone, C. M.; Franke, J. P.; de Zeeuw, R. A.; Ensing, K. *Journal of Chromatography. A* **1999**, *838*, 259-272.

(71) Thormann, W.; Meier, P.; Marcolli, C.; Binder, F. *Journal of Chromatography* **1991**, *545*, 445-460.

(72) Couderc, F.; Causse, E.; Bayle, C. *Electrophoresis* **1998**, *19*, 2777-2790.

(73) Rada, P.; Tucci, S.; Perez, J.; Teneud, L.; Chuecos, S.; Hernandez, L. *Electrophoresis* **1998**, *19*, 2976-2980.

(74) Jiang, J.; Lucy, C. A. *Journal of Chromatography, A* **2002**, *966*, 239-244.

(75) Qian, J.; Wu, Y.; Yang, H.; Michael, A. C. *Analytical Chemistry* **1999**, *71*, 4486-4492.

(76) Baldwin, R. P. *Electrophoresis* **2000**, *21*, 4017-4028.

(77) Dou, Y.-H.; Bao, N.; Xu, J.-J.; Chen, H.-Y. *Electrophoresis* **2002**, *23*, 3558-3566.

(78) Parrot, S.; Bert, L.; Mouly-Badina, L.; Sauvinet, V.; Colussi-Mas, J.; Lambas-Senas, L.; Robert, F.; Bouilloux, J.-P.; Suaud-Chagny, M.-F.; Denoroy, L.; Renaud, B. *Cellular and Molecular Neurobiology* **2003**, *23*, 793-804.

(79) Srinivasan, K.; Bartlett, M. G. *Rapid Communications in Mass Spectrometry* **2000**, *14*, 624-632.

(80) Chen, Y.-R.; Tseng, M.-C.; Chang, Y.-Z.; Her, G.-R. *Analytical Chemistry* **2003**, *75*, 503-508.

(81) Schmitt-kopplin, P.; Frommberger, M. *Electrophoresis* **2003**, *24*, 3837-3867.

(82) Ramstrom, M.; Bergquist, J. *FEBS Letters* **2004**, *567*, 92-95.

(83) Burgi, D. S.; Chien, R. L. *Analytical Chemistry* **1991**, *63*, 2042-2047.

(84) Kruaysawat, J.; Marriott, P. J.; Hughes, J.; Trenerry, C. *Electrophoresis* **2003**, *24*, 2180-2187.

(85) Sun, B.; Macka, M.; Haddad, P. R. *Electrophoresis* **2003**, *24*, 2045-2053.

(86) Chien, R. L.; Burgi, D. S. *Journal of Chromatography* **1991**, *559*, 153-161.

(87) Krivankova, L.; Pantuckova, P.; Bocek, P. *Journal of Chromatography, A* **1999**, *838*, 55-70.

(88) Urbanek, M.; Krivankova, L.; Bocek, P. *Electrophoresis* **2003**, *24*, 466-485.

(89) Shihabi, Z. K. *Electrophoresis* **2000**, *21*, 2872-2878.

(90) Shihabi, Z. K. *Electrophoresis* **2002**, *23*, 1612-1617.

(91) Quirino, J. P.; Terabe, S. *Journal of Capillary Electrophoresis* **1997**, *4*, 233-245.

(92) Kim, J.-B.; Terabe, S. *Journal of Pharmaceutical and Biomedical Analysis* **2003**, *30*, 1625-1643.

(93) Chien, R.-L. *Electrophoresis* **2003**, *24*, 486-497.

(94) Liu, Z.; Sam, P.; Sirimanne, S. R.; McClure, P. C.; Grainger, J.; Patterson, D. G., Jr. *Journal of Chromatography, A* **1994**, *673*, 125-132.

(95) Quirino, J. P.; Terabe, S. *Journal of Chromatography, A* **1997**, *781*, 119-128.

(96) Aguete, E. C.; Gago-Martinez, A.; Leao, J. M.; Rodriguez-Vazquez, J. A.; Menard, C.; Lawrence, J. F. *Talanta* **2003**, *59*, 697-705.

(97) Palmer, J.; Munro, N. J.; Landers, J. P. *Analytical Chemistry* **1999**, *71*, 1679-1687.

(98) Carabias-Martinez, R.; Rodriguez-Gonzalo, E.; Revilla-Ruiz, P.; Dominguez-Alvarez, J. *Journal of Chromatography, A* **2003**, *990*, 291-302.

(99) Choy, T. M. H.; Chan, W.-H.; Lee, A. W. M.; Huie, C. W. *Electrophoresis* **2003**, *24*, 3116-3123.

(100) Quirino, J. P.; Terabe, S. *Science* **1998**, *282*, 465-468.

(101) Quirino, J. P.; Terabe, S.; Bocek, P. *Analytical Chemistry* **2000**, *72*, 1934-1940.

(102) Quirino, J. P.; Terabe, S. *Analytical Chemistry* **2000**, *72*, 1023-1030.

(103) Quirino, J. P.; Terabe, S. *Analytical Chemistry* **1998**, *70*, 1893-1901.

(104) Quirino, J. P.; Terabe, S. *Analytical Chemistry* **1999**, *71*, 1638-1644.

CHAPTER 2

PERFLUOROCARBOXYLIC ACIDS ENHANCED EXTRACTION OF 3-HYDROXYPYRIDINE INTO FC-72 AND TEFLON AF FILMS

Abstract

The unique nature of fluorocarbon solvents makes them significant in selective extraction. The poor solubility of hydrocarbons in fluorous phases has been useful in separation of fluorous compounds from hydrocarbon compounds. Molecular recognition based on the intermolecular associations between a receptor (host) and a substrate (guest) has been widely used in enhancement of extraction selectivity. We therefore studied noncovalent intermolecular associations in fluorous media (fluorous solvents/polymers), and extraction with a fluorous solvent, FC-72, and a fluorous polymer, Teflon AF 2400, as the extracting solvents. The association through hydrogen bonding and electrostatic interactions between fluorinated carboxylic acids and 3-hydroxypyridine improves the extraction of 3-hydroxypyridine into FC-72 and the films prepared from Teflon AF 2400. The association is found to be substantially stronger in FC-72 than in chloroform; however weaker in the fluorous films due to the specific properties of the polymer and sorption of solvents in the films.

2.1 INTRODUCTION

The unique nature of fluorocarbon solvents makes them significant in selective extraction. The poor solubility of hydrocarbons in fluorous phases has been useful in

synthesis by simplifying the post-reaction purification process.[1-6] Selectivity is achieved by attaching a fluorous tag to one of the reactants/reagents, followed by separation of the desired products according to the differences in solubility in fluorous solvents. Fluorous biphasic synthesis and fluorous biphasic catalysis have gained rapid development in recent years, and have provided understanding about separation and reactivity in fluorous phases.[7-9]

Noncovalent intermolecular interactions in fluorous media have been attracting some attention. Williams and coworkers used fluorinated ketones to enhance the solubility of phenol and phenol derivatives in perfluorooctyl bromide, which has possible applications in drug delivery to the acutely diseased lung through pulmonary ventilation fluids.[10] The formation constant for phenol with the most successful ketone is about 30 M^{-1}. Palomo et al. demonstrated the use of perfluroalkanoic acids to solubilize ureas consisting of "light" fluorous tags in fluorocarbon solvents.[11] The perfluorocarboxylic acids dramatically increased the solubility of investigated ureas in the fluorous solvent, and this method was successfully applied to the scavenging of the urea byproducts in flurorous biphasic synthesis. A highly fluorous anion, tetrakis{3,5-bis([perfluorohexyl)-phenyl}borate, has shown potential in coordinating ions, such as cationic metal catalysts, and extracting these ions into fluorous solvents.[12] Vincent et al. reported fully fluorocarbon-soluble coordination complexes of Mn(II) perfluorocarboxylates and perfluorinated triamines.[13] In an interesting work of Chechik and Crooks on dendrimer-encapsulated Pd nanoparticles as fluorous biphasic catalysts, they used poly(hexafluoropropylene oxide-*co*-difluoro-methylene oxide) monocarboxylic acid to complex the terminal amine groups of dendrimers to solubilize the catalysts in the fluorous phase.[14] Kasai et al. examined the

dissociation of perfluoroether lubricants containing hydroxyl terminals following dilution with fluorocarbon solvents, such as FC-72 (a mixture of perfluorohexanes), and hexafluorobenzene.[15] Our study of hydrogen bonding between barbitals and a perfluoroether tagged-receptor consisting of six binding sites in a cyclic cage in FC-72 illustrated certain selectivity for the target drug, phenobarbital. However, synthesis of this receptor is not trivial. It is therefore practically advantageous to investigate a comparative yet simpler receptor in the first step of studying intermolecular interactions in fluorous solvents.

Among the limited number of highly fluorinated compounds suitable for fluorous receptors, perfluorocarboxylic acids are good candidates. A wide variety of perfluorocarboxylic acids are commercially available, from perfluoroalkanoic acids with different lengths to carboxylic acid-terminated perfluoropolyether oligomers such as Krytox® (**1**). Carboxylic acids have been used as receptors/acceptors for many compounds,[16-19] such as the aminopyridines, and the self-assembly of pyrazine carboxylic acids. Perfluorocarboxylic acids have been demonstrated to have superior hydrogen bonding capabilities toward amide-like hydrogen bond acceptors.[11]

Hydroxypyridines are known to play a role in many biological processes and their nucleus is found in a wide range of drugs.[20-22] However, studies of molecular recognition of hydroxypyridines are rare. Guillerez investigated the tautomerism of 6-chloro-2-hydroxypyridine and its association with acetic acid in CCl_4.[23] The formation constant (K_f) was reported to be 3270 M^{-1} for the pyridine form (OH tautomer), and 17900 M^{-1} for the pyridone form (NH tautomer). The inclusion complexes of 2-, 3-, and 4-hydroxypyridines with β-cyclodextrin in aqueous solution have been studied by NMR

and IR.[24] All complexes showed 1:1 stoichiometry, and the association constants were in the range of 40 - 100 M^{-1}. Lynch and Byriel reported crystal structures of 3HP complexes with different carboxylic acids.[25-28] They demonstrated that the crystal structures were affected by the position of the carboxylate group relative to the plane of the 3HP ring. Various crystal structures, tetramers, or polymeric zig-zag networks were observed.

In general, the study of noncovalent associations in fluorous solvents and fluorous polymers is still a fairly new field. Current studies have been mainly focused on enhancement of solubilities of organic targets or lightly fluorinated molecules in fluorous solvents, which certainly has significance in fluorous biphasic synthesis/catalysis. However, the influence of fluorous solvents on the binding strength and on the selectivity of noncovalent associations is far from understood. We have postulated that fluorous solvents could be used as the extracting phase to improve the selectivity of molecular recognition-enhanced extraction. This is based on the vision that fluorous solvents can effectively suppress nonspecific extraction of interfering species, while target compounds are selectively extracted through association with carefully designed receptors soluble in fluorous solvents. In a transport study of solutes through films prepared from Teflon AF 2400 polymers (**2**), we have found that carboxylic acid terminated perfluoroether **1** can be doped into the films.[29, 30] The film acts as a nonvolatile, dimensionally stable extraction medium. Among a series of solutes being investigated, 3-hydroxypyridine (3HP) stands out with enhanced transport apparently due to association with **1** in the film. We have not seen any reports on association in teflon films so far, it is therefore significant to understand the association of 3HP with perfluorocarboxylic acids in fluorous solvents and polymers. Comparison of the association in Teflon AF films, in a fluorous solvent

(FC-72, perfluorohexanes), and in an organic solvent (chloroform) would lead to an insight of the solvent effects on intermolecular noncovalent associations.

2.2 EXPERIMENTAL SECTION

2.2.1 Reagents

FC-72 (perfluorohexanes) was purchased from 3M (Minneapolis, MN). Krytox 157 FSH (FW 7000-7500, **1**) was from Miller-Stephenson Chemical Company Inc (Danbury, CT). Teflon AF 2400 (**2**) was purchased from Dupont (Wilmington, DE). 1,1,2-trifluorotrichloroethane (TCTFE), spectrophotometric grade chloroform, 3-hydroxypridine (3HP), and perfluorodecanoic acid (PFDA) were from Aldrich (Milwaukee, WI). 99.96% $CDCl_3$ was from Cambridge Isotope Laboratories, Inc (Andover, MA). Other chemicals not specified were reagent grade from Aldrich. All aqueous solutions were prepared with deionized water produced from a Milli-Q A10 system (Millipore, Bedford, MA).

2.2.2 Apparatus

UV spectra were acquired with an Agilent 8453E spectrophotometer (Palo Alto, CA). Quartz cuvettes with path lengths of 0.1 cm and 1.0 cm were purchased from Starna Cells (Atascadero, CA). Transport experiments were carried out on a 15-position stirrer (Cole-Parmer, Chicago, IL) equipped with a control of stirring speeds. ^1H NMR spectra were obtained on Bruker Avance 300 or 600 MHz instruments in $CDCl_3$.

2.2.3 Extraction of 3HP and other solutes with 1

All extractions were conducted at room temperature (25±2 °C) in 4-mL glass tubes with glass stoppers. 1 mL chloroform solution of the solute (0.05 mM) was extracted with 1 mL 0.5 mM **1** dissolved in FC-72. Pyridine has a comparatively low molar absorptivity; so higher concentrations, 0.2 mM pyridine and 2 mM **1**, were used in the extraction. The contents in the glass tubes were mixed for 10 minutes on a Vortex (Scientific Industries, Bohemia, NY) and followed by shaking for 10 minutes. The two phases were separated by centrifugation at 6000 rpm for 10 minutes, and both phases were measured by UV spectrophotometry. In the control extractions, the extracting phase was FC-72 without the receptor. All extractions were carried out in duplicate. The average distribution coefficients and the standard errors of the mean (SEM) are reported.

The fraction of a solute remaining in the chloroform phase (q) was calculated based on the UV absorbance at λ_{max} prior to and following the extraction. The distribution coefficient (D_c) was obtained from Eq. 2-1

$$D_c = (1-q)/q\Phi \qquad (2\text{-}1)$$

where Φ is the volume phase ratio ($V_{FC\text{-}72}/V_{CHCl_3}$).The partition ratio, K_D, is equal to D_c obtained in absence of the receptor.

2.2.4 Extraction of 3HP from chloroform to FC-72 and determination of 3HP with capillary electrophoresis (CE)

In the extraction experiments, 10 mL 1 mM 3HP solution prepared in chloroform was transferred to a separatory funnel containing 10 mL FC-72. The two phases were mixed

and shaken for 15 minutes. The FC-72 layer was transferred to a 10 mL tube for centrifugation for 10 minutes, from which an 8 ml aliquot was taken out and dried. 0.7 ml methanol was added to the residue, followed by sonication for 5 minutes. The solution was transferred into a smaller vial, and again the solvent was evaporated. The residue was finally reconstituted in 80 μL 0.01 M acetic acid-sodium acetate buffer (HAc buffer, pH 4.7) for CE analysis. The extractions were carried out at room temperature in duplicate, and each extraction sample was injected three times in CE analysis. The average partition ratio and the pooled standard deviation are reported.

The CE experiments were conducted on an ISCO 3850 Capillary Electropherograph (ISCO Inc., Lincoln, NE), with EZChrom Chromatography Data System (Scientific Software, Inc., San Ramon, CA). The fused silica capillary was 70 cm (45 cm to the detection window) × 50 μm I.D. (Polymicro Technologies, Inc., Phoenix, AZ). The CE separation was conducted in 0.1 M HAc buffer (pH 4.7), using an voltage of +16 kV and a current about 20 μA. Samples were injected for 40 seconds at 0.5 psi vacuum. The UV detection wavelength was 280 nm. The working standard solution was 10 μM 3HP solution prepared in the same HAc buffer used for the extraction samples. The average peak area of three injections was used for calculations.

2.2.5 Determination of the stoichiometry of 3HP-PFDA complex

The stoichiometry of the complex was determined by the method of continuous variation with UV spectrophotometry detection.[31] Solutions of equal concentration of 3HP and PFDA were mixed in various volume ratios, while the total concentration of the two was kept constant. Another set of control samples were prepared in a similar procedure, with

solvent (chloroform) replacing the PFDA solution. The differences in absorbance (at 292 nm) between the PFDA-containing samples and the control were plotted vs. the molar fraction of 3HP (Job's Plot). The stoichiometry was determined at four concentrations, 0.060 mM, 0.10 mM, 0.24 mM, and 1.2 mM.

For a complex H_aG_b, the difference in absorbance between the two solutions (in presence/absence of PFDA) at each mixing ratio is proportional to the concentration of the complex (Eq. 2-2).

$$A_{obs} - \varepsilon_H \cdot [H]_t - \varepsilon_G \cdot [G]_t = (\varepsilon_C - a \cdot \varepsilon_H - b \cdot \varepsilon_G) \cdot [C] \quad (2\text{-}2)$$

where A_{obs} is the observed absorbance of the mixture. $[H]_t$ and $[G]_t$ are the total concentration of the host (PFDA), and the guest (3HP), respectively; $[C]$ is the concentration of the complex; a and b are the stoichiometric coefficients in the complex H_aG_b; ε_C, ε_H, and ε_G are the molar absorptivities of the complex, the host, and the guest, respectively. Because PFDA does not have UV absorbance at 292 nm ($\varepsilon_H = 0$), Eq. 2-2 is simplified to:

$$A_{obs} - \varepsilon_G \cdot [G]_t = (\varepsilon_C - b \cdot \varepsilon_G) \cdot [C] \quad (2\text{-}3)$$

The stoichiometry is determined from the x-coordinate at the maximum ($dy/dx = 0$) of the Job's Plot.

2.2.6 IR spectra and NMR spectra of 3HP complexes with perfluorocarboxylic acids

IR spectra were recorded on an Excalibur FTS 3000 Spectrometer (DigiLab, Randolph, MA) using a flow cell with KBr widows and a 1 mm Pb spacer. The solvent chloroform

used in IR experiments was purified by basic aluminum oxide column. The complex of 3HP-PFDA in $CHCl_3$ was prepared by mixing the same volume of 10 mM 3HP and 10 mM PFDA solutions. The complex of 3HP-**1** in FC-72 was prepared by addition of an equal molar 3HP solid into the solution of **1**, followed by sonication till the added 3HP was dissolved (for about 10 minutes).

^{1}H NMR spectra were obtained on Bruker Avance 300 or 600 MHz instruments in $CDCl_3$ at room 298 K. The complex of 3HP-PFDA in $CDCl_3$ was prepared by mixing equal volume of 0.2 mM 3HP with 2 mM PFDA. The complex in FC-72 was obtained from extracting the $CDCl_3$ solution of 1mL 0.2 mM 3HP with 1mL FC-72 solution of 2 mM **1**. The mixture was shaken for 30 minutes, followed by centrifugation for 10 min. The FC-72 layer was taken out for collecting NMR spectra.

2.2.7 Transport of 3HP through films of 2 and determination of the distribution coefficient of 3HP from solvents to the film.

The films were prepared by casting polymer solutions in FC-72.[29] Two types of films were investigated, films of pure **2**, and films of **2** doped with 50% (w/w) **1**. Transport of 3HP (dissolved in $CHCl_3$) through the film was carried out in a carefully designed three-phase transport apparatus at room temperature (24 ± 2 ºC).[29, 32] The test film was sandwiched between two 4-mL transport cuvettes modified with holes (0.5 cm i.d.) to allow transport. The receiving phase which was contained in a UV transparent cuvette was monitored by a UV spectrometer continuously until steady–state transport was reached.

The distribution coefficient of a solute was obtained through a non-linear curve fit according to Eq. 2-4.[29]

$$Q_t = K_D Cl\left(\frac{Dt}{l^2} - \frac{1}{6} - \frac{2}{\pi^2}\sum_{1}^{\infty}\frac{(-1)^n}{n^2}\exp(-Dn^2\pi^2 t/l^2)\right) \qquad (2\text{-}4)$$

Q_t denotes the total amount of a solute transported through the film at time t, which can be obtained from the recorded solute concentration in the receiving phase. K_D is the partition ratio of the solute. C is the concentration of the solute in the source phase; l is the film thickness, and D is the diffusion coefficient.

2.3 RESULTS AND DISCUSSION

2.3.1 Association of 3HP with perfluorocarboxylic acids and extraction of 3HP into fluorous solvents

A perfluorocarboxylic acid, PFDA, was used as the receptor for extraction of 3HP. 3HP associates with the acid. The UV spectra exhibited red shift following addition of PFDA to 0.2 mM 3HP solution in chloroform (Fig. 2.1). The spectral shift occurred at low concentrations (0.005 - 0.1 mM 3HP), suggesting a large formation constant of the 3HP-PFDA complex. Increasing the molar ratio of the acid to 3HP caused a gradual shift of the maximum wavelength, λ_{max}, from 277 nm to 287 nm. Fig. 2.2 records the change of the UV absorbance at 287 nm of the solutions with various mixing ratios. For 0.2 mM 3HP, about 5 fold PFDA was needed for complete association of 3HP. Higher ratios of PFDA/3HP (up to 40:1) did not cause any change of the peak shape or the UV

absorbance at 287 nm. These results illustrate that only one complex with λ_{max} at 287 nm exists under the conditions of excess acid.

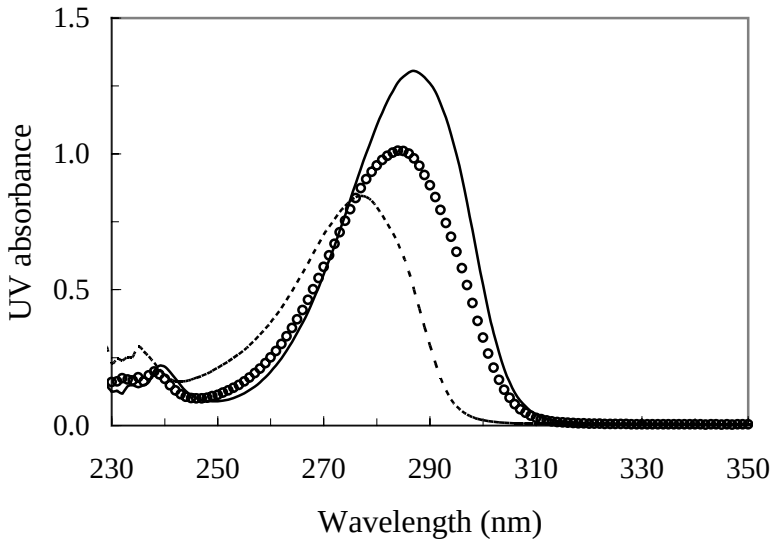

Figure 2.1. UV spectra of 0.2 mM 3HP and mixtures with PFDA in $CHCl_3$

Dash line: 0.2 mM 3HP; dotted line: 1:1 (3HP/PFDA) mixture; and solid line: 1:10 mixture.

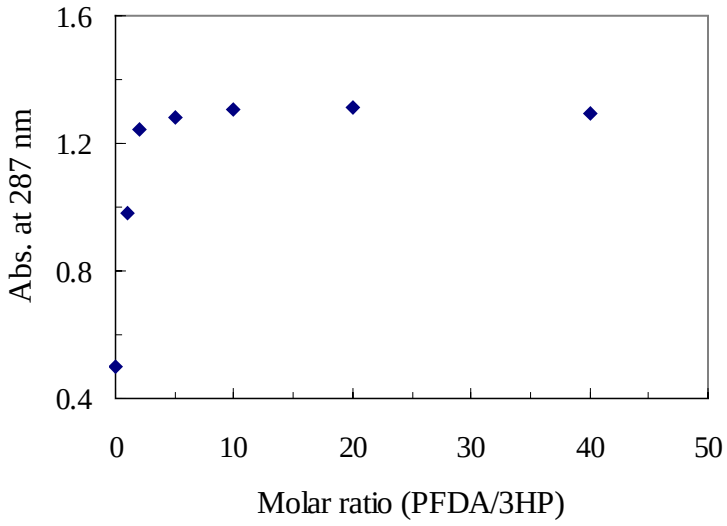

Figure 2.2. UV Absorbance of 3HP (0.2 mM) and the complex formed with excess PFDA (in $CHCl_3$)

However, the fluorous tag ($-C_9F_{19}$) of perflurodecanoic acid is not enough to solubilize the 3HP-PFDA complex into FC-72; the complex showed a small partition ratio from chloroform to FC-72. Carboxylic acids containing longer fluorous tags, such as perfluorotetradecanoic acid, and perfluorooctadecanoic acid, improve the partitioning of the complex to FC-72. However, the limited solubility of these acids in FC-72 (<1 mM) hinders their applications as fluorous receptors. Fluorinated polyethers are structurally more flexible than perfluoroalkanes, therefore they are more suitable for large fluorous tags to achieve desired partitioning from organic solvents to fluorous solvents.[33] A carboxylic acid-terminated poly(hexafluoropropylene oxide) under the brand name Krytox was then chosen to replace PFDA. Krytox is commercially available with different average molecular weights: 2500 (FSL), 4000 (FSM), 7500 (FSH). The one with an average molecular weight of 7500 (**1**, Fig. 2.3) was used in this study.

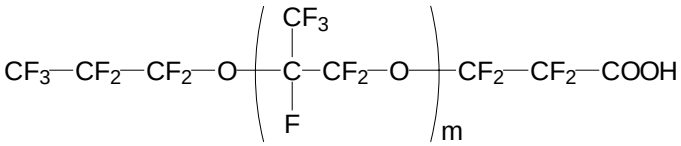

Figure 2.3. Krytox FSH, MW 7500 (**1**)

3HP is virtually not extracted by the fluorous solvent FC-72, so it is practically challenging to determine the small partition ratio of 3HP from chloroform to FC-72. This was achieved by preconcentrating the FC-72 phase 100 fold following the extraction, as well as applying sample stacking injection in CE analysis. The preconcentration was carried out in two steps: first, evaporate FC-72 and reconstitute the residue in a smaller volume of methanol, second, evaporate methanol again and reconstitute the residue in a smaller volume of pH 4.7 HAc buffer.

The final volume of the extraction samples was less than 0.1 mL, so CE was chosen for separation and analysis. CE sample stacking injection improves the analysis sensitivity by allowing injection of a large sample volume while still maintaining narrow separation peaks.[34, 35] Samples were dissolved in a buffer (0.01 M HAc buffer) with a lower conductivity than that of the CE run buffer (0.1 M HAc buffer), and a long injection time (40 s at 0.5 psi vacuum) was used. To minimize the analysis error, two extractions and three injections for each extraction were carried out. Fig. 2.4 shows the CE electropherograms of an extraction sample and the 10 μM 3HP standard. The partition ratio of 3HP from chloroform to FC-72 was determined to be: $(6.7 \pm 0.5) \times 10^{-5}$. This is consistent with the poor solubility of polar organic compounds in fluorous solvents.

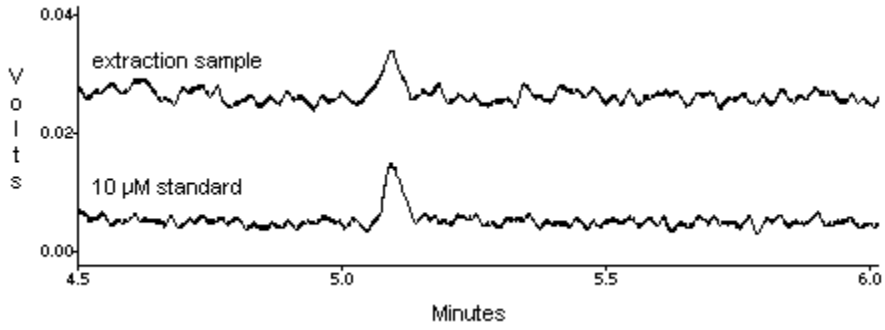

Figure 2.4. CE determination of 3HP extracted into FC-72.

Receptor **1** dramatically enhances the extraction of 3HP. Without **1**, there is virtually no extraction of 3HP into FC-72. With 0.5 mM **1** in FC-72, the distribution coefficient of 3HP increases substantially to 2.10, which means 67% of 3HP was extracted at an initial concentration of 0.05 mM. Fig. 2.5 shows the UV spectrum of the FC-72 phase following extraction.

For comparison, pyridine and phenol were examined under the same extraction conditions. Receptor **1** enhanced the extraction of pyridine too, however to a smaller degree as compared to 3HP. No detectable phenol was found in the FC-72 phase, indicating that **1** does not associate with phenol. Table 2.1 lists the distribution coefficients of the three solutes in presence/absence of **1**. The extraction results demonstrate that the nitrogen on 3HP is responsible for coordinating the carboxylic acid.

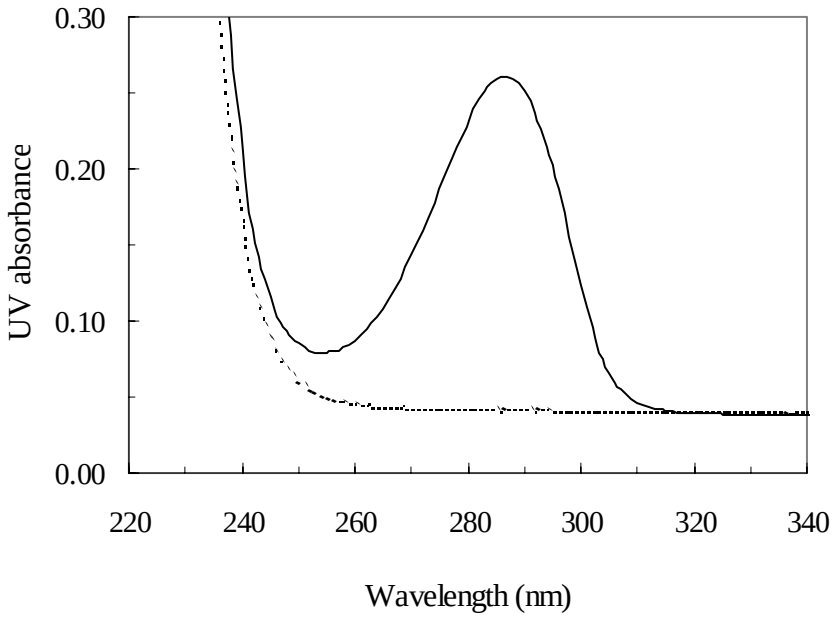

Figure 2.5. UV spectrum of the FC-72 phase after extraction of 3HP with 0.5 mM **1**. Dotted line: control; solid line: extraction of 3HP with **1**.

Table 2.1. Distribution coefficients of solutes

Solute	Without **1**	With **1**[a]
3HP	[b]$(6.7 \pm 0.5) \times 10^{-5}$	2.1 ± 0.1
pyridine	< 0.01	1.8 ± 0.1
phenol	< 0.01	< 0.01

[a]Extractions of the solutes from chloroform solution to FC-72 were carried out using excess **1**. The listed values are the average of duplicate measurements, and the errors are the standard error of the mean. [b]The error is the pooled standard deviation.

2.3.2 Complex stoichiometry and formation constant in $CHCl_3$

It is essential to know the stoichiometry of the complex for calculation of the formation constant. The stoichiometry of 3HP-PFDA complex was determined by continuous variation method at four concentrations in chloroform, 0.060 mM, 0.10 mM, 0.24 mM, and 1.20 mM, gave the same ratio of 1:1, as shown in Fig. 2.6.

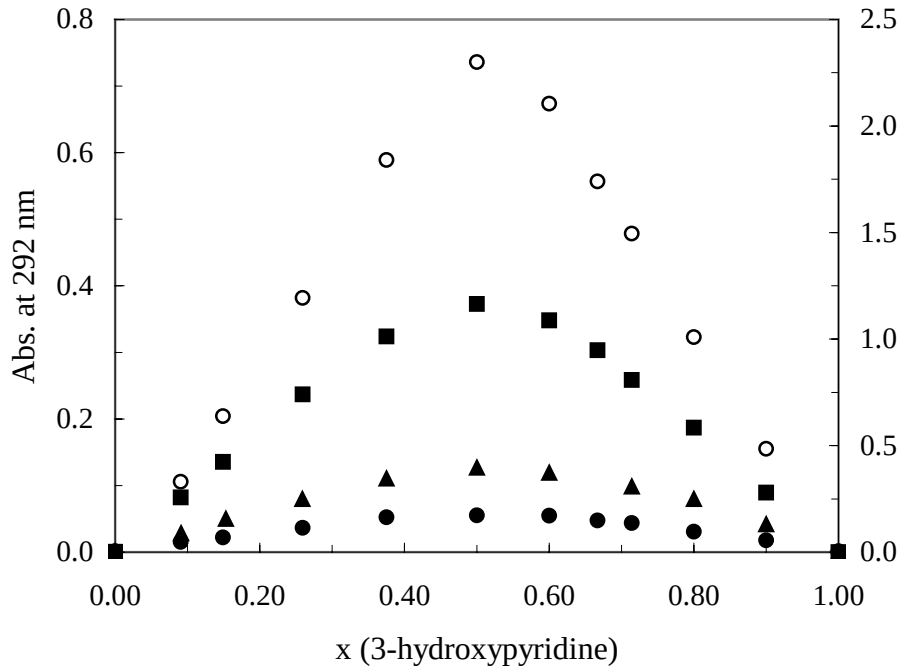

Figure 2.6. Job's plot for determination of the stoichiometry of 3HP-PFDA complex in $CHCl_3$.

Curves from bottom to top: 0.060, 0.10, 0.24 mM (left y-axis), and 1.20 mM (right y-axis) total concentration.

The formation constant, K_f, can be deduced through a non-linear curve fit according to Eq. 2-5.

$$K_f = \frac{[C]}{(C_{total}\,x - [C])(C_{total}\,(1-x) - [C])} \qquad (2\text{-}5)$$

where C_{total} is the total concentration of the host plus the guest; x is the molar fraction of the guest; [H], [G], [C], are the concentrations of the host, the guest, and the complex respectively in the mixture. [C] is a function of the measured UV absorbance as shown in Eq. 2-3.

Both the formation constant (K_f) and the molar absorptivity of the complex (ε_C) can be obtained through non-linear fit. However, the non-linear fit gives more accurate results if ε_C is known; in which case K_f is the only unknown parameter in Eq. 2-5. The molar absorptivity of 3HP-PFDA complex was therefore determined. Solutions of 3HP with various concentrations were mixed with excess PFDA. Calculations were conducted to make sure that >99% 3HP was in complex form in each solution. The UV spectra of all solutions gave λ_{max} at 287 nm, which confirmed that 3HP was completely associated with the acid. Fig. 2.7 shows the standard curve of the complex. The molar absorptivity of the complex (ε_C) was determined to be 5885 $M^{-1}cm^{-1}$ at 287 nm, and 5303 $M^{-1}cm^{-1}$ at 292 nm (R^2 = 0.9995). At the same time, the molar absorptivity of 3HP at 292 nm was determined to be 732 $M^{-1}cm^{-1}$ (R^2 = 0.9994).

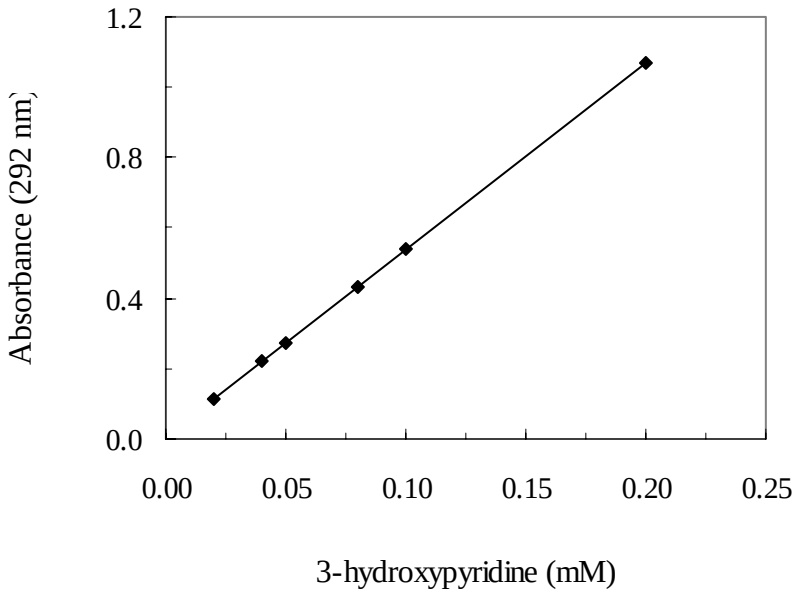

Figure 2.7. Standard curve of 3HP-PFDA complex in $CHCl_3$

The formation constants obtained from nonlinear fit of 0.060, 0.1, 0.24 mM 3HP/PFDA mixtures is listed in Table 2.2. The average formation constant is deduced to be 4.8×10^4 M^{-1}. Data obtained for the 1.20 mM 3HP/PFDA mixture was excluded in the nonlinear fit because the fit error was large due to the fairly complete association at this concentration.

Table 2.2. Formation constants of 3HP-PFDA complex in $CHCl_3$

Concentration (mM)	Formation Constant (M^{-1})
0.06	3.8×10^4
0.10	5.3×10^4
0.24	5.3×10^4
Average	$(4.8 \pm 0.5) \times 10^4$ (SEM, n = 3)

This formation constant is certainly large for a single hydrogen bond. It is also much larger than the value reported by Barrow for the pyridine-acetic acid complex in $CHCl_3$ (70 M^{-1}), and in CCl_4 (220 M^{-1}).[36] A 1:1 complex was reported to form through the hydrogen bond between the -COOH on acetic acid and the nitrogen on pyridine. Barrow also studied the association of pyridine and trifluoroacetic acid (TFA) in chloroform.[36] He found that a proton transfer from acid to pyridine occurred for strong acids such as TFA, resulting in an ion-pair species. PFDA is a strong acid like TFA; thus proton transfer is possible in 3HP-PFDA complex. The complex structure was then investigated.

2.3.3 Complex structure

Studies of the tautomeric equilibria of 3HP by UV,[37-40] NMR,[41-44] and theoretic calculations[21, 45, 46] have demonstrated that the equilibria are in favor of the pyridine form (OH tautomer) over the zwitterionic form (NH tautomer) in the gas phase and in solvents with low polarity. The equilibria shift in the direction of the zwitterionic form as the dielectric constant of the solvent increases, and reach a ratio about 1:1 in water.[38, 40, 46] The UV spectra of 3HP we obtained in $CHCl_3$ exhibited one single peak at 277 nm with no detectable shift of λ_{max} from 0 to 1 mM concentration range. The liner regression analysis of UV absorbance vs. concentration of 3HP showed a correlation coefficient (R^2) of 0.9999. The NMR spectra of 3HP showed no large peak shift of any of the four hydrogens on the pyridine ring from 0.05 mM to 1 mM. These results indicate that 3HP exists as monomeric *hydroxypyridine* form in $CHCl_3$ at the investigated concentrations (< 1 mM).

Association of 3HP with perfluorocarboxylic acid occurs between the pyridine nitrogen and the carboxylic acid, as suggested by the extraction of 3HP, pyridine, and phenol with **1**. Because perfluorocarboxylic acids are strong acids, and pyridine nitrogen is basic, does the ion-pair complex form? In a study by Johnson and Rumon regarding the solid state complexes of pyridine with substituted benzoic acids,[47] it is suggested that proton transfer from the acid to the pyridine nitrogen occurs when aqueous *pKa* differences between acid and base are greater than 3.75. Such is the case of the pyridine complexes with 2,4-dinitrobenzoic acid, and trifluoroacetic acid.[47] Proton transfer has also been observed in the pyridine complexes with dichloroacetic acid and TFA in benzene and dichloromethane solutions,[18] as well as the complex of substituted pyridines with TFA in different solvents.[48] Lynch and coworkers have reported similar proton transfer phenomenon in crystal structures of 3HP complexes with 2,4,6-trinitrobenzoic acid, 4-nitrobenzoic acid, and 2,6-dichloro-benzoic acid.[25, 28]

To confirm if proton transfer occurred in 3HP- PFDA complex, HCl-saturated $CHCl_3$ was added stepwise to 3HP solution (in $CHCl_3$). The UV spectra of 3HP shifted to higher wavelength of 288 nm with addition of HCl-saturated $CHCl_3$ (Fig. 2.8). The molar absorptivity of the protonated 3HP was determined to be 7250 $M^{-1}cm^{-1}$ at 288 nm, which is slightly larger than the molar absorptivity of the 3HP-PFDA complex (5885 $M^{-1}cm^{-1}$ at 287 nm). The similarity in the UV spectra of HCl-protonated 3HP and the 3HP-PFDA complex suggests that proton transfer occurs in the latter case. The IR spectrum of PFDA (5 mM in $CHCl_3$) showed two peaks at 1780.3 cm^{-1}, and 1797.7 cm^{-1}, belonging to the $\nu_{C=O}$ of PFDA dimer and monomer, respectively. These two peaks are closed to the $\nu_{C=O}$ bands of TFA dimer (1782 cm^{-1}) and monomer (1805 cm^{-1}) in CH_2Cl_2 as reported by

Barczynski et al.[18] In the 1:1 mixture of 3HP and PFDA (5mM each), these two peaks from PDFA disappeared; a new peak appeared at 1664.6 cm^{-1} could be attributed to ν_{COO^-} vibration. This is similar to the case of TFA-pyridine complex which shows a band at 1662 cm^{-1},[47] and the case of TFA complex with 2,4,6-trimethylpyridine which shows a band at 1685 cm^{-1}.[18] These bands are close to the ν_{COO^-} vibrations in TFA salts: 1680 cm^{-1} in CH_3COONa (crystal),[47] and 1688 cm^{-1} in $CH_3COOH^-N^+(Bu)_4$ (in CH_2Cl_2).[18]

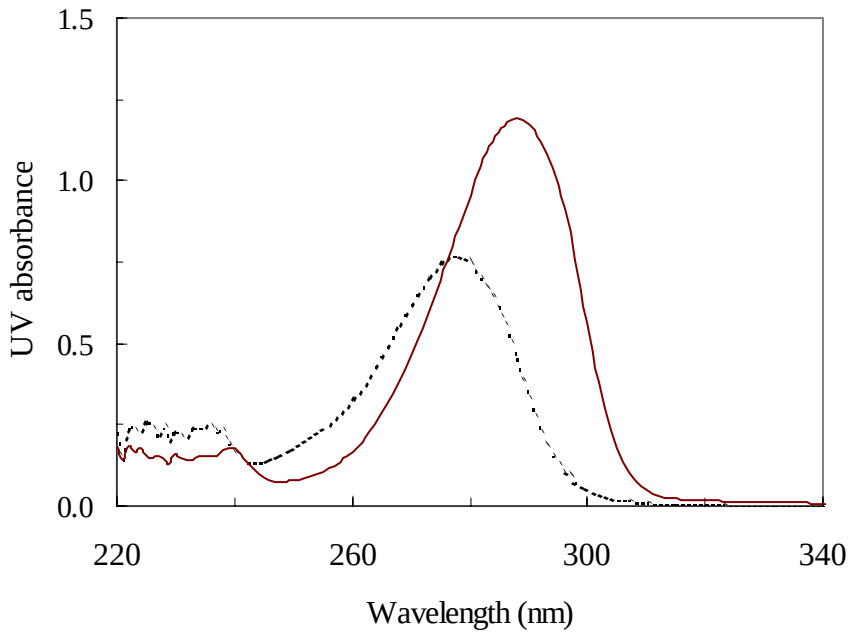

Figure 2.8. UV spectra of 3HP solution before (dash line) and after (solid line) addition of HCl-saturated $CHCl_3$.

2.3.4 Noncovalent association of 3HP and 1 in FC-72

The formation constant of a complex can be obtained from the extraction experiments. Under the condition of the receptor being in large excess of the acceptor, the formation constant, K_f, can be deduced from Eq. 2-6

$$K_f = (1 - q - qK_D\Phi)/(qK_D\Phi[R]_t) \quad (2\text{-}6)$$

where q is the fraction of 3HP remaining in the chloroform phase following extraction; K_D is the partition ratio in absence of the receptor; and $[R]_t$ is the total concentration of the receptor in the extracting solvent.

The complex has been shown to take a 1:1 stoichiometry in chloroform, with the association being between the nitrogen of 3HP and the carbonyl group of the carboxylic acid. Does the complex in fluorous solvents possess the same structure? We investigated the IR spectra of the two complexes: 3HP-PFDA in $CHCl_3$, and 3HP-**1** in FC-72. Higher concentration solutions, 5 mM solutions, were used in these experiments. 3HP had three peaks in $CHCl_3$: 1583.6 cm^{-1} and 1460.1 cm^{-1} attributed to the 3HP ring, and 1280.7 cm^{-1} attributed to the ν_{C-O} band. PFDA had a peak at 1780.3 cm^{-1} from of the dimer (in $CHCl_3$); while **1** had a peak at 1776.4 cm^{-1} from $\nu_{C=O}$ of the dimer (in FC-72). The $\nu_{C=O}$ band of the acid dimer shifted to 1674.2 cm^{-1} in the 3HP-PFDA complex, and to 1664.6 cm^{-1} in the 3HP-**1** complex. The $\nu_{C=O}$ bands of free **1** and 3HP-**1** complex are close to the values reported by Doan and coworkers: 1775 cm^{-1} for the acid dimer, and 1676 - 1690 cm^{-1} for the sodium salt dimer of the perfluoropolyether.[49] The two bands of 3HP ring shifted to higher wavenumbers in the two complexes (Fig. 2.9). The IR spectra of the

3HP-PFDA complex and the 3HP-**1** complex are very similar, suggesting similar complex structures in $CHCl_3$ and FC-72.

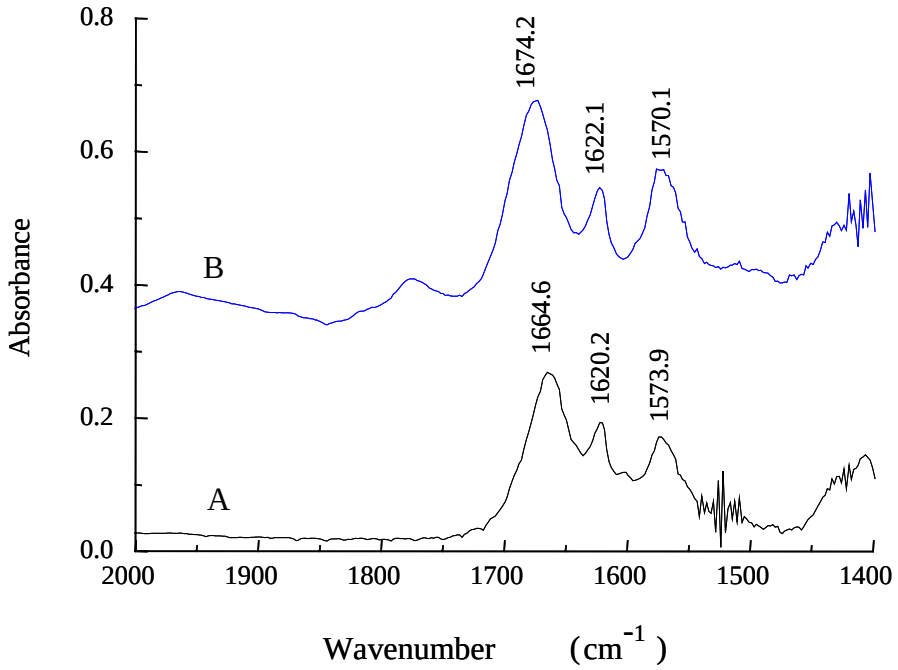

Figure 2.9. IR spectra of 3HP-PFDA complex in $CHCl_3$ (A) and 3HP-**1** (B) complex in FC-72 (5 mM solutions)

Proton NMR spectra of the two complexes in $CDCl_3$ and in FC-72 provided some structure information (Table. 2.3). The hydrogens in the pyridine ring of 3HP: H-2, H-4, and H-5, showed large downfield chemical shifts after complexation. H-6 showed very small shift in the two complex. The two complexes have similar coupling modes, H-2 as a wide unresolved single peak, H-6 as doublet, H-4 and H-5 as doublet-doublet. In FC-72, H-2 and H-6 of 3HP-**1** complex present a larger downfield shift compared to 3HP-PFDA complex, probably due to a stronger interaction of 3HP with the receptor **1**.

Table 2.3. ^{1}H NMR chemical shifts of 3HP and 3HP complex with acids at 298 K (ppm)

Compound	H-2	H-4	H-5	H-6
3HP	8.28 (dd)	7.20 (dd)	7.19 (dd)	8.23 (dd)
3HP-PFDA	9.04 (s)	7.91 (dd)	7.76 (dd)	8.16 (d)
3HP-**1**	9.58 (s)	7.94 (dd)	7.71 (dd)	8.40 (d)

600 MHz ^{1}H NMR spectra of 0.2 mM 3HP-PFDA complex in $CDCl_3$, and 3HP-**1** complex in FC-72. Peak abbreviation: s, singlet; d, doublet; dd, doublet-doublet.

Combining the results of UV, IR and NMR spectra, we propose a 1:1 3HP-**1** complex in FC-72. The formation constant between 3HP and **1** in FC-72 is then deduced to be $(6.2 \pm 0.7) \times 10^{7}\ M^{-1}$ (SEM, n = 2) when using 0.5 mM **1**. This formation constant in FC-72 is remarkably large, compared to the value between 3HP and PFDA in $CHCl_3$. The reason is likely related to the extremely low partition ratio of 3HP to the fluorocarbon solvent FC-72 ($(6.7 \pm 1.7) \times 10^{-5}$), as well as the strong tendency of the hydrogen bonded ion pair being associated in the nonpolar fluorocarbon solvent.

2.3.5 Noncovalent association in Teflon AF films

Among the two Teflon AF products available: Teflon AF 2400 containing 87 mol% PDD, and Teflon AF 1600 containing 65% mol PDD,[50] Teflon AF 2400 (**2**, Fig. 2.10) is more permeable, thus it is more suitable for transport of solutes. Receptor **1** is miscible with the polymer, and plasticizes the polymer. The transition temperature, T_g, deceases to -40 °C for the polymer doped with 50% **1** (w/w) compared to 240 °C for pure **1.** Consisting of a –COOH terminal, **1** is also a convenient receptor in fluorous polymer **2**.

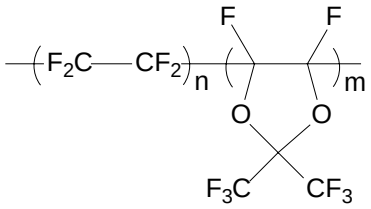

Figure 2.10. Teflon AF (**2**)

To investigate the association of 3HP with **1** in the film, a film of **2** doped with 50% of **1** was soaked in a 0.1 mM chloroform solution of 3HP overnight at room temperature, allowing the association to complete. The film surface was quickly washed with $CHCl_3$ and dried in air. The untreated film was used as the blank in UV spectrophotometric measurements. The film treated with 3HP solution showed similar UV spectra to that of the complex formed in $CHCl_3$ and FC-72 (Fig. 2.11), with the same λ_{max} of 287 nm.

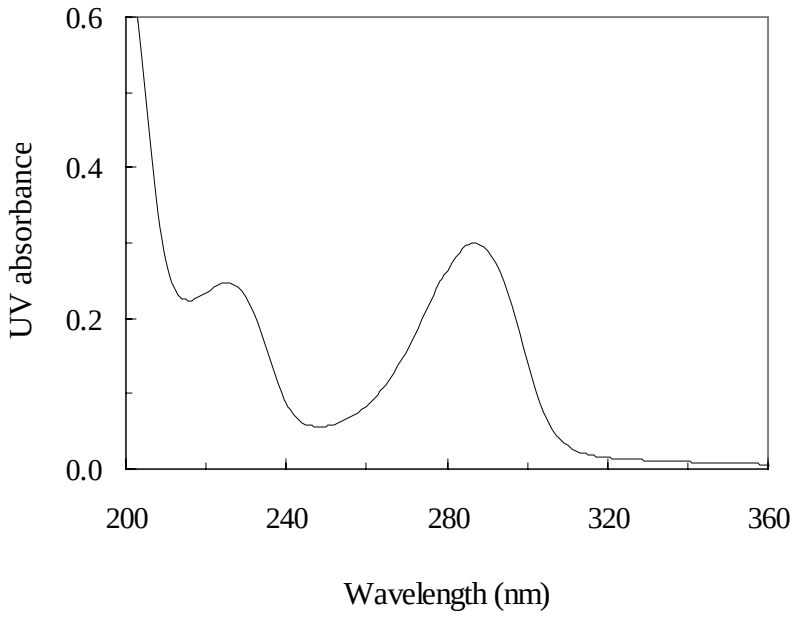

Figure 2.11. UV spectrum of the **1**-doped film treated with 3HP solution. The film contained 50% (w/w) **1**.

Similar to the liquid-liquid extraction experiments, the formation constant of 3HP and **1** in the fluorous polymer can be obtained by determination of the distribution coefficients of 3HP in presence and in absence of receptor **1**. The distribution coefficient of 3HP obtained from transport experiments was 0.016 ± 0.03 (SEM, n = 7) for the film of **2**, and 1.8 ± 0.2 (SEM, n = 3) for the film doped with 50% **1** (approximate concentration of 0.13 M). The formation constant is then deduced to be 840 M^{-1}. Table 2.4 lists the distribution coefficients of 3HP and the formation constants of the complex in FC-72 and in the film.

Table 2.4. Distribution coefficients of 3HP and association constants of the complex in films and FC-72

	Film of **2**	FC-72
D_c in absence of **1**	0.016 ± 0.03 (n = 7)	$(6.7 \pm 1.7) \times 10^{-5}$ (n = 2)
D_c with 0.13 M **1**	1.8 ± 0.2 (n = 3)	37 ± 2 (n = 2)
K_f (M^{-1})	840	4.3×10^6

D_c: distribution coefficient, K_f: formation constant. The errors are the standard errors of the mean of multiple measurements.

The formation constant of 3HP-**1** complex in the film is remarkably smaller than the value determined in FC-72 at the same receptor concentration. This is caused by the differences between the polymer films and FC-72. Under the conditions of absence of the receptor, the distribution coefficient of 3HP from chloroform to the film is substantially larger than the value from chloroform to FC-72. We have found that this is due to the large free volume of the film as well as solvent sorption into the film (Chapter 3).[29] The fractional free volume (FFV) of **2** is 0.327; gases have shown large solubility and permeability in the film.[51, 52] We have determined the chloroform concentration sorbed in the film, which reaches 7.9/100g polymer (1.13 M,).[29] The sorbed solvent plasticizes the film, changes the fluorous nature of the film, and results in much higher solubility for organic solutes as compared to fluorous solvents. On the other hand, the distribution coefficients of 3HP from chloroform to the film containing 0.13 M **1** is smaller than the value from chloroform to FC-72 containing the same concentration of **1**, which reflects a less enhancement of extraction with the receptor. The formation constant in the film is

therefore much lower than the value obtained in FC-72. The association between **1** and 3HP increases the extractability of the polar solute 3HP by 15000 times in FC-72, and 41 times in the film.

2.4 CONCLUSION

Non-covalent associations through hydrogen bonding and electrostatic interactions have been shown to improve the extraction of a polar solute 3HP into a fluorous solvent FC-72, and into a fluorous polymer **2**. Association occurs between the 3HP nitrogen and the carboxyl group of the acid (perfluorodecanoic acid, or COOH-terminated perfluoroether **1**). Proton transfer process is observed in these complexes. As a result, the ion-pairing hydrogen bonding species have large formation constants. The association between 3HP and carboxylic acid is substantially stronger in the fluorous solvent than in chloroform due to the strong tendency of the hydrogen bonded ion pair being associated in the nonpolar fluorocarbon solvent. However, similar strong association is not observed in the fluorous polymer **2**. The formation constant obtained in the plasticized film is a couple orders lower than that in chloroform, which is related to the characteristics of the polymer and plasticization of the film by the contacted solvents. In a practical sense, the dramatic enhancement of the extraction of 3HP by fluorous carboxylic acid show the sort of selectivity in extraction that we seek for more complex systems.

2.5 REFERENCES

(1) Gladysz, J. A. *Science* **1994**, *266*, 55-56.

(2) Horvath, I. T.; Rabai, J. *Science* **1994**, *266*, 72-75.

(3) Horvath, I. T. K., Gabor; Cook, Raymond A.; Bond, Jeffrey E.; Stevens, Paul A.; Rabai, Jozsef; Mozeleski, Edmund J. *Journal of the American Chemical Society* **1998**, *120*, 3133-3143.

(4) Studer, A.; Hadida, S.; Ferritto, R.; Kim, S.-Y.; Jeger, P.; Wipf, P.; Curran, D. P. *Science* **1997**, *275*, 823-826.

(5) Luo, Z.; Zhang, Q.; Oderaotoshi, Y.; Curran, D. P. *Science* **2001**, *291*, 1766-1769.

(6) Gladysz, J. A., Curran, Dennis P., Horvath, Istvan T. *Handbook of Fluorous Chemistry*; Wiley-VCH: Weinheim, 2004.

(7) Linclau, B.; Sing, A. K.; Curran, D. P. *Journal of Organic Chemistry* **1999**, *64*, 2835-2842.

(8) Barthel-Rosa, L. P.; Gladysz, J. A. *Coordination Chemistry Reviews* **1999**, *190-192*, 587-605.

(9) Richter, B. d. W., Elwin; van Koten, Gerard; Deelman, Berth-Jan. *Journal of Organic Chemistry* **2000**, *65*, 3885-3893.

(10) Williams, T. D.; Jay, M.; Lehmler, H. J.; Clark, M. E.; Stalker, D. J.; Bummer, P. M. *Journal of Pharmaceutical Sciences* **1998**, *87*, 1585-1589.

(11) Palomo, C.; Aizpurua, J. M.; Loinaz, I.; Fernandez-Berridi, M. J.; Irusta, L. *Organic Letters* **2001**, *3*, 2361 -2364.

(12) van den Broeke, J.; Deelman, B.-J.; van Koten, G. *Tetrahedron Letters* **2001**, *42*, 8085-8087.

(13) Vincent, J.-M.; Rabion, A.; Yachandra, V. K.; Fish, R. H. *Angewandte Chemie, International Edition in English* **1997**, *36*, 2346-2349.

(14) Chechik, V.; Crooks, R. M. *Journal of the American Chemical Society* **2000**, *122*, 1243-1244.

(15) Kasai, P. H.; Spiese, C. *Tribology Letters* **2004**, *17*, 823-833.

(16) Chen, H.; Weiner, W. S.; Hamilton, A. D. *Current Opinion in Chemical Biology* **1997**, *1*, 458-466.

(17) Garcia-Tellado, F.; Goswami, S.; Chang, S. K.; Geib, S. J.; Hamilton, A. D. *Journal of the American Chemical Society* **1990**, *112*, 7393-7394.

(18) Barczynski, P.; Dega-Szafran, Z.; Szafran, M. *Journal of the Chemical Society, Perkin Transactions 2: Physical Organic Chemistry (1972-1999)* **1987**, 901-906.

(19) Vishweshwar, P.; Nangia, A.; Lynch, V. M. *Journal of Organic Chemistry* **2002**, *67*, 556-565.

(20) Fuss, A.; Koch, V. *Synthesis* **1990**, 604-608.

(21) Kiruba, G. S. M.; Wong, M. W. *Journal of Organic Chemistry* **2003**, *68*, 2874-2881.

(22) Wondrak, G. T.; Roberts, M. J.; Jacobson, M. K.; Jacobson, E. L. *Journal of Biological Chemistry* **2004**, *279*, 30009-30020.

(23) Guillerez, J.; Bensaude, O.; Dubois, J. E. *Journal of the Chemical Society, Perkin Transactions 2: Physical Organic Chemistry* **1980**, 620-623.

(24) Ramusino, M. C.; Pichini, S. *Carbohydrate Research* **1994**, *259*, 13-19.

(25) Byriel, K. A.; Kennard, C. H. L.; Lynch, D. E.; Smith, G.; Thompson, J. G. *Australian Journal of Chemistry* **1992**, *45*, 969-981.

(26) Lynch, D. E.; Smith, G.; Byriel, K. A.; Kennard, C. H. L. *Acta Crystallographica, Section C: Crystal Structure Communications* **1992**, *C48*, 533-536.

(27) Lynch, D. E.; Smith, G.; Byriel, K. A.; Kennard, C. H. L.; Whittaker, A. K. *Australian Journal of Chemistry* **1994**, *47*, 309-319.

(28) Lynch, D. E.; Lad, J.; Smith, G.; Parsons, S. *Crystal Engineering* **1999**, *2*, 65-77.

(29) Zhao, H.; Ismail, K.; Weber, S. G. *Journal of the American Chemical Society* **2004**, *126*, 13184-13185.

(30) Zhao, H., Wu, N, Zhang, J., Zhang, X., Crowley, K., Weber, S. G. *Journal of the American Chemical Society* **2005**, Accepted.

(31) Hirose, K. *Journal of Inclusion Phenomena and Macrocyclic Chemistry* **2001**, *39*, 193-209.

(32) Zhang, X.; Zhao, H.; Chen, Z.; Nims, R.; Weber, S. G. *Analytical Chemistry* **2003**, *75*, 4257-4264.

(33) Eleuterio, H. S. *Journal of Macromolecular Science, Chemistry* **1972**, *6*, 1027-1052.

(34) Baker, D. R. *Capillary Electrophoresis*; Wiley, New York, N. Y., 1995.

(35) Burgi, D. S.; Chien, R. L. *Analytical Chemistry* **1991**, *63*, 2042-2047.

(36) Barrow, G. M. *Journal of the American Chemical Society* **1956**, *78*, 5802-5806.

(37) Gordon, A.; Katritzky, A. R. *Tetrahedron Letters* **1968**, 2767-2770.

(38) Metzler, D. E.; Harris, C. M.; Johnson, R. J.; Siano, D. B.; Thomson, J. A. *Biochemistry* **1973**, *12*, 5377-5392.

(39) Sanchez-Ruiz, J. M.; Llor, J.; Cortijo, M. *Journal of the Chemical Society, Perkin Transactions 2: Physical Organic Chemistry* **1984**, 2047-2051.

(40) Llor, J.; Asensio, S. B. *Journal of Solution Chemistry* **1995**, *24*, 1293-1305.

(41) Kwiatkowski, J. S. *Journal of Molecular Structure* **1971**, *10*, 245-251.

(42) Stefaniak, L. *Tetrahedron* **1976**, *32*, 1065-1067.

(43) Del Giudice, M. R.; Settimj, G.; Delfini, M. *Tetrahedron* **1984**, *40*, 4067-4080.

(44) Llor, J.; Lopez-Mayorga, O.; Munoz, L. *Magnetic Resonance in Chemistry* **1993**, *31*, 552-556.

(45) Karelson, M. M.; Katritzky, A. R.; Szafran, M.; Zerner, M. C. *Journal of Organic Chemistry* **1989**, *54*, 6030-6034.

(46) Wang, J.; Boyd, R. J. *Journal of Physical Chemistry* **1996**, *100*, 16141-16146.

(47) Johnson, S. L.; Rumon, K. A. *Journal of Physical Chemistry* **1965**, *69*, 74-86.

(48) Dega-Szafran, Z.; Dulewicz, E. *Organic Magnetic Resonance* **1981**, *16*, 214-219.

(49) Doan, V.; Koeppe, R.; Kasai, P. H. *Journal of the American Chemical Society* **1997**, *119*, 9810-9815.

(50) Buck, W. H., Resnick, P. R., 183rd Meeting of the Electrochemcial Socienty, Honolulu, HI, USA 1993.

(51) Pinnau, I.; Toy, L. G. *Journal of Membrane Science* **1996**, *109*, 125-133.

(52) Merkel, T. C.; Bondar, V.; Nagai, K.; Freeman, B. D.; Yampolskii, Y. P. *Macromolecules* **1999**, *32*, 8427-8440.

CHAPTER 3

SEPARATION WITH TEFLON AF FILMS*[*]

Abstract

Fluorous media have great potential for selective extraction (e.g. as applied to organic synthesis). Fluorous polymer films would have significant advantages in fluorous separations. We investigated poly(2,2-bis(trifluoromethyl)-4,5-difluoro-1,3-dioxide-co-tetrafluoroethylene (Teflon AF 2400, T_g = 240 °C), a stable and permeable fluorous polymer, as a transport/extraction medium for solutes for the first time. Films cast from the polymer solution appear defect-free (SEM; AFM) and do not transport large (MW ~500) polar solutes. Rigid aromatic solutes are transported (from chloroform solution to chloroform receiving phase) in a size dependent manner (log permeability is proportional to -0.0067 times critical volume). Benzene's permeability is about two orders of magnitude higher than in comparable gas phase experiments. The films show selectivity for fluorinated solutes in comparison to the hydrogen-containing control. Transport rates are dependent on the solvent making up the source and receiving phases. The effect of solvent is, interestingly, not due to changes in partition ratio, rather it is due to changes in the solute diffusion coefficient in the film. Solvents plasticize the films. A less volatile compound, -COOH terminated poly(hexafluoropropylene oxide), plasticizes the films (T_g = -40 °C). Permeabilities are decreased in comparison to plasticizer-free films apparently

[*] Part of the information in this chapter has been published on *Journal of the American Chemical Society* **2004**, *126*, 13184-13185

because of decreased diffusivity of solutes. The slope of dependence of log permeability on critical volume is not changed, however.

3.1 INTRODUCTION

Simple partitioning of solutes, with or without the aid of synthetic receptors,[1-8] is of inestimable value in chemistry. Selective partitioning, with solvents and/or synthetic receptors that solvate/bind to specific types of compounds, is particularly reliable. Fluorous liquids are selective solvents for fluorous compounds, a property that is useful in synthesis.[9-16] In practical situations, dimensionally stable solvents, such as supported liquids contained in polymer membranes are beneficial.[17-20] With this in mind, we investigated an amorphous glassy fluorous polymer, Teflon AF, as a transport medium for solutes. Teflon AF is a copolymer of tetrafluoroethylene (TFE) and 2,2-bistrifluoromethyl-4,5-difluoro-1,3-dioxole (PDD) (Fig. 3.1). Two products available are Teflon AF 2400 (87 mol% PDD, T_g 240 ºC, **1**), and Teflon AF 1600 (65% mol PDD, T_g 160 ºC).[21]

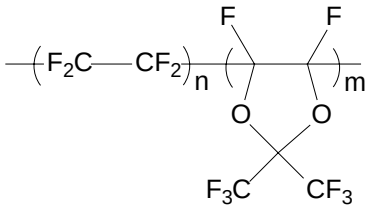

Figure 3.1. Teflon AF

While sharing many significant characteristics of other known teflon polymers, such as chemical inertness and thermal stability, Teflon AF polymers possess some unique properties resulted from the amorphous structure. The polymers have extremely low refractive indices, and have been applied to in liquid core waveguide analysis.[22-24] Teflon AF is highly permeable to low molecular weight gases and has been studied in gas separation[22, 25-27] and pervaporation.[28,29] The polymers are mechanically stiff, and are moderately soluble in some fluorinated solvents at room temperature, thus thin and dimensional stable films can be prepared easily through solvent casting. The film is transparent within a wide UV-Vis and IR range,[21] which enables analysis of the films with these spectroscopic techniques.

Teflon AF 2400 has a large fractional free volume (FFV) of 0.327,[27] which is much larger than most glassy plastics, including other teflon polymers. Transport of gas phase species (penetrants) through Teflon AF films has shown that the films have permeability coefficients for gases that are second only to poly(trimethylsilyl propyne) (PTMSP), a well-known highly permeable polymer.[26, 27] The films demonstrate moderate selectivity to a variety of gases. Studies of sorption[30-33] and diffusion[34-36] of penetrants in Teflon AF films have led to insights into how gases are separated with these films. Permeability of organic vapors increases with the vapor pressure, which suggests possible plasticization of the polymer.[27, 37] High free volume elements on the order of a 5 - 7 Å are found to exist in the polymer as determined by positron annihilation lifetime spectroscopy.[26, 37, 38] A study of penetrant diffusion in Teflon AF 1600 films by NMR showed that the films contained large disordered regions that consist of these high free volume elements.[34, 35] The disordered regions appeared to be interspersed with lower free volume regions, and

the apparent diffusion constants of penetrants showed strong dependence on diffusion time. A recent study by Merkel et al. demonstrated enhancement of permeability for comparatively larger molecules by physically dispersing silica nanoparticles in the Teflon AF polymer films.[39, 40] The reports of pervaporation of organic solvents through these films also showed high permeability of some common organic liquids.[28, 29]

Carboxylic acid terminated poly(hexafluoropropylene oxide) (**2**, Fig. 3.2) has been used as a high-performance lubricant in severe environments, such as aerospace engines and satellite instruments.[41] The excellent lubricity of perfluoropolyether oligomers stems partly from their exceptionally weak intermolecular cohesive force. There are three products commercially available in this series: Krytox FSL (FW 2500), FSM (FW 3500 - 4000), and FSH (FW 7500 - 8000). Krytox FSH (**2**) was used in our study.

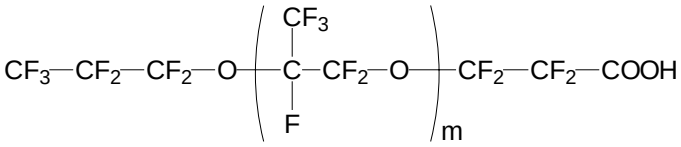

Figure 3.2. Krytox (**2**)

2 has good solubility in fluorous solvents because of the perfluoropolyether backbone. The carboxylic acid terminal makes it also a candidate of receptors soluble in fluorous solvents or polymers. In our premier study of modification of Teflon AF films with fluorous additives, we found that **2** was miscible with the polymer, and plasticized the polymer.[42] The films of **1** doped with **2** were physically softer than films of **1**, like any other plasticized polymers. The **2**-doped films showed quite different transport properties

compared to films of **1**. It is therefore of unique significance to study **2** as a plasticizer of Teflon AF polymers and as a receptor that can be impregnated into the polymer films.

This work is to study the transport of solutes through films of Teflon AF 2400 (**1**), in an effort to explore the potential of this material in selective transport and solid phase extraction. We investigate the factors that could affect the solute permeability through the films. These factors include the characteristics of the solutes (solute size, polarity, and structure), and the solvents (chloroform, methanol, water, 1,1,2-trichlorotrifluoroethane) used in transport. The partitioning equilibria and diffusion kinetics of solutes in the film will be studied, which helps reveal how solvents influence the solute permeability. Films of **1** doped with nonvolatile perfluoropolyether plasticizer **2** are investigated for the first time. Plasticization of the fluoropolymer films by **2** and its effects on transport of solutes will be discussed.

3.2 EXPERIMENTAL SECTION

3.2.1 Reagents

Teflon AF 2400 (**1)** was purchased from Dupont (Wilmington, DE). Krytox 157 FSH (FW 7000 - 7500, **2**) was from Miller-Stephenson Chemical Company Inc (Danbury, CT). FC-72 (perfluorohexanes) was obtained from 3M (Minneapolis, MN). Acid red 37 (**3**) and Reichardt's dye (**4**) were purchased from Aldrich (Milwaukee, WI). 1,1,2-Trifluorotrichloroethane (TCTFE), and spectrophotometric grade chloroform were from Aldrich (Milwaukee, WI). The analytes used in transport experiments, benzene, naphthalene, anthracene, toluene, pyridine, 2-hydroxypyridine, 3-hydroxypyridine,

pyrazine, benzyl alcohol, benzoic acid, α,α,α-trifluorotoluene, pentafluorobenzoic acid were used as received. All aqueous solutions were prepared with deionized water produced from a Milli-Q A10 system, (Millipore, Bedford, MA).

3.2.2 Apparatus

The surfaces and the cross-sections of the films were imaged by scanning electron microscopy FE-SEM (Philips, Model: XL 30 FEG). The topography of the film was imaged by Atomic Force Microscopy (AFM) (Digital Instruments, Model NanoScope IIIa). UV spectra were obtained on an Agilent 8453E spectrophotometer (Palo Alto, CA). Quartz cuvettes with path lengths of 0.1 cm and 1.0 cm were purchased from Starna Cells (Atascadero, CA). IR spectra were obtained on an Excalibur FTS 3000 Spectrometer (DigiLab, Randolph, MA). Transport experiments were carried out on a 15-position stirrer (Cole-Parmer, Chicago, IL equipped with a control of stirring speeds. The homemade glass transport cuvette (1 × 1 × 4 cm) had well-polished walls and a hole of 0.5 cm id on the wall in contact with the film. Film thicknesses were measured by a Starrett micrometer (Athol, MA) with an accuracy of ±1 μm.

3.2.3 Preparation of the films

Films of **1** were cast from a 1 wt% solution of **1** in FC-72. A defined amount of solution was transferred into a glass petri dish that has a flat bottom (7.5 cm i.d.) and a glass cover. The solvent was allowed to evaporate overnight at room temperature, and the formed film was stripped from the petri dish. Soaking the film in water for a short time helped peal off the film more easily. The film was dried in an oven at 110 °C for 2 hours,

and stored in a container at room temperature. The film was cut into small pieces (about 1 × 1 cm) with scissors for transport experiments.

To prepare films doped with the perfluoroether **2**, the dopant was dissolved in FC-72 and mixed with 1% solution of **1** in the desired proportions. The films were formed under the conditions described above, and was pealed off with a scalpel readily without the water-soaking procedure. The film was then left in a vacuum oven for one hour at room temperature. Drying at high temperature was not used because the doped films shrank at elevated temperatures.

3.2.4 Transport of solutes through films

Transport of solutes was conducted on a home-made, three-phase transport device (Fig. 3.3) at room temperature (24 ± 2 ºC).[43] The subject film was sandwiched between two pieces of viton rubber in which holes of a diameter of 0.5 cm (an area of 0.196 cm^2) were cut to define the transport area. The rubber-secured film was then clamped between two transport cuvettes. A multiple position stirrer controlled a small stirring bar in each cuvette at a stirring speed of 300 rpm. The source phase contained 3 mL solute-containing solution at a defined concentration. The receiving phase contained 3 mL solvent at the beginning of the experiments. The solute concentration in the receiving phase was monitored by UV spectrophotometry until steady transport was reached.

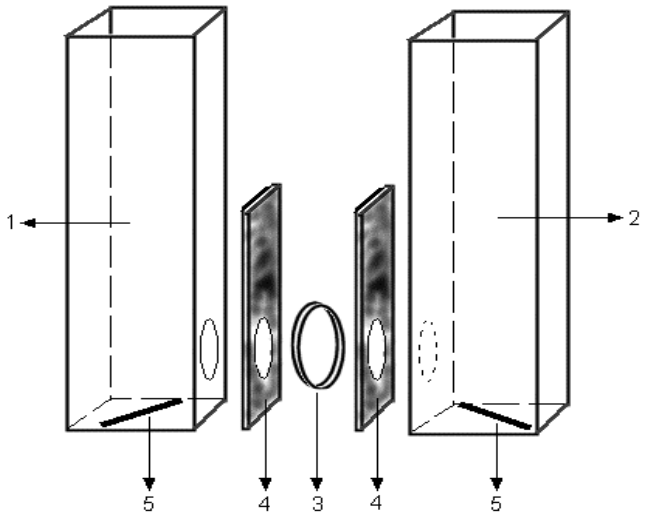

Figure 3.3. Schematic diagram of the transport apparatus.

1, cuvette for the source phase; 2, cuvette for the receiving phase; 3, film; 4, Vition ruber; 5, stirring bars.

The steady-state flux, J, of a solute through the film is obtained from Eq. 3-1.

$$J = (dC_r/dt)(V/A) \quad (\text{mol}\cdot\text{s}^{-1}\cdot\text{cm}^{-2}) \tag{3-1}$$

A is the effective film area, V is the volume of the receiving phase, and dC_r/dt is the accumulation rate of the solute in the receiving phase at steady state. The permeability coefficient, P, is deduced from the flux.

$$P = J\cdot l / (C_s - C_r) \approx J\cdot l / C_{s0} \quad (\text{cm}^2\cdot\text{s}^{-1}) \tag{3-2}$$

Where l is the thickness of the film. C_s and C_r are the concentrations of the solute in the source phase and the receiving phase, respectively. Because C_r is negligible at the beginning period of transport, C_s–C_r is close to the initial concentration of the solute in the source phase, C_{s0}. The permeability coefficient depends on the nature of the solute, the film type, and the temperature.

3.2.5 Determination of diffusion coefficients (*D*) and partition ratios (K_D) of solutes

The experiment was carried out in a similar transport device while a quartz cuvette was employed for the receiving phase in order to obtain continuous UV measurements of the receiving phase. Thick films were used in order to observe the kinetic process till the steady state was reached. The thick film was prepared by firmly stacking multiple thin films (about 20 μm) together after dipping the thin films in a mixture of 4% FC-72 and 96% TCTFE briefly. The film was then washed with dichloromethane and dried at 110 °C in an oven. Films with various thicknesses were chosen according the diffusion speed of a solute. An average thickness of 269 μm was used in determination of the diffusion of benzene in films of **1**, and 100 μm for benzene in **2**-doped films. Thinner films (about 50 μm) were used in determination of the diffusion of 3-hydroxypyridine. Multiple parallel experiments were conducted to minimize the experiment deviation.

In the transport experiment, the concentration of a solute in the receiving phase is recorded according to time. Under the conditions that the membrane is initially at zero concentration and the receiving phase maintains zero concentration during the initial transport period, the accumulation of a substance in the receiving phase can be described by Eq. 3-3.[44]

$$Q_t = C_1 l\left(\frac{Dt}{l^2} - \frac{1}{6} - \frac{2}{\pi^2}\sum_1^{\infty}\frac{(-1)^n}{n^2}\exp(-Dn^2\pi^2 t/l^2)\right) \qquad (3\text{-}3)$$

Q_t denotes the total amount of diffusing substance that has passed through the membrane in time t per membrane area; it has a unit of mol·cm^{-2}. D is the diffusion coefficient of the diffusing substance; l is the membrane thickness; C_1 is the concentration of the diffusing substance at the membrane interface contacting the source phase. This equation is an

infinite series; we decide that "n" in the third term as 10 is enough. For a diffusing substance with a concentration C_s in the source phase, then C_1 can be deduced through the partition equation.

$$C_1 = C_s K_D. \tag{3-4}$$

where K_D is the partition ratio of the substance from the source phase to the membrane. Then the diffusion equation is changed to:

$$Q_t = K_D C_s l\left(\frac{Dt}{l^2} - \frac{1}{6} - \frac{2}{\pi^2}\sum_1^{\infty}\frac{(-1)^n}{n^2}\exp(-Dn^2\pi^2 t/l^2)\right) \tag{3-5}$$

3.2.6 Sorption of solvent in film of 1 measured by FTIR

Saturated chloroform vapor with a pressure of 26.2 kpa (25 °C)[45] was introduced to an IR flow cell (with a 1.0 mm lead spacer, and two 13 mm i.d. KBr windows) by nitrogen gas at a defined flow rate (Fig. 3.4). The IR absorbance of the flow cell was monitored by an FTIR spectrometer until equilibrium was reached. To determine the solvent sorption in film of **1**, a small piece of film (1 cm diameter) with a thickness of 20 μm was placed in the flow cell. The control experiments were carried out under the same conditions without films, which was used to calculate the IR molar absorptivity of chloroform vapor. The net sorption of chloroform in the film was obtained from the difference of the IR absorbance with/without the film. We noticed that the C-Cl vibration shifted from 772 cm^{-1} for the vapor to 768 cm^{-1} for the vapor sorbed in the film, so the IR absorbance was measured at 772 cm^{-1} for vapor and 768 cm^{-1} for films, respectively.

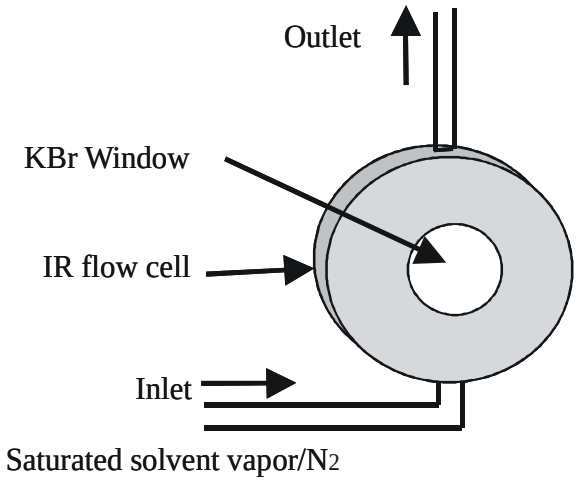

Figure 3.4. The device for measurement of solvent sorption in films.

3.3 RESULTS AND DISCUSSION

3.3.1 Integrity of films and transport apparatus

SEM and AFM were used to image the topography and possible defects of the films. The solution-cast films appear homogeneous both on the film surfaces and through the cross-section. No obvious pinholes or cracks were observed (Fig. 3.5 and Fig. 3.6). AFM measurements were carried out on two types of films: film of **1** and film of **1** doped with 50% **2** (w/w). The films were cast on silicon wafers for a stiff and flat substrate. AFM results showed that the films had highly smooth surface. Within 10 μm range scan, the roughness (RMS) was 0.4 nm for the film of **1**, and 1.1 nm for the doped film. The smooth surface of the films of **1** has enabled applications of Teflon AF polymers in surface polishing,[46] and allows preparation of thin stable films containing minimal defects.

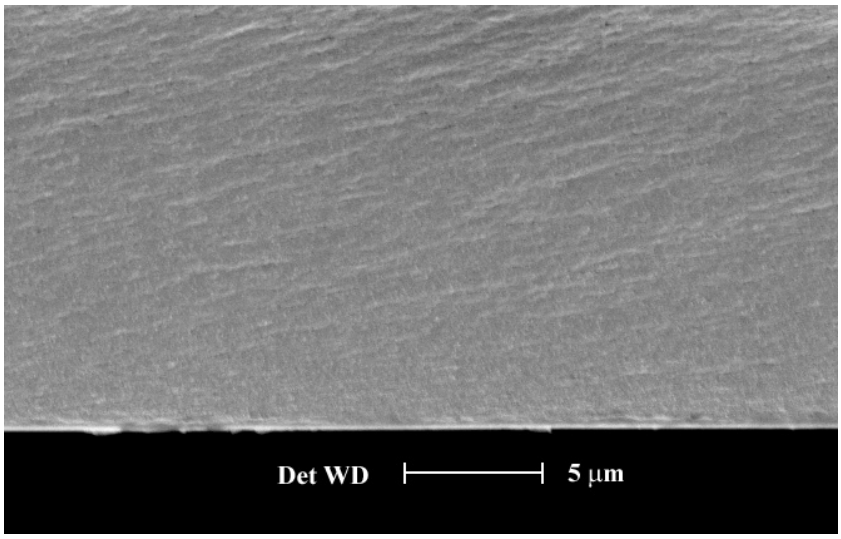

Figure 3.5. SEM image of the cross-section of the film of **1**.

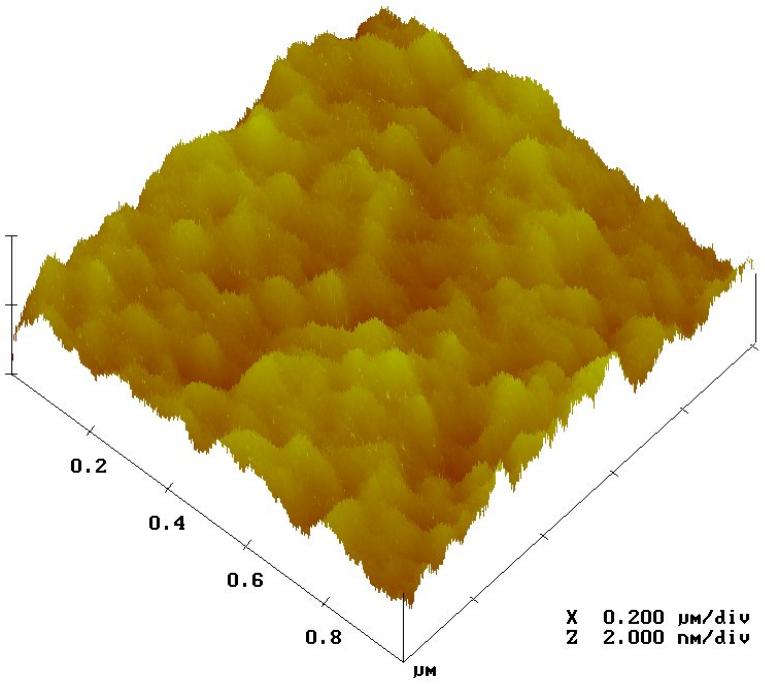

Figure 3.6. AFM image of the surface the film of **1**.

The integrity of the film and the transport apparatus were tested with two dyes that have high molecular weight, high molar absorptivity, but different polarities (Fig. 3.7). An aqueous solution of **3** and a chloroform solution of **4** were used as the source phases, while water or chloroform were employed as the receiving phases, respectively. No measurable absorbance was observed in the receiving phase after three days in repeated experiments. Under the detection sensitivity, the permeability coefficients of is estimated to be no more than 7.3×10^{-11} $cm^2 \cdot s^{-1}$ for **3**, and no more than 1.2×10^{-12} $cm^2 \cdot s^{-1}$ for **4**. This proved that the film did not contain defects that allowed significant passage of somewhat large polar molecules.

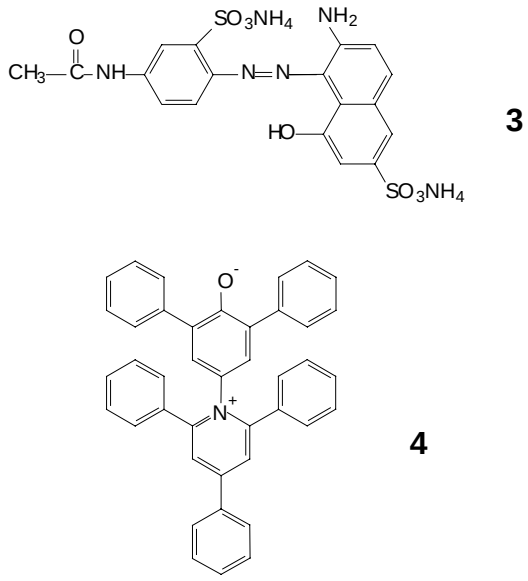

Figure 3.7. Acid red 37 (**3**) and Reichardt's dye (**4**).

For the organic solutes that we have investigated, the relative standard deviations of the measured permeability coefficients are from 10% to 14% within the same batch of films,

and 12% to 25% among different batches of films in over three years study. The films had good long-term stability, and showed no changes in transport properties after months of storage at room temperature.

3.3.2 Dependence of permeability coefficients on film thickness

The permeability coefficients of benzene measured from films of various thicknesses agreed within the variation between different batches of films, indicating that permeability coefficients are independent of the film thickness (Table 3.1, first 3 entries).

Table 3.1. Permeability coefficients of benzene through films of **1** with various thickness

Film thickness (μm)	Film density ($g \cdot mL^{-1}$)	P /(10^{-9} $cm^2 \cdot s^{-1}$)
7.8[a]	1.61 ± 0.10	41
12[a]	1.65 ± 0.06	33
37[a]	1.46 ± 0.03	37
269[b]	/	33

[a]The film density and permeability coefficients are the mean values of duplicate measurements. The errors for film density are standard deviation of the mean. The pooled standard deviation of the permeability coefficients for the first three entries is 4×10^{-9} $cm^2 \cdot s^{-1}$. [b]The films were prepared by stacking multiple thin films (about 20 μm) together; the permeability coefficient is the mean values of seven measurements, with a standard deviation of mean of 6×10^{-9} $cm^2 \cdot s^{-1}$.

The evaporation conditions during film preparation were found to affect the density of the formed films, and result in variation of the film permeability. Compared to thin films, it is more difficult to control the density of thick films with the same preparation procedures. So, the thick films used in kinetic transport experiments were prepared by stacking a number of thin films together. The thickness of thick films prepared in this way was measured and compared with the sum of the thicknesses of the individual films of the stack. Stacks with thicknesses more than 20% different than expected were not used. The quality of the thick films was confirmed by comparing the permeability coefficients of solutes with the values obtained from the thin films. The average permeability coefficient of benzene through the thick films is 3.3×10^{-8} $cm^2 \cdot s^{-1}$, which is close to that through thin films.

3.3.3 Diffusion coefficients (*D*) and partition ratios of solutes (K_D)

Diffusion coefficients can be determined by lag-time method[47] or nonlinear fit of the transport curve.[44] The transport curve records the amount of solute accumulated in the receiving phase versus transport time. The lag time is determined by extrapolating the steady state flux versus time; the point across the x ordinate gives the value of the lag time. The diffusion coefficient is then deduced from the lag time. Compared to the lag time method, the nonlinear fit method produces more precise results by fitting the whole transport curve, therefore the latter one was used in our study. Two typical solutes were studied, a neutral solute, benzene, and a polar solute, 3-hydroxypyridine. Fig. 3.8 shows a transport curve of benzene and the best nonlinear fit. Table 3.2 lists the diffusion coefficients and partition ratios of the two solutes.

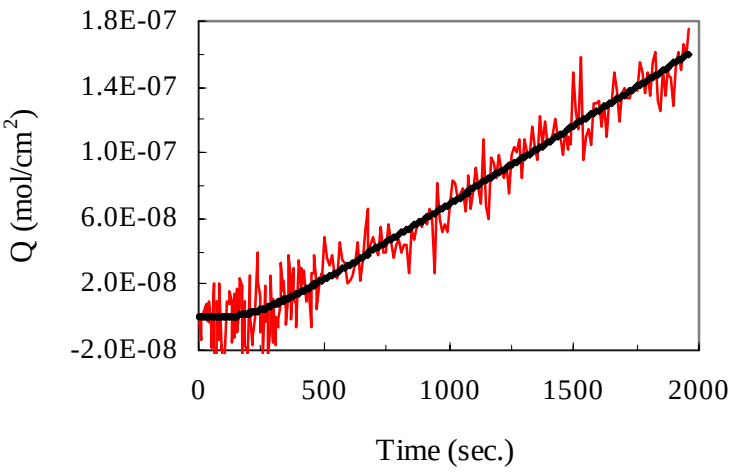

Figure 3.8. Transport curve of benzene and the best fit.

The transport was carried out at 24 ± 2 °C at 300 rpm stirring speed through a film of **1** with a thickness of 277 μm and a transport area of 0.20 cm^2. The source phase contained 0.1 M benzene solution prepared in $CHCl_3$. Red line: transport curve of benzene; thick black line: best fit.

Table 3.2. Diffusion coefficients (D) and partition ratios (K_D) of benzene and 3-hydroxypyridine in films of **1**

Solute	D /($cm^2 \cdot s^{-1}$)	K_D
benzene	$(1.2 \pm 0.3) \times 10^{-6}$	0.04 ± 0.01
3-hydroxypyridine	$(3.3 \pm 0.4) \times 10^{-8}$	0.02 ± 0.003

The listed values are the average of seven measurements. The errors are standard deviation of the mean.

The diffusion coefficient of benzene is determined to be 1.2×10^{-6} $cm^2 \cdot s^{-1}$, and the partition ratio (from $CHCl_3$ to **1**) is 0.040. Benzene vapor has been reported to have a diffusion coefficient of 4.9×10^{-10} $cm^2 \cdot s^{-1}$ in Teflon AF 1600.[48] Benzene liquid in a pervaporation study showed a diffusion coefficient of 4.93×10^{-8} $cm^2 \cdot s^{-1}$ in Teflon AF 1600 film, and 1.9×10^{-7} $cm^2 \cdot s^{-1}$ in Teflon AF 2400 film.[28] The diffusion of gases in Teflon AF 1600 is about a factor of 10 slower than in **1**. Thus, the diffusion coefficient of the solute benzene is remarkably 2 - 3 orders of magnitude larger than that of the gaseous benzene.

Interestingly, the partition ratio of the polar solute, 3-hydroxypyridine, is only slightly smaller that that of benzene. However, the diffusion coefficient of 3-hydroxypyridine is substantially lower than that of benzene. The permeability coefficient of 3-hydroxypyridine is 5.8×10^{-10} $cm^{2\cdot} s^{-1}$, compared to 3.3×10^{-8} $cm^{2\cdot} s^{-1}$ for benzene. Obviously, the difference of permeability of the two solutes mainly arises from the differences in their diffusion coefficients.

3.3.4 Dependence of permeability coefficients on the solute molecular size

Neutral, rigid aromatic solutes were used to investigate the dependence of permeability on the molecular size. There have been reports of the permeability of benzene vapor through Teflon AF 2400 films, therefore the permeability coefficient of benzene obtained in solute transport is converted to the unit of Barrer (10^{-10} $cm^3(STP) \cdot cm \cdot cm^{-2} \cdot s^{-1}$) for comparison. Taking the vapor pressure of benzene at 25 °C (p^0) as 95.25 mmHg,[45] the equilibrium vapor pressure of 0.1 M benzene in chloroform, p, is deduced to be 0.0618 cmHg from Eq. 3-6.

$$p = p^0 x\gamma \quad (3\text{-}6)$$

Where, x is the mole faction of benzene in 0.1 M $CHCl_3$, γ is the activity coefficient, which is estimated to be 0.81 from literature.[49] The permeability coefficient is converted to Barrer according to Eq. 3-7.

$$P = J \cdot l / \Delta p \quad (3\text{-}7)$$

Where, J is the flux of benzene, l is the film thickness, and Δp denotes the difference of the equilibrium pressure between the source phase (the feed pressure) and the receiving phase (the permeate pressure). The value of Δp is close to the feed pressure, p, at the beginning period of permeation when the permeate pressure is very low. The permeability of benzene dissolved in chloroform (3.3×10^{-8} $cm^2 \cdot s^{-1}$) is then transferred to 1.2×10^4 Barrer. This value is about two orders of magnitude higher than that can be extrapolated from gas permeation.[28, 37]

Although films of **1** are highly permeable, the permeability of solutes decreases rapidly as molar volume increases. The permeability coefficient of anthracene was only 1/74 of benzene, indicating a size-sieving character of the film. The critical volume (V_c) is a convenient measure of the size of a molecule. A plot of the permeability coefficients vs. the critical volumes (V_c)[45] of the solutes is shown in Fig. 3.9. Linear regression of *LogP* vs. V_c for these solutes gave a slope of –0.0067, and a correlation coefficient of 0.99.

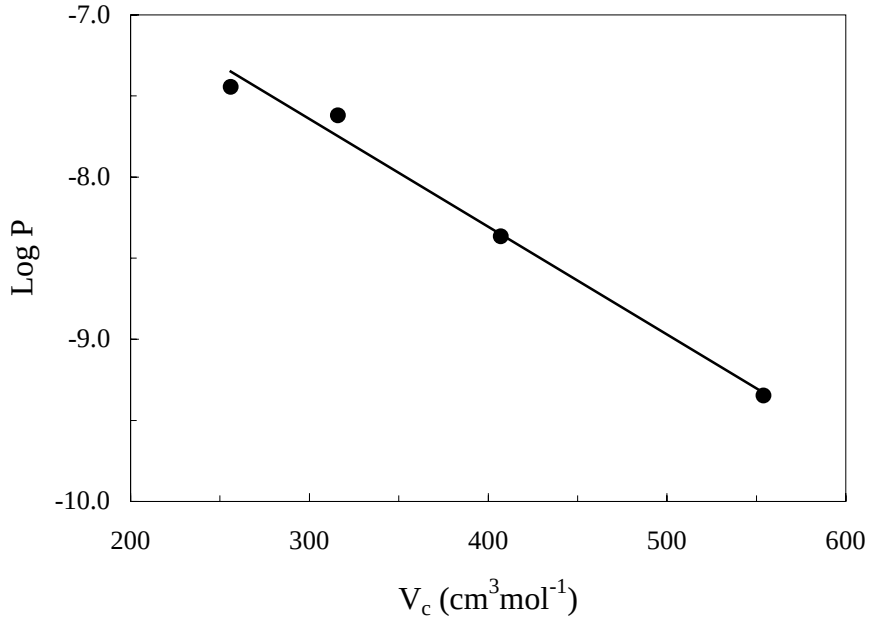

Figure 3.9. Dependence of permeability coefficients ($cm^2 \cdot s^{-1}$) on solute size. The four solutes are benzene, toluene, naphthalene, and anthracene.

This observation is in agreement with other reports about separation of gases through Teflon AF films[27, 32, 37] and pervaporation of organic liquids through these films[28] where high molecular weight gases or organic liquids showed lower permeability than the smaller ones. Polyakov and coworkers published a nice figure to compare the dependence of permeability on molecular size (critical volume) of various polymer films (Fig. 3.10).[28] The slope of -0.0067 we observed from transport of solutes is comparable to that obtained in the pervaporation studies[28] and in gas permeation with film of **1**, while is smaller than those glassy polymers that have strong size-sieving characteristics such as polysufone (PSF), and polycarbonate.[28]

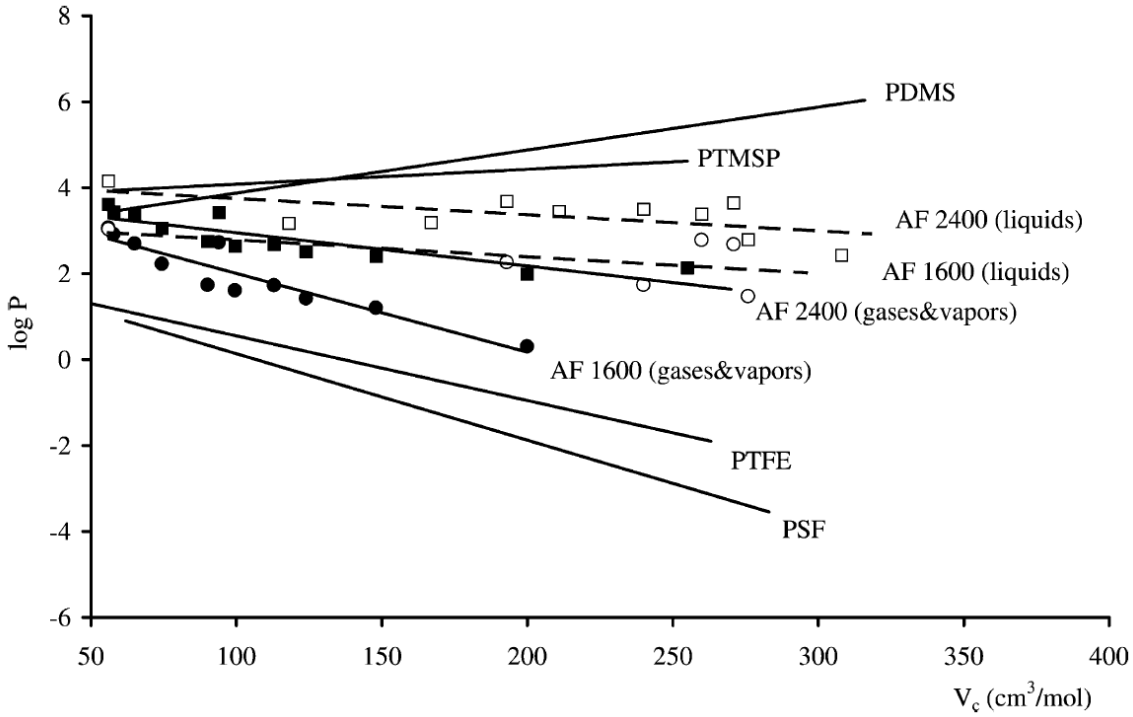

Figure 3.10. Dependence of permeability coefficient *P* (Barrer) on critical volume. (PDMS—40 °C; PTMSP—23 °C; PTFE—25 °C; PSF—23 °C. (Polyakov, 2003)[28]

3.3.5 Dependence of permeability on C_{s_0}

Benzene and pyrazine in chloroform showed constant permeability coefficients regardless the initial concentrations in the source phase (Fig. 3.11).

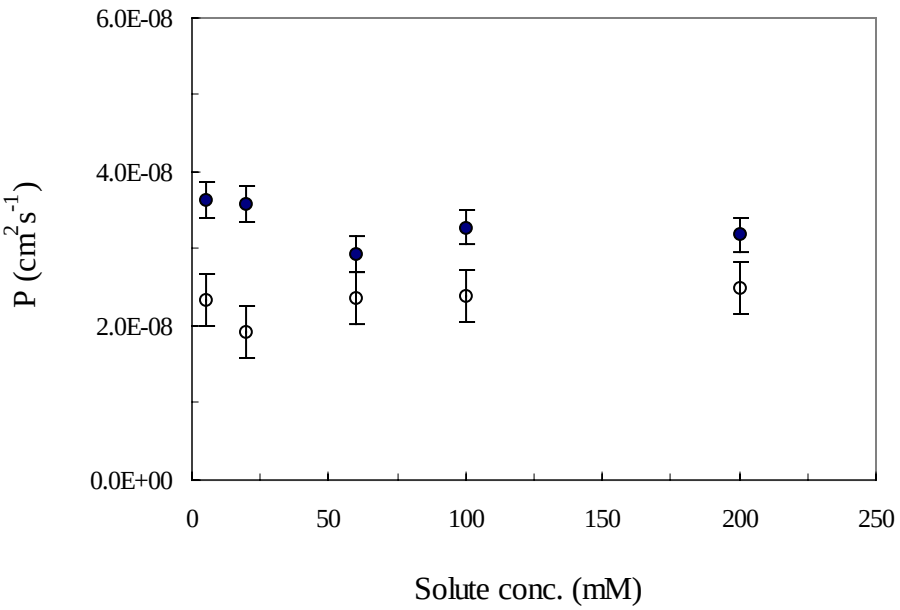

Figure 3.11. Dependence of the permeability coefficients of benzene and pyrazine on the initial concentrations of solutes in the source phase (C_{s0}).

C_{s0} of benzene (•), and pyrazine (o) were 5, 20, 60, 100, and 200 mM. The error bars are from a pooled standard deviation.

The transport characteristics of benzene and pyrazine are consistent with the solution-diffusion transport mode.[50] In this transport mode, the transport process consists of partitioning of a solute from the source phase into the film, diffusion of the solute through the film, and release of the solute to the receiving phase. The permeability coefficient (P) is the product of the diffusion coefficient (D) and the partition ratio of a solute from the source phase to the film (K_D) as shown in Eq. 3-8.[2] In this case, the permeability coefficient is independent of the solute concentration.

$$P = D \cdot K_D \qquad (3\text{-}8)$$

However, solutes such as benzoic acid and pentafluorobenzoic acid showed changes in permeability coefficients with C_{s0}, with higher permeability coefficients at lower C_{s0} (Fig. 3.12).

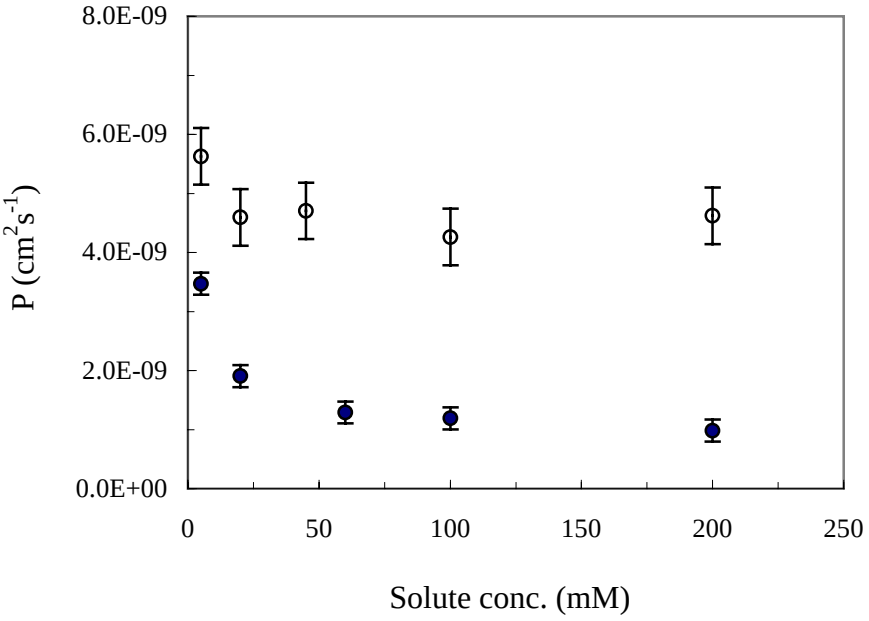

Figure 3.12. Dependence of the permeability coefficients of benzoic acid and pentafluorobenzoic acid on C_{s0}.

The experimental conditions were the same as in Fig. 3.11. Solutes: benzoic acid (•), pentafluorobenzoic acid (o). The error bars are from a pooled standard deviation.

Carboxylic acids are well known to dimerize. Benzoic acid has a dimerization constant of 87 in 1,2-dichloroethane (37 °C),[51] and 516 in benzene (25 °C).[52] Dimerization of carboxylic acids is solvent dependent; higher dimerization constants have been demonstrated in solvents with lower dielectric constants.[53] Considering that the dielectric

constant of chloroform (ε = 4.8) is in between 1,2-dichloroethane (ε = 10.36) and benzene (ε = 2.3),[51] it is reasonable to assume that the dimerization constant of benzoic acid is in the range of 10^2 M^{-1} in chloroform. With this dimerization constant, the monomer fraction in the concentration range of 5 mM to 200 mM changes from about 60% (at 5 mM) to about 15% (at 200 mM). As we have shown, the film of **1** is sensitive to the molecular size of the solutes. The monomer has a much larger permeability than the dimer. Dimerization of benzoic acid leads to a lower concentration of benzoic acid monomer in the source phase, which results in a decreased permeability coefficient.

The dimerization constant of benzoic acid is probably higher in the film than in chloroform, considering the nonpolar nature of the film. However, the partition ratios of solutes from chloroform to the film are generally small, for example, 0.04 for a nonpolar molecule, benzene, and 0.02 for a polar molecule, 3-hydroxypyridine. As a result, the concentration of benzoic acid monomer in the film is small, and the dimerization equilibrium in the film does not likely affect the permeability strongly at that concentration. The correspondence of the concentration range over which the permeability changes and the dissociation constant in $CHCl_3$ supports the notion that the dimerization equilibrium in the solvent has the major effect on the observed permeability changes with concentration. Pentafluorobenzoic acid has a smaller dimerization constant than benzoic acid.[54] We observed that the solute concentration affected the permeability coefficients of pentafluorobenzoic acid to a smaller degree.

The permeability coefficients of 2-hydroxypyridine and 3-hydroxypyridine changed with C_{s0} too (Fig. 3.13, Fig. 3.14), which shows that selfassociation of these solutes affect the

transport. More discussion about the dimerization of 2-hydroxypyridine will be in section 3.3.6

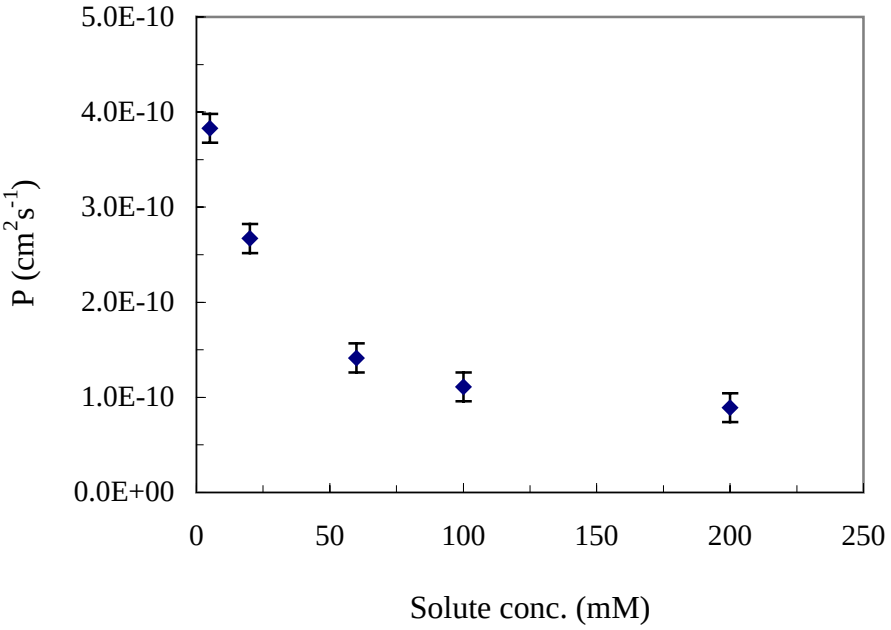

Figure 3.13. Dependence of the permeability coefficients of 2-hydroxypyridine on C_{s0}.

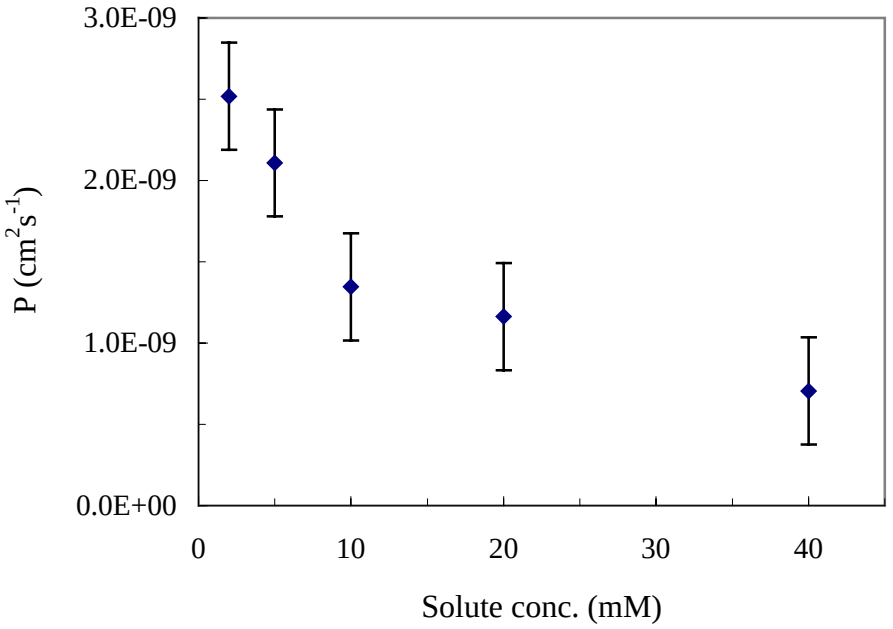

Figure 3.14. Dependence of the permeability coefficients of 3-hydroxypyridine on C_{s0}.

3.3.6 Permeability of fluorinated solutes and polar solutes

The permeability coefficients of fluorinated solutes and polar solutes are shown in Table 3.3. The four neutral aromatic hydrocarbons are included in the table for comparison. For part of the solutes, the permeability coefficients obtained at a lower concentration, 5 mM, are also listed.

Fluorinated solutes showed higher permeability than their nonfluorinated analogs. The permeability coefficient of α,α,α-trifluorotoluene is twice the value of toluene, and the permeability coefficient of pentafluorobenzoic acid is three times the value of benzoic acid. Films of **1** have been reported to have a higher dissolving power for perfluorocarbon gases than their hydrocarbon analogs because of the fluorous nature of

the polymer.[32] For example, the concentration of C_2F_6 sorbed in **1** is reported to be 13% higher than that of C_2H_6 at 15 atm feed pressure. However, because of the larger molecular size, perfluorocarbon gases have significantly lower permeability than the hydrocarbon analogs despite favorable solubility.[32] In contrast, in this work, the permeability coefficients of dissolved fluorinated solutes are still substantially larger than that of the hydrocarbon analogs. Preference of films of **1** for fluorocarbons hints at possible applications in separation of fluorocarbons from hydrocarbons with this type of films.

Table 3.3. Permeability coefficients of solutes through films of **1**

Solutes	Number	P /(10^{-9} $cm^2 \cdot s^{-1}$)[a]	P /(10^{-9} $cm^2 \cdot s^{-1}$)[b]
α,α,α,-trifluorotoluene	1	47[b]	/
benzene	2	33	36
toluene	3	24	/
pyrazine	4	21	23
pyridine	5	14	/
benzyl alcohol	6	6.2	/
pentafluorobenzoic acid	7	4.8	5.6
naphthalene	8	4.3	/
benzoic acid	9	1.5	3.5
3-hydroxypyridine	10	0.58	2.1
anthracene	11	0.45	/
2-hydroxypyridine	12	0.13	0.38

Transport was carried out with solutes in chloroform as the source phase through the film with an effective area of 0.20 cm^2 and a thickness of 9 ± 1 μm at room temperature (24 ± 2 °C). The reported permeability coefficients are the mean values of duplicate measurements. [a]0.1 M solution, [b]0.005 M solution as the source phase. The pooled standard deviation is

The polarity of the solutes was found to influence the permeability. In the group of solutes: benzene, pyridine, and pyrazine that have similar molecular size, the permeability decreased with increased polarity. The same phenomenon was found in the

group of solutes: toluene and benzyl alcohol. The observation agrees with the general view that polar solutes have smaller partition ratios into the Teflon environment thus results in lower permeability.

2-Hydroxypyridine has a remarkably low permeability coefficient considering its molecular size. This is caused by its dimerization. 2-Hydroxypyridine dimerizes and tautomerizes in solvents.[55-57] Keto-monomer (2-pyridone) is more stable than enol-monomer (2-hydroxypyridine) in chloroform, so the dimeric equilibrium is primarily between 2-pyridone and its dimer (Fig. 3.15).[56]

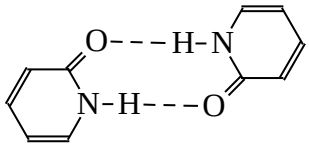

Figure 3.15. 2-Pyridone dimer

The self-association constant of 2-pyridone is large and increases when the polarity of the solvent decreases. Dimerization constants were reported to be 6.5×10^2 M^{-1} in $CHCl_3$, and 2.5×10^4 M^{-1} in CCl_4.[56] The low permeability of 2-pyridone in transport is a result of the low fraction of monomer in the chloroform solution (8.4% in a 0.1 M solution), and the cyclic structure of the dimer. In contrast to benzoic acid discussed in the former section, dimerization of 2-pyridone is stronger and the dimer has a more rigid structure. Self-association of 2-pyridone is likely stronger as well in the film. All these factors lead to a very low permeability coefficient.

3.3.7 Solvent effects on solute transport

Pyrazine was chosen as the model solute to study the solvent effects because it presents satisfactory solubility in solvents with a large range of polarities. Chloroform, methanol, and water influence the transport of pyrazine as shown in Table 3.4. In chloroform, the permeability coefficient was three times larger than that in methanol, and five times larger than that in water.

Table 3.4. Permeability coefficients of pyrazine in different solvents

Solvent	P /(10^{-9} $cm^2 \cdot s^{-1}$)	Ratio
Chloroform	21 ± 0.7	1.0
Methanol	6.6 ± 0.4	0.32
Water	4.1 ± 0.1	0.20

(Transport was carried out through films of **1** with 20 mM pyrazine in each solvent as the source phase while the receiving phase containing the same solvent as the source phase. The errors are standard deviation of mean (n = 2). Other conditions were the same as in Table 3.3. The ratios are the permeability coefficients compared to the value obtained from chloroform.)

The permeability coefficient of pyrazine is the product of the partition ratio and the diffusion coefficient. The effect of solvents on the permeability coefficient can be predicted if we assume that the solvent does not influence the film properties, so the diffusion coefficients of the solute in the film will be identical in all experiments. The only effect of solvents on permeability would then be the difference in partition ratios.

Define the permeability of a solute in the film in the presence of solvent *j* as P_j; similarly, define the partition ratio of a solute from solvent *j* to solvent *k* as $K_{j,k}$. Then we obtain Eq. 3-9.

$$P_{H_2O} / P_{CHCl_3} = K_{H_2O,\,film} / K_{CHCl_3,\,film} = K_{H_2O,CHCl_3} \qquad (3\text{-}9)$$

If solvent does not influence diffusion coefficient of the solute in the film, then the ratio of the permeability coefficients for pyrazine (P_{H_2O}/P_{CHCl_3}) should be comparable to the partition ratio $K_{H_2O,CHCl_3}$. The former is 0.20 from our study, while the latter is 3.9.[58] The two values are clearly not identical. This tells us that the assumption that solvent does not influence the diffusion of the solutes is wrong. Solvents act not only to influence the partitioning, they also likely change the film properties which consequently change the diffusion of solutes.

In an investigation of pervaporation of organic solvents through Teflon AF 2400 films, Polyakov and coworkers found that ten organic solvents with a wide range of polarity showed small difference of solubility in the films (within 2 times), which is substantially smaller than the variation of their permeability coefficients.[28] We have measured the partition ratios of two solutes with very different polarities, benzene and 3-hydroxypyridine, from $CHCl_3$ to films of **1.** The values are remarkably similar, 0.04 and 0.02, respectively. All of this indicates that the changes of the permeability coefficients of pyrazine (solute) in various solvents are primarily caused by the differences in its diffusion coefficient in the film, not from the differences in its partition ratio.

If solvents influence permeability by increasing solute diffusion coefficients, we hypothesized that a cosolvent that was compatible both with the source (and receiving)

phase and the film would have a significant effect. The effect of halogen atoms on solubility has been demonstrated in the pervaporation study through Teflon AF films.[28] The solubility of chlorinated methane increases in the order of CCl_4 > $CHCl_3$ > CH_2Cl_2, with the solubility of CCl_4 showing twice the value of CH_2Cl_2. 1,1,2-trichlorotrifluoroethane (TCTFE) is a good solvent for many fluorinated and nonfluorinated compounds, and is soluble in chloroform (used as a source/receiving phase solvent). A variety of proportions of TCTFE were mixed with chloroform solutions of naphthalene as the source phase. The results (shown in Fig. 3.16) demonstrate that addition of TCTFE in the source phase enhanced the permeability. Fluorinated solvents such as TCTFE probably have higher solubility than non-fluorinated solvents in Teflon AF films, which plasticizes the films and increases the transport of solutes.

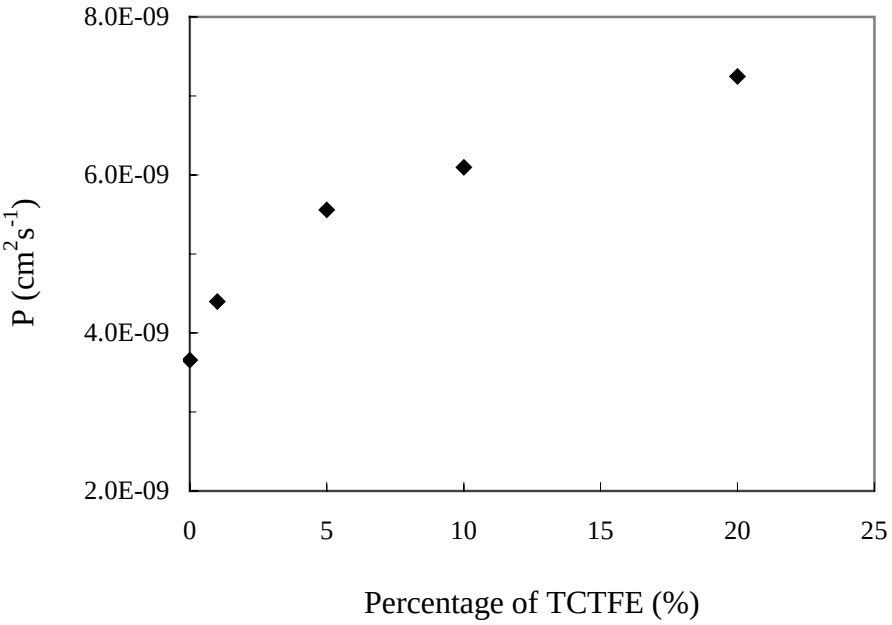

Figure 3.16. Addition of 1,1,2-trichlorotrifluoroethane (TCTFE) to chloroform in the source phase enhanced the permeability of naphthalene.

The percentage of TCTFE mixed with chloroform (*v/v*) in the source phase varied as 0%, 2%, 5%, 10%, and 20%. The receiving phase contained only chloroform.

3.3.8 "Dry" films and "wet" films

By "dry" films, we mean the films that are not in contact with solvents, which is the case in gas permeation. By "wet" films, we mean the films that are exposed to solvent, as the case in transport of solute. To compare the partition ratio for a solute to a "dry" film and to a "wet" film, it is helpful to consider the partition equilibria shown in Fig. 3.17. We will compare measured K_D^{lf} for benzene (solute) to the value of $K_D^{lg}K_D^{gf}$. The latter product is a hypothetical K_D^{lf*} for benzene (solute) to a 'dry' film.

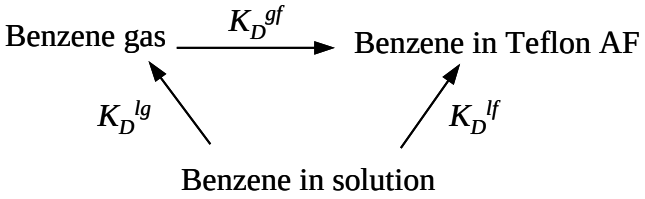

Figure 3.17. Partitioning equilibria

The partition ratio K_D^{gf} is calculated from inverse gas chromatography (benzene vapor sorption into film of **1**) using Eq. 3-10. The net retention volume, V_g, of benzene at room temperature can be extrapolated as 600 $cm^3 \cdot g^{-1}$ from the plot of V_g vs. temperature reported by Bondar et al.[30] The density of the film, ρ_s, is 1.73 $g \cdot cm^{-3}$.[59] The partition ratio from gas phase to the film (K_D^{gf}) is then deduced to be 1038 from Eq. 3-10.

$$K_D^{gf} = V_g \cdot \rho_s \qquad (3\text{-}10)$$

The concentration of benzene vapor equilibrated with 0.1 M benzene solution is deduced to be 3.32×10^{-5} M (Eq. 3-11) at 298 K.

$$C^g = p / (RT) \qquad (3\text{-}11)$$

With known C^g and C^l, the partition ratio of benzene from 0.1 M chloroform solution to gas phase (K_D^{lg}) is obtained to be 3.32×10^{-4} through Eq. 3-12.

$$K_D^{lg} = C^g / C^l \qquad (3\text{-}12)$$

The partition ratio of benzene from chloroform solution to the *chloroform-free* Teflon AF film, K_D^{lf*} is then calculated to be 0.34. This value is about eight times larger than K_D^{lf} we measured, which is only 0.04. The difference of K_D^{lf*} and K_D^{lf} suggests that the "wet" films used in transport of solutes are different from the "dry" films used in gas

permeation. The “wet” films present unique properties due to in contact with the solvent. It would be helpful to measure the solvent uptake in the films and evaluate the impact of the sorbed solvents on the films.

3.3.9 Sorption of chloroform in films of 1

Uptake of solvents in films is often obtained by soaking a film in solvents and then monitoring the weight increase of the film.[28, 60] Having concerns that the volatility of the organic solvents might affect the measurement, we developed an IR method to determine the film saturated by the solvent vapor. Fig. 3.18 shows an example of IR absorbance of the film following sorption of chloroform vapor. The equilibrium concentration of chloroform in the film was measured to be 7.9 ± 0.2 g/100 g polymer (1.13 M, SEM, n = 5), which is close to the value reported in a pervaporation study measured by the weighing method 9.11 g/100 g polymer.[28]

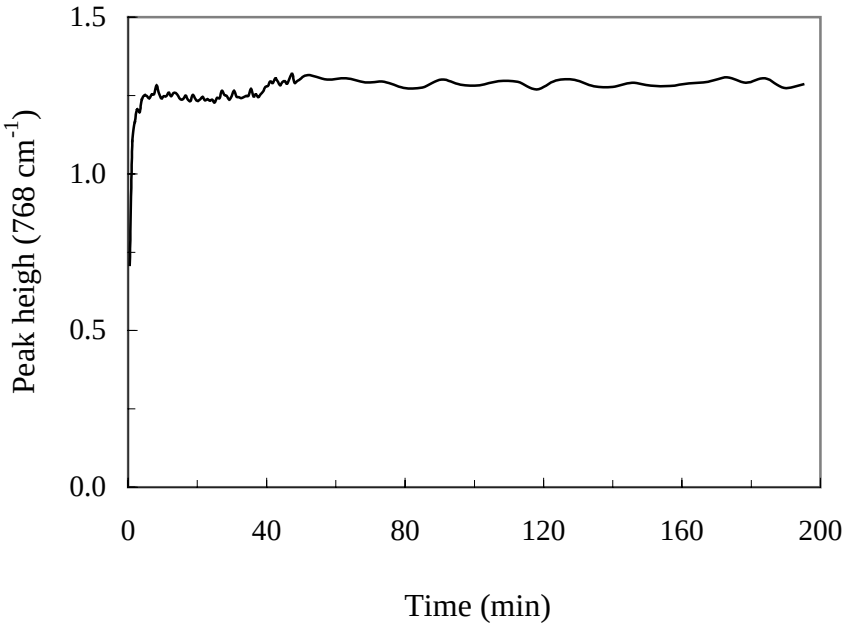

Figure 3.18. Sorption of chloroform in films of **1** monitored by FTIR.

Thick solid line, with film of **1** in the IR flow cell; thin solid line, control (without film).

The C-H stretch is known to be solvatochromic.[61] Interestingly, the IR spectra of chloroform as gas vapor, as liquid, as a solute in FC-72 and in film **1** show marked differences (Fig. 3.19, and Table 3.5). The spectroscopic evidence demonstrates that chloroform is not in an environment like bulk chloroform, neither is it in an environment like a fluorous solvent.

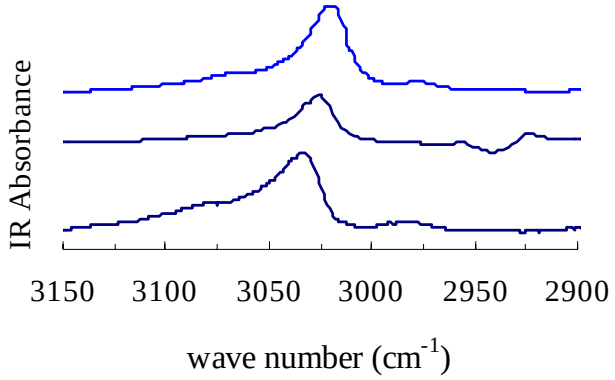

Figure 3.19. IR spectra (absorbance) of chloroform in solution and in the film of **1**. From top to bottom: pure chloroform liquid; chloroform sorbed in the film; 1% chloroform in FC-72. Spectrophotometric grade chloroform liquid was measured by placing a drop of liquid between two NaCl plates. The solution of 1% chloroform diluted in FC-72 was measured in an IR flow cell with a 1.0 mm spacer.

Table 3.5. Vibrational frequencies of $CHCl_3$

Chloroform	ν (cm-1)
gas	3034 [61]
liquid	3020
1% solution in FC-72	3034
in **1**	3025

The surprisingly strong sorption of solvents in Teflon AF films is consistent with the dual sorption model describing the gas behavior in Teflon AF,[30, 32] in which **1** was demonstrated to have high Langmuir sorption capacity and large Henry constants compared to other glassy polymers. The Langmuir sorption capacity represents saturated

partitioning into voids, while the Henry constant represents dissolving in the polymer matrix. We conclude that, because the film sorbs solvent, it becomes more organic-like, though the solvent is not identical to the bulk solvent. Extrapolating published data[30] for small gases leads to estimates of Henry's constant and Langmuir sorption for $CHCl_3$. They predict that, of the sorbed $CHCl_3$ from exposure of **1** to saturated vapor or pure liquid, about 40% is dissolved while 60% is sorbed into the free volume. Sorption of solvents decreases the K_D of benzene (solute) compared to benzene vapor because the large free volume, which is void space for benzene vapor, is chloroform-filled. At the same time, partitioning of chloroform into the film matrix (Henry's Law) plasticizes the film, dramatically increasing the diffusion coefficient of benzene solute vs. benzene vapor.

3.3.10 Transport through films of 1 doped with perfluoroether 2

The apparent plasticization of the films by organic solvents is interesting, and leads to very large increases in solute diffusivity. It would be significant if the film could be plasticized with fluorous additives which might help maintain the fluorous nature of the film while providing better control of the solute diffusion and solubility that affect the film selectivity.[43, 62] Poly(hexafluoropropylene oxide) terminated with a carboxylic acid (**2**) was found to be miscible with **1** at any proportion. It is known that **2** has an IR absorbance at 1775 cm^{-1} from the C=O stretch of the carboxylic acid dimer.[63] Films of **1** doped with various percentages of **2** showed the expected absorption peak around 1774 cm^{-1} (Fig. 3.20). We did not see any IR evidence for the dissociation of the carboxylic acid dimer into the monomer.

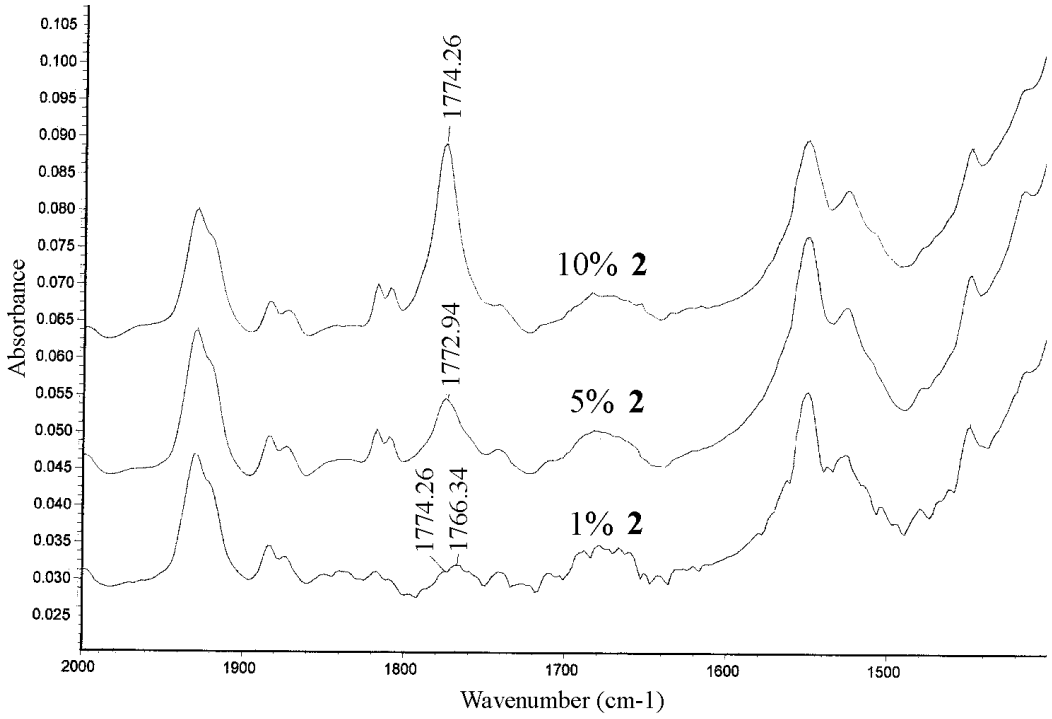

Figure 3.20. IR spectra of films of **1** doped with varied percentages of **2** (*w/w*)

It was found that **2** plasticized films of **1**. The glass transition temperature, T_g, of **1** doped with 50% **2** (w/w) was measured to be –40 °C, compared to 240 °C for film of **1**. The solute permeability coefficients in **2**-doped films are shown in Table 3.6. For comparison with films of **1**, the ratios of the permeability coefficients in the two types of films (P_1/P_2) are also presented.

Table 3.6. Permeability coefficients of solutes through films of **1** doped with 50% **2** (w/w)

Analyte	P_2 /(10^{-9} $cm^2 \cdot s^{-1}$)[a]	P_1/P_2[b]
α,α,α-trifluorotoluene	6.0	7.7
benzene	3.5	9.7
toluene	2.5	9.7
pyrazine	1.7	12
pyridine	1.4	9.8
benzyl alcohol	0.74	8.4
pentafluorobenzoic acid	0.45	11
naphthalene	0.33	13
benzoic acid	0.10	15
3-hydroxypyridine	0.12	4.7
anthracene	0.043	10
2-hydroxypyridine	0.016	7.8

[a]The experimental conditions were the same as that in Table 3.3, except replacing films of **1** with the doped films. The permeability coefficients are the mean values of duplicate experiments. [b]P_1/P_2 is the ratio of average permeability coefficients in the film of **1** to that in the doped film.

The permeability of benzene in the **2**-doped film is still considerably larger than its permeability as a gas-phase penetrant. However its permeability, and the permeabilities of other solutes, are lower than the permeabilities in the absence of **2**. The average ratio of the permeability coefficients in the two types of films (P_1/P_2) is about 10.

Interestingly, the linear correlation of log *P* and the critical volume of the four neutral aromatic solutes holds, giving a slope of –0.0066 and a correlation coefficient of 0.98. This slope is essentially the same as the value of –0.0067 for films of **1**, which shows that the plasticized film is sensitive to the critical volume of the solutes to the same degree as films of **1**.

There are two possible reasons for reduced permeation, namely, decreased partitioning of solutes from the solvent into the film, and decreased diffusion of solutes in the film. Table 3.7 lists the partition ratios and the diffusion coefficients of benzene in the two types of film. The partition ratio of benzene in the **2**-doped film is not significantly smaller than that in the film of **1**. On the other hand, the diffusion coefficient decreases about a factor of 10 in the doped film, changing from 1.2×10^{-6} $cm^2 \cdot s^{-1}$ in the film of **1** to 9.5×10^{-8} $cm^2 \cdot s^{-1}$ in the **2**-doped film.

Table 3.7. Partition ratios (K_D) and the diffusion coefficients (D) of benzene in the film of **1** and the **2**-doped film

Film	K_D	D ($cm^2 \cdot s^{-1}$)
Film of **1**	0.04 ± 0.01	$(1.2 \pm 0.3) \times 10^{-6}$
Doped film	0.03 ± 0.003	$(9.5 \pm 0.8) \times 10^{-8}$

The reported values are the average and the standard deviation of the mean from seven measurements for film of **1**, and from three measurements for the **2**-doped film (50% **1**-50% **2**, *w/w*).

The plasticized film showed similar selectivity for fluorinated solutes as the film of **1**. The permeability coefficient of α,α,α-trifluorotoluene is 2.4 times the value of toluene, and the permeability coefficient of pentafluorobenzoic acid is 4.5 times the value of benzoic acid in the plasticized film. These values are 2.0, and 3.2, respectively for the films of **1**. The fluorous plasticizer **2** seems to increase the selectivity of film to fluorinated solutes slightly. This is very encouraging. It hints the possibility of using proper fluorous plasticizers smaller than **2** in modification of the films of **1** for selective transport of fluorinated compounds while maintaining satisfactory permeability.

The permeability coefficient ratio, P_1/P_2, of the solutes that consist of hydrogen bond groups showed deviation from the average value of 10. Particularly, 3-hydroxypyridine and 2-hydroxypyridine showed an "enhanced" transport in the plasticized film compared to the neutral solutes. Both UV-Vis and IR spectra demonstrated hydrogen bonding between the hydroxypyridines with **2**. Fig. 3.21 shows the IR spectra of films doped with 50% **2** after transport of solutes. Compared to the film control and the films used in transport of a neutral solute, naphthalene, for the films used in transport of 2-hydroxypyridine and 3-hydroxypyridine, the acid dimer bond disappeared; meanwhile new vibration bands appeared in the range of 1500 – 1700 cm^{-1}. These vibration bands were not observed in the pure Teflon AF films after transport of these two solutes. Evidences from IR spectra indicate than intermolecular associations between the two hydroxypyridines and **2** occur in the plasticized film.

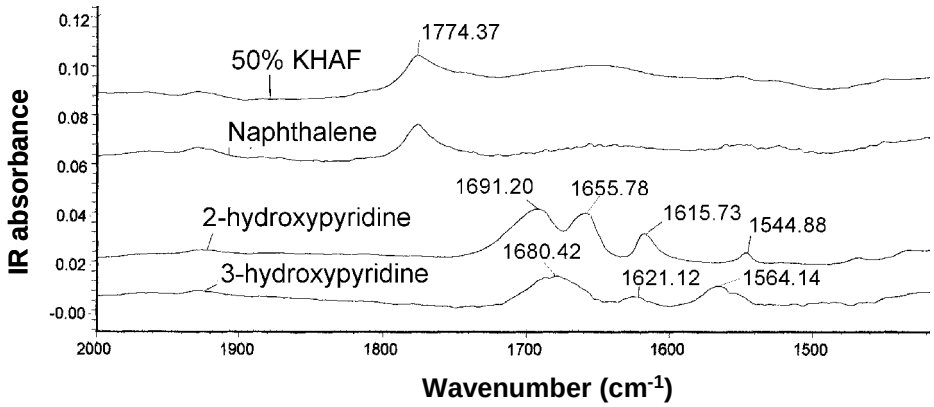

Figure 3.21. IR absorption spectra of films of **1** doped with 50% **2** after transport of solutes

We measured the distribution coefficient of 3-hydroxypyridine from chloroform to the films doped with 50% **2** (about 0.13 M **2**). The distribution coefficient increased remarkably to a value of 1.8 ± 0.2 (SEM, n = 3), compared to 0.02 in pure film **1**. Although the diffusion coefficients of 3-hydroxypyridine decreased significantly in the plasticized film ((8.9 ± 2.0) × 10^{-11} cm^2s^{-1}, compared to 3.3 ×10^{-8} cm^2s^{-1} in pure film **1**), the permeability coefficients only decreased 4.7 times as a result of the interactions with **2**. The smaller enhancement of transport of 2-hydroxypyridine compared to 3-hydroxypyridine is probably caused by the strong dimerization of 2-hydroxypyridine. Dimerization of 2-hydroxypyridine could compete with the interactions with **2**, and weaken the association with the receptor. The hydrogen bond interactions of 3-hydroxypyridne with fluorous carboxylic acid is discussed in detail in Chapter 2.

3.4 CONCLUSION

We have studied the transport of a series of solutes with different polarity and functional groups through Teflon AF 2400 films (**1**) and the fluorous films doped with a perfluoropolyether plasticizer (**2**). The films showed selectivity according to the solute size, polarity, and are in favor of the transport of fluorinated solutes in comparison to the hydrogen-containing control. Transport rates are dependent on the solvent making up the source and receiving phases, which plasticizes the film and consequently changes the diffusion of solutes in the film dramatically. Nonvolatile fluorous plasticizers, -COOH terminated poly(hexafluoropropylene oxide) (**2**) strongly plasticizes the films. Permeabilities are decreased in comparison to **2**-free films. Complexation of **2** with 2-hydroxypyridine and 3-hydroxypyridine in the fluorous polymer has been observed for the first time.

We speculate that the occupation of free volume by **2** significantly alters the diffusion of small molecules even as it increases the polymer chain mobility. We are led to this conclusion from considering that our work, and other studies of solute dynamics[19,28-30,32] in the films are consistent with the idea that diffusion takes place by solute moving from one region of free volume to another. Plasticization by low molecular weight solvents enhances solute diffusion even as it occupies free volume because the solvent molecules themselves are diffusing rapidly. When plasticization is by polymeric **2** however, the free volume is lowered while the environment within the free volume becomes viscous in comparison to solvent-saturated films, although the environment becomes less restricted than that of dry films. Plasticization of Teflon AF polymers by fluorous plasticizers leads to the envision that proper nonvolatile fluorous solvents can be introduced into the films

in a similar manner as that in organic polymer membranes, and can increase the control of the film selectivity and transport rates.

3.5 REFERENCES

(1) Chang, S. K.; Van Engen, D.; Fan, E.; Hamilton, A. D. *Journal of the American Chemical Society* **1991**, *113*, 7640-7645.

(2) Visser, H. C.; Reinhoudt, D. N.; de Jong, F. *Chemical Society Reviews* **1994**, *23*, 75-81.

(3) Valenta, J. N.; Dixon, R. P.; Hamilton, A. D.; Weber, S. G. *Analytical Chemistry* **1994**, *66*, 2397-2403.

(4) Valenta, J. N.; Weber, S. G. *Journal of Chromatography, A* **1996**, *722*, 47-57.

(5) Rebek, J., Jr. *Chemical Communications (Cambridge)* **2000**, 637-643.

(6) Ghaddar, T. H.; Castner, E. W.; Isied, S. S. *Journal of the American Chemical Society* **2000**, *122*, 1233-1234.

(7) Chou, H.-C.; Hsu, C.-H.; Cheng, Y.-M.; Cheng, C.-C.; Liu, H.-W.; Pu, S.-C.; Chou, P.-T. *Journal of the American Chemical Society* **2004**, *126*, 1650-1651.

(8) Goswami, S.; Ghosh, K.; Dasgupta, S. *Tetrahedron* **1996**, *52*, 12223-12232.

(9) Horvath, I. T.; Rabai, J. *Science* **1994**, *266*, 72-75.

(10) Horvath, I. T. K., Gabor; Cook, Raymond A.; Bond, Jeffrey E.; Stevens, Paul A.; Rabai, Jozsef; Mozeleski, Edmund J. *Journal of the American Chemical Society* **1998**, *120*, 3133-3143.

(11) Studer, A.; Hadida, S.; Ferritto, R.; Kim, S.-Y.; Jeger, P.; Wipf, P.; Curran, D. P. *Science* **1997**, *275*, 823-826.

(12) Luo, Z.; Zhang, Q.; Oderaotoshi, Y.; Curran, D. P. *Science* **2001**, *291*, 1766-1769.

(13) Gladysz, J. A.; Curran, D. P. *Tetrahedron* **2002**, *58*, 3823-3825.

(14) Gladysz, J. A., Curran, Dennis P., Horvath, Istvan T. *Handbook of Fluorous Chemistry*; Wiley-VCH: Weinheim, 2004.

(15) Curran, D. P.; Luo, Z. *Journal of the American Chemical Society* **1999**, *121*, 9069-9072.

(16) Palomo, C.; Aizpurua, J. M.; Loinaz, I.; Fernandez-Berridi, M. J.; Irusta, L. *Organic Letters* **2001**, *3*, 2361 -2364.

(17) Bartsch, R. A.; Way, J. D. *Chemical separations with liquid membranes*; Washington, DC : American Chemical Society, 1996.

(18) Li, S.; Sun, L.; Chung, Y.; Weber, S. G. *Analytical Chemistry* **1999**, *71*, 2146-2151.

(19) Paugam, M.-F.; Bien, J. T.; Smith, B. D.; Chrisstoffels, L. A. J.; de Jong, F.; Reinhoudt, D. N. *Journal of the American Chemical Society* **1996**, *118*, 9820-9825.

(20) Zhang, X.; Zhao, H.; Weber, S. G. *Analytical Chemistry* **2002**, *74*, 2184-2189.

(21) Buck, W. H., Resnick, P. R., 183rd Meeting of the Electrochemcial Socienty, Honolulu, HI, USA 1993.

(22) Dasgupta, P. K.; Genfa, Z.; Poruthoor, S. K.; Caldwell, S.; Dong, S.; Liu, S.-Y. *Analytical Chemistry* **1998**, *70*, 4661-4669.

(23) Waterbury, R. D.; Yao, W.; Byrne, R. H. *Analytica Chimica Acta* **1997**, *357*, 99-102.

(24) Liu, Z.; Pawliszyn, J. *Analytical Chemistry* **2003**, *75*, 4887-4894.

(25) Nemser, S. M.; Du Pont Canada Inc.: US5051113, 1991.

(26) Alentiev, A. Y.; Yampolskii, Y. P.; Shantarovich, V. P.; Nemser, S. M.; Plate, N. A. *Journal of Membrane Science* **1997**, *126*, 123-132.

(27) Pinnau, I.; Toy, L. G. *Journal of Membrane Science* **1996**, *109*, 125-133.

(28) Polyakov, A. M.; Starannikova, L. E.; Yampolskii, Y. P. *Journal of Membrane Science* **2003**, *216*, 241-256.

(29) Polyakov, A. M.; Starannikova, L. E.; Yampolskii, Y. P. *Journal of Membrane Science* **2004**, *238*, 21-32.

(30) Bondar, V. I.; Freeman, B. D.; Yampolskii, Y. P. *Macromolecules* **1999**, *32*, 6163-6171.

(31) Merkel, T. C.; Bondar, V.; Nagai, K.; Freeman, B. D. *Macromolecules* **1999**, *32*, 370-374.

(32) Merkel, T. C.; Bondar, V.; Nagai, K.; Freeman, B. D.; Yampolskii, Y. P. *Macromolecules* **1999**, *32*, 8427-8440.

(33) De Angelis, M. G.; Merkel, T. C.; Bondar, V. I.; Freeman, B. D.; Doghieri, F.; Sarti, G. C. *Macromolecules* **2002**, *35*, 1276-1288.

(34) Meresi, G.; Wang, Y.; Cardoza, J.; Wen, W. Y.; Jones, A. A.; Gosselin, J.; Azar, D.; Inglefield, P. T. *Macromolecules* **2001**, *34*, 4852-4856.

(35) Meresi, G.; Wang, Y.; Cardoza, J.; Wen, W. Y.; Jones, A. A.; Inglefield, P. T. *Macromolecules* **2001**, *34*, 1131-1133.

(36) Wang, Y.; Inglefield, P. T.; Jones, A. A. *Polymer* **2002**, *43*, 1867-1872.

(37) Alentiev, A. Y.; Shantarovich, V. P.; Merkel, T. C.; Bondar, V. I.; Freeman, B. D.; Yampolskii, Y. P. *Macromolecules* **2002**, *35*, 9513-9522.

(38) Davies, W. J.; Pethrick, R. A. *Eur. Polym. J.* **1994**, *30*, 1289-1293.

(39) Merkel, T. C.; He, Z.; Pinnau, I.; Freeman, B. D.; Meakin, P.; Hill, A. J. *Macromolecules* **2003**, *36*, 8406-8414.

(40) Merkel, T. C.; Freeman, B. D.; Spontak, R. J.; He, Z.; Pinnau, I.; Meakin, P.; Hill, A. J. *Science* **2002**, *296*, 519-522.

(41) Kasai, P. H. *Macromolecules* **1992**, *25*, 6791-6799.

(42) Zhao, H.; Ismail, K.; Weber, S. G. *Journal of the American Chemical Society* **2004**, *126*, 13184-13185.

(43) Zhang, X.; Zhao, H.; Chen, Z.; Nims, R.; Weber, S. G. *Analytical Chemistry* **2003**, *75*, 4257-4264.

(44) Crank, J. *The Mathematics of diffusion*; Oxford University Press: New York, 2001.

(45) Lide, D. R. *CRC Handbook of Chemistry and Physics*; CRC Press: Boca Raton, NY, 1998.

(46) Leistner, A. J. *Applied Optics* **1993**, *32*, 3416-3424.

(47) Koval, C. A.; Spontarelli, T.; Thoen, P.; Noble, R. D. *Industrial & Engineering Chemistry Research* **1992**, *31*, 1116-1122.

(48) Podgorsek, R. P.; Sterkenburgh, T.; Wolters, J.; Ehrenreich, T.; Nischwitz, S.; Franke, H. *Sensors and Actuators, B: Chemical* **1997**, *B39*, 349-352.

(49) Kojima, K.; Tochigi, K.; Kurihara, K.; Nakamichi, M. *J. Chem. Eng. Data* **1991**, *36*, 343-345.

(50) Wijmans, J. G.; Baker, R. W. *Journal of Membrane Science* **1995**, *107*, 1-21.

(51) Coetzee, J. F.; Lok, R. M.-S. *Journal of Physical Chemistry* **1965**, *69*, 2690-2696.

(52) Barela, R.; Liwski, G.; Szatylowicz, H. *Fluid Phase Equilibria* **1995**, *105*, 119-127.

(53) Williams, D. H.; Gale, T. F.; Bardsley, B. *Journal of the Chemical Society, Perkin Transactions 2: Physical Organic Chemistry* **1999**, 1331-1334.

(54) Zhukova, V. A.; Tarasova, L. I.; Sheikh-Zade, M. I. *Teoreticheskaya i Eksperimental'naya Khimiya* **1978**, *14*, 396-398.

(55) Beak, P. *Accounts of Chemical Research* **1977**, *10*, 186-192.

(56) Takasuka, M.; Saito, T.; Nakai, H. *Vibrational Spectroscopy* **1996**, *13*, 65-74.

(57) Chou, P.-T.; Wei, C.-Y.; Hung, F.-T. *Journal of Physical Chemistry B* **1997**, *101*, 9119-9126.

(58) Abraham, M. H.; Platts, J. A.; Hersey, A.; Leo, A. J.; Taft, R. W. *Journal of Pharmaceutical Sciences* **1999**, *88*, 670-679.

(59) Aleksan, R.; Amadon, A.; Besson, P.; Bourgeois, P.; Le Meur, J.; Robert, J. P. *Nuclear Instruments & Methods in Physics Research, Section A: Accelerators, Spectrometers, Detectors, and Associated Equipment* **1996**, *371*, 578-579.

(60) Walsby, N.; Sundholm, F.; Kallio, T.; Sundholm, G. *Journal of Polymer Science, Part A: Polymer Chemistry* **2001**, *39*, 3008-3017.

(61) Devaure, J.; Turrell, G.; Pham Van, H.; Lascombe, J. *Journal de Chimie Physique et de Physico-Chimie Biologique* **1968**, *65*, 1064-1071.

(62) Lysander, A. J.; Chrisstoffels, F. J.; Reihoudt, D. N. In *Chemical separations with liquid membranes*; Way, J. D., Ed.; American Chemical Society: Washington, DC, 1996, pp 18-56.

(63) Doan, V.; Koeppe, R.; Kasai, P. H. *Journal of the American Chemical Society* **1997**, *119*, 9810-9815.

CHAPTER 4

DETERMINATION OF BARBITURATES BY CZE AND MEKC WITH ON-LINE CONCENTRATION

Abstract

Sample stacking techniques in capillary zone electrophoresis (CZE) and micellar electrokinetic chromatography (MEKC) have gained increasing popularity for improvement of CE sensitivity. We first investigated the optimal stacking conditions of four barbitals with CZE in which Tris-TAPSO buffer (pH 8.0) was utilized as the separation buffer. MEKC was applied for a more complicated sample mixture of eight barbiturate drugs and analogs. The separation was conducted in the same Tris-TAPSO buffer containing 24 mM SDS under. Under the MEKC separation conditions, sample stacking was best when dissolving the drug mixture in a high pH solution (20 mM NaOH solution, pH 12.10). Investigations have shown that the high pH sample solution is essential for stacking by ionizing the analytes, thus decreasing their affinity for the SDS micelles. Consequently, stacking similar to that in CZE can be achieved for all the investigated analytes with a wide distribution of retention factors (0.1- 2.5), while without any effects on the separation. Both normal stacking mode and transient ITP stacking mechanism are involved, depending on the sample matrix. Besides sample buffer pH, the conductivity of the sample matrix, SDS concentration, and injection time are optimized. This method has been applied to analysis of spiked serum samples

following a solid phase microextraction (SPME) pretreatment. The SPME procedures include a forward extraction with a plasticized PVC film and a back-extraction with 20 mM NaOH solution.

4.1 INTRODUCTION

Capillary Electrophoresis (CE) has developed to a powerful separation and analysis technique. However, the low concentration sensitivity with on-line photometric detection has been a disadvantage due to the small optical path length of the CE capillaries. The minimum detectable concentration without preconcentration lies in the micromolar range for good absorbers.[1] Some detection techniques suffer less from this problem because of better detection sensitivity, such as laser induced fluorescence,[2, 3, 4] electrochemical detection,[5, 6] and mass spectrometric detection.[7, 8]

Higher detection sensitivity can be achieved with sample stacking, in which a large volume of sample is injected without sacrificing the separation efficiency. In the normal stacking mode in capillary zone electrophoresis (CZE), the sample is prepared in a solvent that has a lower conductivity than the run buffer.[9] When a voltage is applied across the capillary, a greater field is developed across the sample plug, which causes the sample ions to move faster within the sample plug than in the CE run buffer. Analytes become stacked as narrow zones at the interfaces of the sample plug and the run buffer.

Micellar electrokinetic chromatography (MEKC) has the ability to separate electrically neutral species.[10-14] Separation is based on the different affinities of the neutral compounds for the charged micelles in the run buffer that work as a pseudostationary phase. Stacking in MEKC is different from that in CZE, because neutral analytes do not

respond to the electric field. Neutral compounds are stacked through association with the charged micelles and migrate as analyte-micelle complexes. Nice reviews have been published about stacking/sweeping in MEKC.[12,15-18] Among all the on-capillary concentration techniques, the normal stacking mode,[19-21] field amplified polarity switching injection,[19, 22] high salt stacking,[23-25] and sweeping[26-28] are widely used. These MEKC stacking methods work particularly well for analytes with large retention factors (strong affinity for micelles), but not for polar anlaytes with small retention factors.

Barbitals and hydantoins are sedatives and anticonvulsants. Phenobarbital and 5,5-diphenylhydantoin are among the prescriptions for treatment of head trauma and epilepsy.[29] Toxic barbiturate levels in serum are 7-80 $mg \cdot L^{-1}$, therefore the monitoring of these drugs in serum, plasma, and urea has clinic significance.[1,30] HPLC,[31-34] CZE,[30, 35-41] and MEKC[42-45] have been applied to separation of barbiturates. In analysis of complicated samples, MEKC has been widely used because of its ability to separate both polar and non-polar compounds. MEKC with cyclodextrin was reported on separation of isomers of these therapeutic drugs.[41,46] In our study of molecular recognition-enhanced extractions, mixtures of barbitals and their analogs at low concentrations need quantitative analysis. Fig. 4.1 shows the structures of the compounds. Former work in this lab has established the CZE separation conditions for the mixture of barbitals and hydantoin.[37] The separation was conducted in a pH 7.8 Tris (Tris-(hydroxymethyl)aminomethane) - TAPSO (3-[N-tris(hydroxymethyl)-methylamino]-2-hydroxy-propane sulfonic acid) buffer with hydrodynamic injection (normal injection time) and UV detection. The first part of our study is to improve the CZE analysis sensitivity of a mixture of four barbitals by adapting normal sample stacking techniques.

The second part of this study is to establish a sample stacking method in MEKC for more complicated mixtures, in which the wide distribution of retention factors of the components causes difficulty in achieving a good separation and stacking at the same time. We investigated approaches to stack analytes with a wide range of polarity, especially analytes with small retention factors in MEKC.

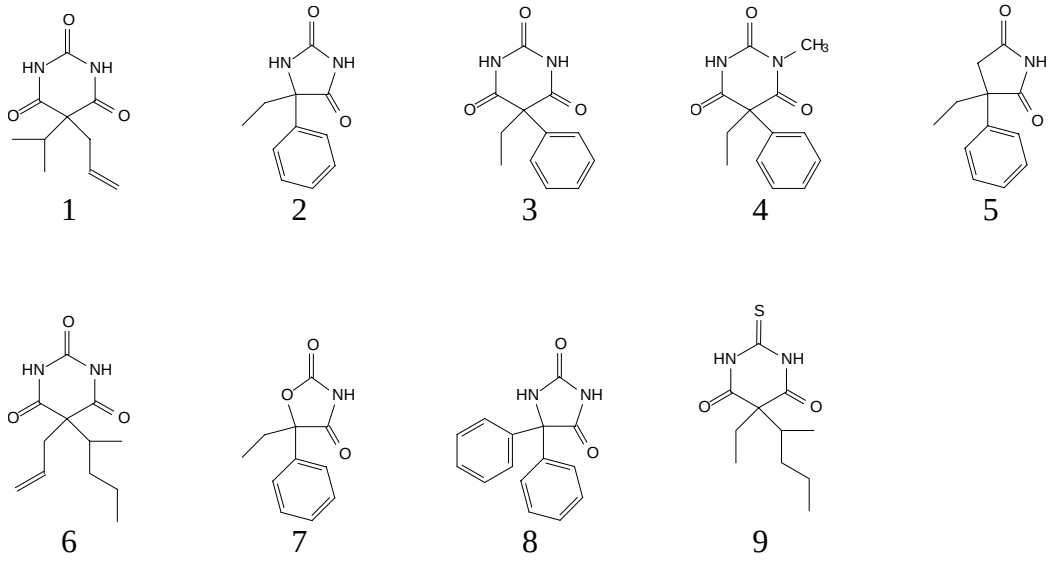

Figure 4.1. Chemical structures of barbituric acids and analog

1. aprobarbital (AB), 2. 5-ethyl-5-phenyl-hydantoin (EPH), 3. phenobarbital (PB), 4. mephobarbital (MB), 5. 2-ethyl-2-phenyl-succinimide (EPS), 6. secobarbital (SB), 7. 5-ethyl-5-phenyl-2,4-oxazolidinedione (EPO), 8. 5,5-diphenyl-hydantoin (PH), and 9. thiopental (TP).

4.2 EXPERIMENTS

4.2.1 Reagents

Tris(hydroxymethyl)aminomethane (Tris), 3-[N-tris(hydroxymethyl)-methylamino]-2-hydroxy-propane sulfonic acid (TAPSO), sodium dodecyl sulphate (SDS), are from Aldrich (Milwaukee, WI). Aprobarbital (AB), secobarbital (sodium salt, SB), mephobarbital (MB), phenobarbital (PB), 5,5-diphenylhydantoin (PH), and lyophilized bovine serum were purchased from Sigma (St. Louis, MO). DL-2-Ethyl-2-phenylsuccinimide (EPS), DL-5-ethyl-5-phenylhydantoin (EPH), and 5-ethyl-5-phenyl-oxazolidinedione (EPO) were gifts from Dr. Nims (Laboratory of Comparative Carcinogenesis, Chemistry Section, National Cancer Institute at Frederick, Frederick, Maryland). PVC (high molecular weight, Selectophore) and dioctyl sebacate (DOS, Selectophore) were from Fluka Chemical Co. (Ronkonkoma, NY). Santicizer 141 (90% octyl diphenyl phosphate) was a gift from Monsanto (St. Louis, MO). Sudan III (1-(4-(phenylazo)phenylazo)-2-naphthol)) and other chemicals that are not specified were purchased from Aldrich (Milwaukee, WI). Water used in all the experiments was deionized water purified with Milli-Q A10 System (Millipore, Bedford, MA).

4.2.2 Apparatus

All CE separations were performed on an ISCO 3850 Capillary Electropherograph (ISCO Inc., Lincoln, NE), with EZChrom Chromatography Data System (Scientific Software, Inc., San Ramon, CA) or PeakSimple Chromatography Data System (SRI Instruments Inc., Las Vegas, NV) for data collection, and EZdata System (Q. Liang, http://www.chemilab.net) for data analysis. An uncoated fused silica capillary (Polymicro

Technologies, Inc., Phoenix, AZ) with 50 μm I.D. and 70 cm length was employed in CE separation. A new CE capillary was conditioned with 1.0 *M* sodium hydroxide for 1 hour followed by 0.1 *M* sodium hydroxide for 2 hours. Before running samples, the capillary was flushed with water and then the run buffer. The capillary was conditioned with the same procedure and stored in 0.1 *M* sodium hydroxide everyday after experiments. All CE separations were conducted at room temperature (25 ± 2 °C). The conductivity measurements were carried out on a conductivity meter (Model 604, Amber Science Inc., Eugene, OR) calibrated with two KCl standard solutions (1.408 $ms \cdot cm^{-1}$, 12.85 $ms \cdot cm^{-1}$). An Accumet pH meter equipped with an Orion Ross reference electrode (Fisher Scientific) was used for pH measurements.

4.2.3 Separation of four barbiturates with sample stacking-CZE

The run buffer was prepared by adjusting the pH of 0.11 M Tris solution to pH 8.00 with TAPSO. The aqueous stock solution of the sample mixture contained 0.1 mM phenobarbital, secobarbital, thiopental, and mephobarbital each. The stock solution was diluted with 20 mM pH 10.00 NaOH-borate buffer to desired concentration for CE analysis. A positive voltage of 20 - 25 kV was applied to a capillary with a separation length of 45-50 cm and a current about 20 μA. UV absorbance was monitored at the wavelength of 230 nm. Non-stacking CE used hydrodynamic injection at 0.5 psi vacuum for 5 seconds; stacking CE used a longer injection time (5 - 100 seconds) at the same vacuum.

4.2.4 Separation of eight barbiturates and analogs with MEKC and comparison with CZE

The separation buffer for MEKC was 90 mM Tris-TAPSO containing 24 mM SDS (pH 8.00). For comparison with CZE, the same Tris-TAPSO buffer without SDS was employed. The non-stacking experiments used hydrodynamic injection of 5 seconds at 0.5 psi vacuum; stacking experiments used hydrodynamic injections of 5 to 100 s at the same vacuum. All separations were conducted under positive electrode polarity, with a voltage of 27 kV applied to a capillary with a total length of 70 cm (45 cm to the detection window), giving an average current of 19 μA in CZE and 28 μA in MEKC. UV absorbance was monitored at the wavelength of 210 nm for maximum sensitivity for all the eight compounds. The velocity of the electroosmotic flow (EOF) was determined by injection of methanol as the neutral marker; the velocity of the SDS micelles was obtained from the migration time of Sudan III.

The phosphate sample buffers were prepared by mixing 40 mM Na_2HPO_4 solution with 40 mM NaOH solution at various ratios to obtain the desired pH values. A series of phosphate buffers with pH values of 10.54, 11.00, 11.50, 12.00, and 12.24 were prepared. The stock solution of the drug mixture contains 100 μM each analyte (dissolved in D.I. water). It was diluted by the investigated sample buffers to the desired concentrations for CE analysis.

4.2.5 SPME pretreatment and analysis of spiked serum samples

The procedures for SPME device preparation, extraction, and back-extraction have been established in this lab.[37, 47] Briefly, a stainless steel rod (1.1 mm O.D.) was dip-coated to

form films of santicizer-plasticized PVC. To prepare the spiked serum samples, aliquots of deionized water containing various concentrations of drugs were injected to the vial containing lyophilized bovine serum to the specified volume. The spiked serum samples were then diluted by the same volume of acidic buffer (25 mM pH 4.50 acetate buffer) to favor the extraction. Each extraction was conducted by immersing a SPME probe into a 125 μL sample solution for 15 minutes, followed by rinsing the probe with D. I. water to remove any serum adsorbed on the probe surface. The probe was then transferred into a Teflon tube (1.2 mm i.d., Small Parts, Miami Lakes, FL) containing 10 μL 20 mM NaOH and was allowed to sit for 30 minutes. At the end of the back extraction, the probe was removed from the Teflon tube and a 1 mL syringe was used to push out the back extraction solution into a sample vial for CE analysis.

4.3 RESULTS AND DISCUSSION

4.3.1 Analysis of barbitals with sample stacking-CZE

Four barbiturates, secobarbital (SB), mephobarbital (MB), thiopental (TP), and phenobarbital (PB), were separated by CZE using a Tris-TAPSO separation buffer. Buffers with various pH, from 7.8 to 8.6, were evaluated; the pH 8.0 Tris-TAPSO buffer gave the best separation. In sample stacking analysis, the injection time was longer than that for normal injection (5 s). Conditions for sample stacking, for instance, the concentration of the sample buffer and the injection time, were investigated. A basic buffer, pH 10.0 borate-NaOH buffer was used to dissolve barbital mixtures. Comparing the concentration of the sample buffer at 5, 10, 20, 50 mM, all of them showed similar stacking efficiency, with 20 mM borate slightly better. 20 mM borate-NaOH sample

buffer was therefore chosen in our experiments. Interestingly, the conductivity of the separation buffer is about the same as that of the 20 mM borate sample buffer. Normal stacking mode works when the conductivity of sample buffer is smaller than that of the separation buffer, which means that only the 5 mM, and 10 mM borate buffer can be used for normal stacking mode. This indicates that there is another stacking mechanism involved when the sample matrix is 20 mM or 50 mM borate buffer. This will be discussed later with MEKC stacking (Section 4.3.5).

Various injection times, 5, 20, 40, 60, 100 seconds, under a 0.5 psi vacuum were tested for analysis of a sample containing 5 μM each barbital (Fig. 4.2). The peak heights and peak areas of all the four barbitals increased with longer injection time. The half peak width (peak width at the half peak height) did not broaden accordingly (Fig. 4.3). The highest stacking efficiency (with the narrowest peak width) was reached at 20-second injection when the peak heights were 4 times the values with 5-second injection. Longer injection time would increase the detection sensitivity but sacrifice the separation, thus the final choice depends on the samples being analyzed.

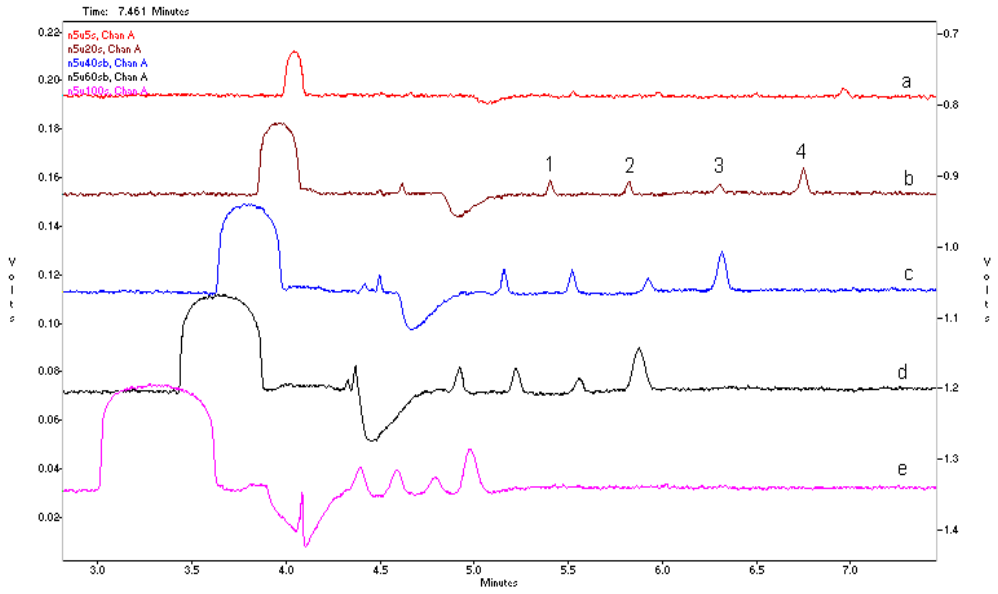

Figure 4.2. The effect of injection time on CZE sample stacking.

From a to e: 5, 20, 40, 60, 100 seconds injection under 0.5 psi vacuum. The mixture samples contained 5 μM SB (1), MB (2), TP (3), and PB (4) each in a 20 mM pH 10.0 borate-NaOH buffer.

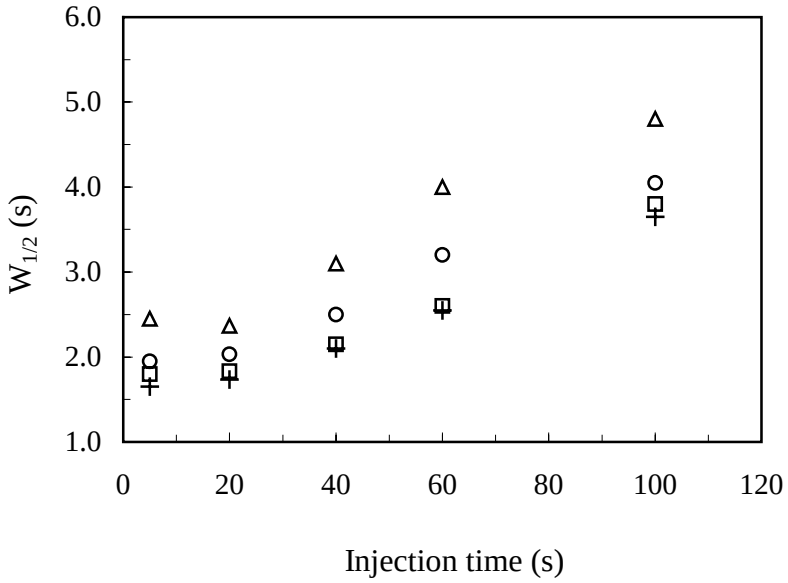

Figure 4.3. Half peak width versus injection time. Symbols, triangles, PB; squares, MB; crosses, SB; and circles, TP.

The standard curves of the barbiturates analyzed by sample stacking CZE (40 s injection) showed correlation coefficients close to 0.999 for all the four analyzed barbiturates. The limits of detection (LOD, S/N = 3) were improved 5-6 times when using a 60-second injection compared to a 5-second injection. The LOD was 1.7.0 μM for TP, 0.9 μM for MB and SB, and 0.5 μM for PB.

4.3.2 Separation with MEKC and comparison with CZE

Eight analytes were separated by CZE using pH 8.00 Tris-TAPSO buffer, and by MEKC with the same buffer containing 24 mM SDS, as shown in Fig. 4.4. In CZE, the migration time of these compounds corresponds to their pK_a values: the ones with higher pK_a values are less ionized at pH 8.00, and show migration velocities closer to EOF. PH (5,5-

diphenylhydantoin) was the only exception. This was probably because of its bulky size compared to other compounds. The peaks of two compounds, EPS (pK_a 9.17) and EPH (pK_a 8.85), are very close to each other, and are close the initial void peak in CZE. In sample stacking mode, these two peaks moved closer to the void peak when the void peak became much larger (Fig. 4.5). Meanwhile, the two analytes can not be base-line separated. Quantification of these peaks was thus affected in stacking CZE. We finally chose MEKC over CZE for better separation and higher sensitivity with applying sample stacking.

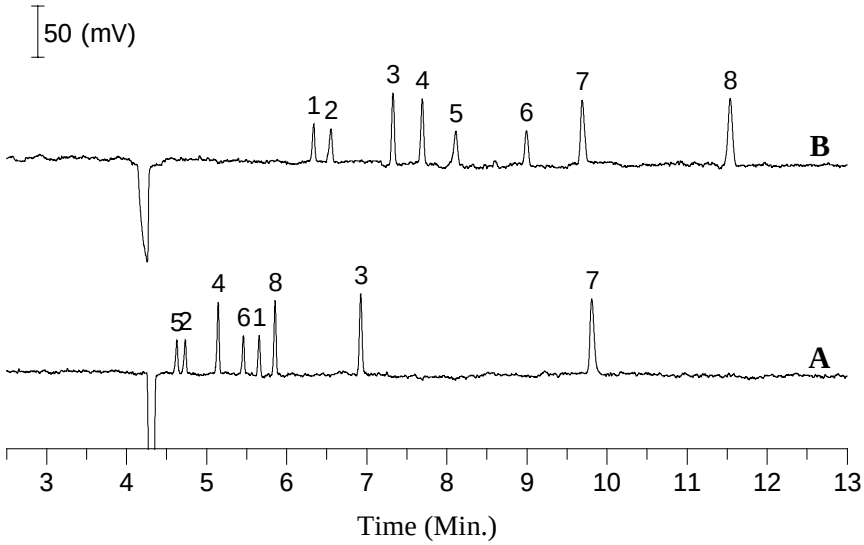

Figure 4.4. Separation of barbiturates and barbital analogs by CEZ (A) and MEKC (B). The separation was carried out on a 70 cm fused silica capillary applied with a voltage of +27 kV. CZE separation buffer: 90 mM Tris-TAPSO solution (pH 8.00). MEKC separation buffer: 90 mM Tris-TAPSO solution (pH 8.00) containing 24 mM SDS. Injection: 5 s at 0.5 psi vacuum. Detection wavelength: 210 nm. Sample concentration: 100 μM for each (dissolved in water). Peak identification: 1 (AB), 2 (EPH), 3 (PB), 4 (MB), 5 (EPS), 6 (SB), 7 (EPO), and 8 (PH).

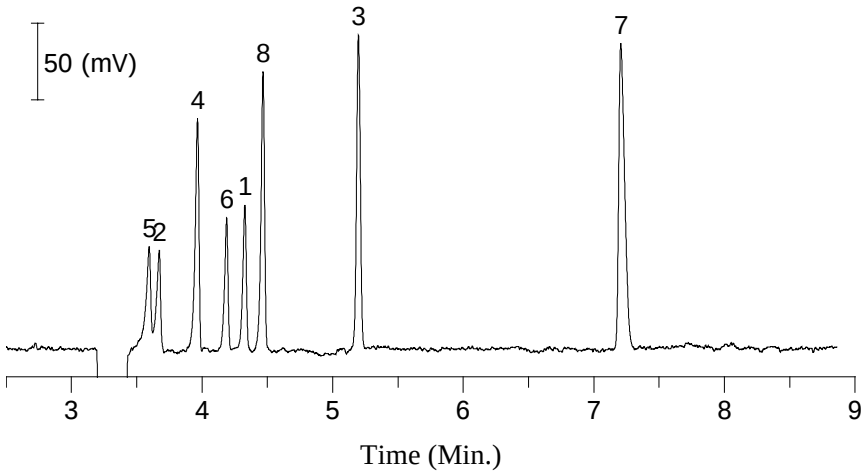

Figure 4.5. Large volume injection in CZE. Separation conditions and peak identification are the same as in Fig. 4.4 A, except the injection time was increased to 30 seconds.

In MEKC, the order of the migration time of the eight analytes was different from that in CZE due to interactions with the SDS micelles. Five compounds, PH, EPS, SB, MB, and EPH had longer migration time than that in CZE, while AB, PB, and EPO showed similar migration time as in CZE. The shift of the migration time of a solute corresponds to its retention factor (k') that defines the affinity of a compound for the micelle pseudostationary phase. The retention factor of an anionic solute in micellar solution, k_i', can be calculated by comparing the separation in CZE and in MEKC according to Eq. 4-1.[9]

$$k_i' = (\mu_i - \mu_{EP(i)}) / (\mu_{mc} - \mu_i) \qquad (4\text{-}1)$$

where μ_i is the observed electrophoretic mobility of an anion in a micellar solution, $\mu_{EP(i)}$ is the observed mobility of the anion in absence of the micelles, and μ_{mc} is the mobility of the micellar phase that can be measured by Sudan III. As shown in Table 4.1, the

retention factors of these compounds are in the range of 0.1 to 2.5 at the selected MEKC conditions.

Table 4.1. The retention factors of the analytes for SDS micelles

Analyte	AB	EPH	PB	MB	EPS	SB	EPO	PH
Peak No.	1	2	3	4	5	6	7	8
pK_a[48]	7.83	8.85	7.63	7.97	9.17	7.81	5.55	8.33
	±0.20	±0.50	±0.20	±0.60	±0.50	±0.20	±0.70	±0.50
Retention factor (k_i')[a]	0.24	0.64	0.17	0.89	1.4	1.3	0.10	2.5

[a]The retention factors were measured under the same conditions as in Fig. 4.4B.

4.3.3 Effects of SDS concentration on MEKC sample stacking

To achieve normal mode sample stacking, the samples were dissolved in water. The efficiency of sample stacking was different in MEKC compare to that in CZE. Effective stacking was obtained for all eight compounds in CZE with sample dissolved in a water matrix, while quite a few analytes presented wide and asymmetric peaks in MEKC (Fig. 4.6).

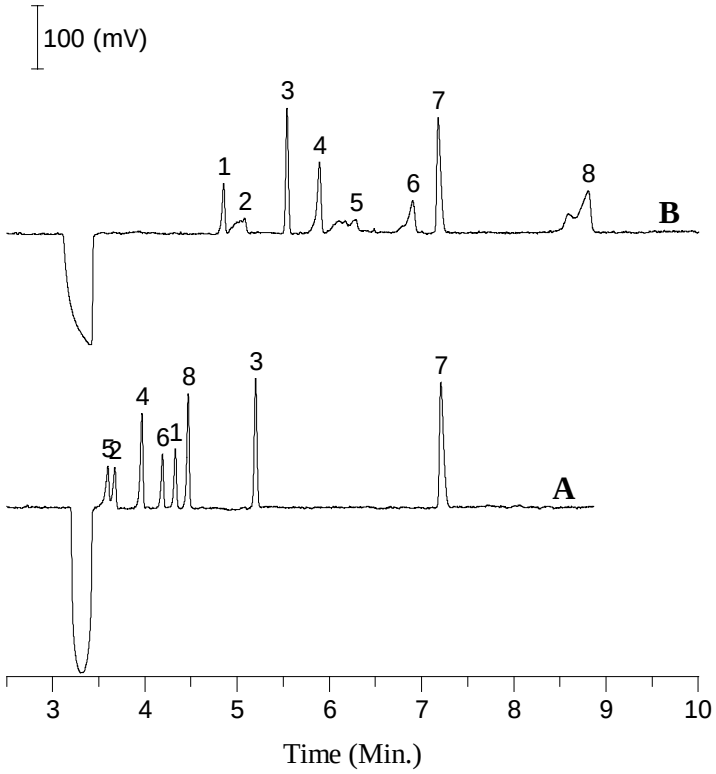

Figure 4.6. Sample stacking in CZE (A) and MEKC (B).

The conditions were the same as that in Fig. 4.3, except that the sample was dissolved in D.I. water with a concentration of 50 μM for each analyte, and the injection time was increased to 30 s. Peak identification: 1 (AB), 2 (EPH), 3 (PB), 4 (MB), 5 (EPS), 6 (SB), 7 (EPO), and 8 (PH).

The compounds that showed poor stacking behavior (wide and/or asymmetric peaks) are EPH, EPS, MB, SB, and PH. All of them have comparatively large retention factors, *i.e.*, stronger affinity toward SDS micelles. PH, which has the highest retention factor (2.5) among the eight, presents the worst peak shape. The peak widths of these analytes were found to increase with higher SDS concentrations. Fig. 4.7 shows the comparison of the half peak widths at various SDS concentrations with samples dissolved in 20 mM pH

11.00 phosphate buffer. Higher SDS concentrations resulted in an increase of the peak width. The same trend was obtained for samples dissolved in 20 mM pH 12.00 phosphate buffer, with overall smaller peak width as compared to results obtained for the pH 11.00 buffer. We therefore conclude that the interaction of the solutes with micelles is unfavorable to the sample stacking under our MEKC separation conditions.

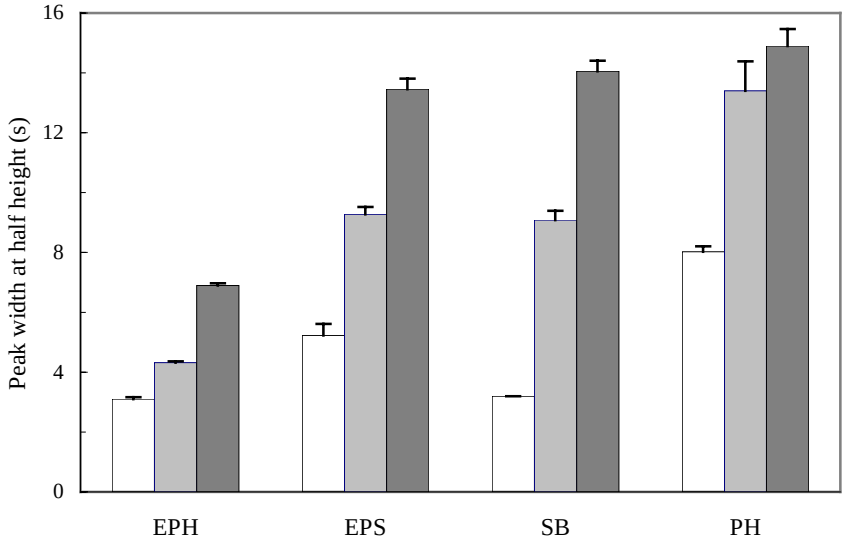

Figure 4.7. Effects of the SDS concentration on peak widths in MEKC stacking. MEKC run buffer: 90 mM Tris-TAPSO solution (pH 8.00) containing 10 mM SDS (blank bars), 24 mM SDS (gray bars), and 40 mM SDS (black bars). The error bars were the standard deviations of duplicate experiments. The mixture of the four analytes was dissolved in a 20 mM pH 11.00 phosphate buffer, and the injection time was 30 s.

Note that all the analytes have electrophoretic mobility even without association with the SDS micelles, which means that they are all charged or partially charged at the separation pH (8.00). When a high voltage was applied following the vacuum injection, the analytes

that had weak associations with micelles, such as AB, BP, and EPO, were efficiently stacked at the rear interface of the sample zone similar as in CZE stacking. The analytes having interactions with SDS micelles were not stacked as well with this stacking mode. To stack neutral analytes or analytes with large retention factors with normal staking mode, Liu dissolved samples in a low-conductivity sample buffer that contained 9 mM SDS, a concentration slightly higher than the critical micelle concentration (CMC) of SDS, but lower than that in the run buffer.[19] Quirino et al. achieved normal stacking by dissolving neutral samples in water or in a low-concentration buffer (1/10 dilution of the run buffer but containing no SDS).[21] They utilized a high concentration of SDS (100 mM) for the separation buffer, which allowed micelles to form even after dilution in the sample zone. The decreased SDS concentration in the sample zone compared to that in the run buffer is due to the faster mobility of SDS micelles in the sample zone.[16] Stacking could be achieved if the concentration of SDS in the sample zone was higher than CMC. Actually, they proved that two other surfactants with lower CMCs than SDS showed better stacking efficiency. Apparently, the conditions required for MEKC normal stacking mode are not satisfied in our case. One possible reason is the lower SDS concentration (24 mM) we used for the separation buffer.

4.3.4 Effects of buffer pH on MEKC sample stacking

Considering that the affinities of all the eight analytes for SDS micelles are not very strong (<2.5), it is possible to achieve stacking similar to in CZE if the interactions with the micelles are suppressed during the stacking process. We therefore dissolved the samples in high pH buffers to encourage the ionization of these analytes thus decrease

their affinity for the micelles. Among the phosphate buffers with various pH, higher pH buffers improved the peak shape, as shown in Fig. 4.8.

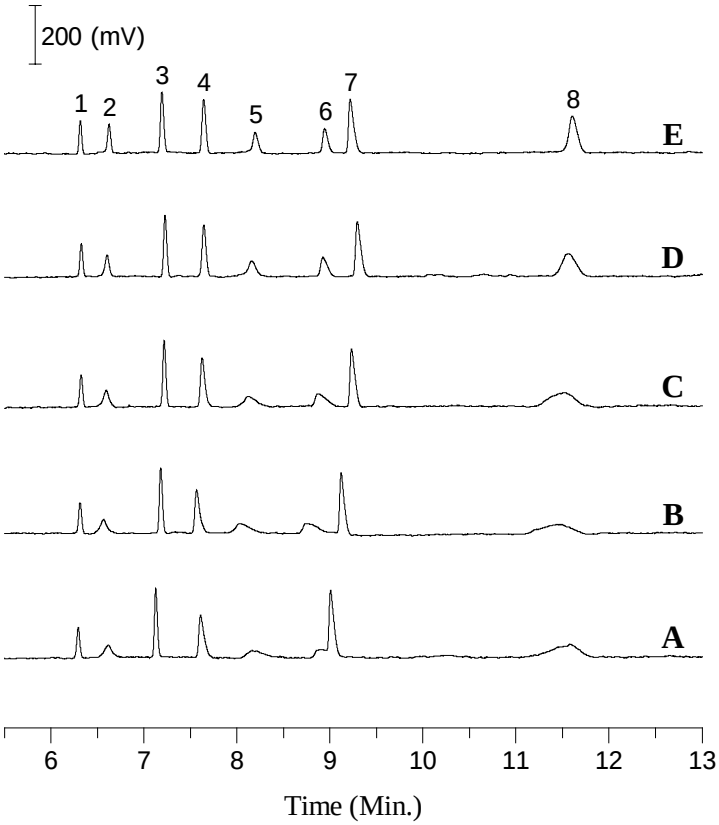

Figure 4.8. The effect of the pH of sample buffers on sample stacking.

MEKC run buffer: 90 mM Tris-TAPSO solution (pH 8.00) containing 24 mM SDS. Injection time: 30 s. Analytes: 50 μM for each, 1 (AB), 2 (EPH), 3 (PB), 4 (MB), 5 (EPS), 6 (SB), 7 (EPO), and 8 (PH). Samples were dissolved in 20 mM phosphate buffers with various pH values: A (pH 10.54), B (pH 11.00), C (pH 11.50), D (pH 12.00), and E (pH 12.24).

To ensure that it was the pH of the sample buffer instead of the buffer composition that caused the stacking, sodium hydroxide solution (pH 12.10) with the same concentration (20 mM) was compared with the pH 12.24 phosphate buffer. Both of them showed similar stacking efficiency for all the investigated compounds, with sodium hydroxide solution showing a little better performance. Table 4.2 lists the half peak widths of the eight analytes obtained in these sample buffers. NaOH solutions were finally chosen to dissolve the samples. To be noted, the compounds that are stacked well at lower pH sample buffers, such as AB, PB, and EPO, maintain efficient stacking in high pH sample buffers.

Table 4.2. Peak widths at half height in MEKC stacking using various sample buffers

Peak width at half height (s)	AB	EPH	PB	MB	EPS	SB	EPO	PH
pH 10.54[a]	2.2	5.3	2.2	3.6	11.5	6.9	3.6	18.7
pH 11.00[a]	2.2	4.7	2.2	3.4	10.5	10.7	3.3	22.3
pH 11.50[a]	2.1	4.2	2.3	3.1	8.3	8.1	3.5	19.3
pH 12.00[a]	2.1	3.0	2.4	2.9	5.5	4.9	3.8	10.4
pH 12.24[a]	2.0	2.4	2.4	2.9	3.7	3.8	3.8	6.3
pH 12.10[b]	1.9	2.3	2.4	2.5	3.2	3.1	3.8	4.3

The listed data were the average of duplicate experiments, with relative standard deviations ranging from 0.1% to 13%, with poorly stacked compounds giving comparatively high deviations. Note: [a]phosphate buffer; [b]20 mM NaOH solution.

Evidently, it is essential to control the pH of the sample buffer for stacking of all the eight analytes. The high pH buffers suppress the interactions of the negatively charged analytes with the SDS micelles, allowing all the analytes to be stacked as in CZE stacking. This is different from other reports we have seen in literature. In MEKC, the affinity of analytes toward micelles is usually favorable for stacking, which is seen in normal stacking mode, field-amplified polarity switching stacking, high salt stacking, and sweeping. The difference in our case is that the analytes under investigation have low retention factors (0.1 to 2.5) for SDS micelles. SDS is utilized to adjust the migration of the mixture components for better separation. It becomes difficult to achieve stacking for all of them with any of the MECK stacking methods that work particularly well for neutral molecules and less polar molecules. The high pH of the sample matrix provides a convenient solution to this problem.

4.3.5 Optimal concentration of the sample matrix

To find the best concentration of the sample matrix, samples were dissolved in NaOH solutions with concentrations ranging from 5 mM to 50 mM, while a 30 s-injection was used. Stacking occurred at all these concentrations, with the best stacking efficiency (the most narrow half peak width) in 20 mM NaOH solution (Figure 4.9). The slightly increased peak widths as using 5 mM NaOH solution compared to 10 mM NaOH solution probably is caused by its comparatively lower pH values (pH 11.65) at this concentration (pH = 11.86 for 10 mM NaOH).

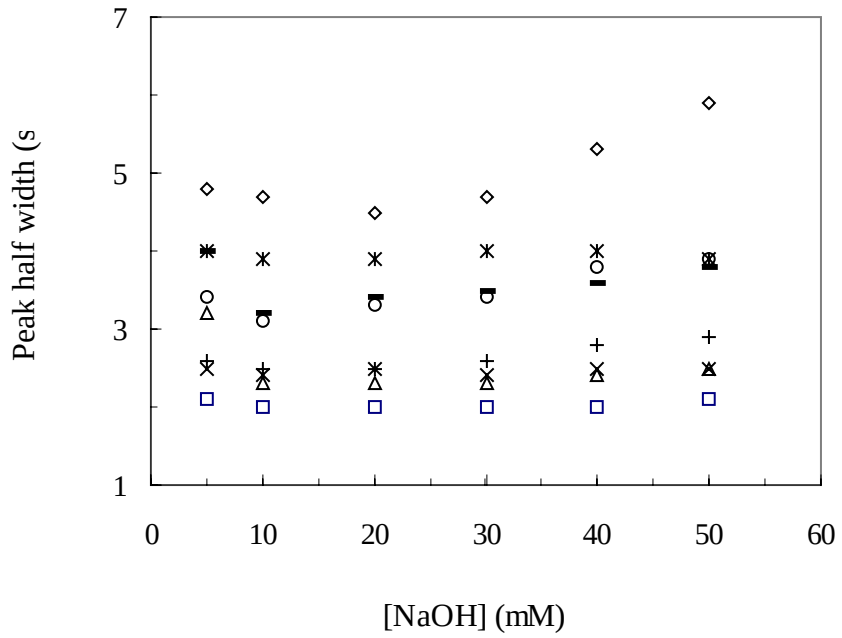

Figure 4.9. Effects of the concentration of the sample buffer on the stacking efficiency. Separation conditions were the same as in 4.8. The samples were dissolved in NaOH solutions with various concentrations. Analytes: PH (◊), EPO (∗), SB (○), EPS (–), MB (+), PB (×), EPH (Δ), and AB (□).

The conductivities of the separation buffers and the sample matrix are examined. The ratio of the conductivity (separation buffer/sample matrix) is defined as the enhancement factor γ. It is interesting to notice that the stacking occurs for γ in certain range, from 2.5 for the 5 mM NaOH as the sample matrix to 0.3 for the 50 mM NaOH as the sample matrix. The best stacking occurred with 20 mM NaOH sample matrix ($\gamma = 0.64$). Normal stacking mode similar to CZE can explain the stacking occurred when $\gamma > 1$, in which the conductivity of the sample matrix is lower than that of the separation buffer. However, when $\gamma < 1$, another mechanism must be involved, which also induces the stacking occurred when 20 mM phosphate buffers (pH 10.5 to 12.2, γ from 0.95 to 0.60) were

used as the sample matrices. Because a salt/base is introduced in both cases, it hints at a transient isotachophoresis (transient ITP) mechanism, where OH^- in the sample matrix works as the leading ion, and the TAPSO ion in the separation buffer functions as the terminating ion. To verify this, the sample was dissolved in a 4 mM phosphate buffer (pH 11) containing various concentrations of NaCl (0 to 100 mM, γ from 3.76 to 0.26, respectively). The peak shape of EPH, EPS, SB, PH was improved with addition of NaCl; and the best stacking occurred with the sample matrix containing 40 mM NaCl ($\gamma = 0.56$). This conductivity ratio is close to that of the 20 mM NaOH sample matrix ($\gamma = 0.64$) which showed the best stacking. Further increase of NaCl concentration to 60 mM, and 100 mM caused decreased peak height and broadened peaks. Cl^- (as in NaCl) is a very common leading ion added to sample matrices in transient ITP-CZE or transient ITP-MEKC stacking of anionic analytes due to its high ionic mobility and ease to use.[18, 24, 49, 50] The other four analyte that have low retention factors, AB, PB, EPO, and MB, presented no big differences in peak width and peak height with NaCl concentration investigated. A similar phenomenon was observed in CZE stacking of the mixture of four barbitals: SB, MB, TP, and PB.

4.3.6 Optimal injection time and stacking efficiency

The peak areas increased linearly with the injection time, while peak widths did not widen accordingly. Fig. 4.10 shows a plot of peak widths vs. injection time. The differences of half peak widths were less than 10% when the injection time was 40 s or less.

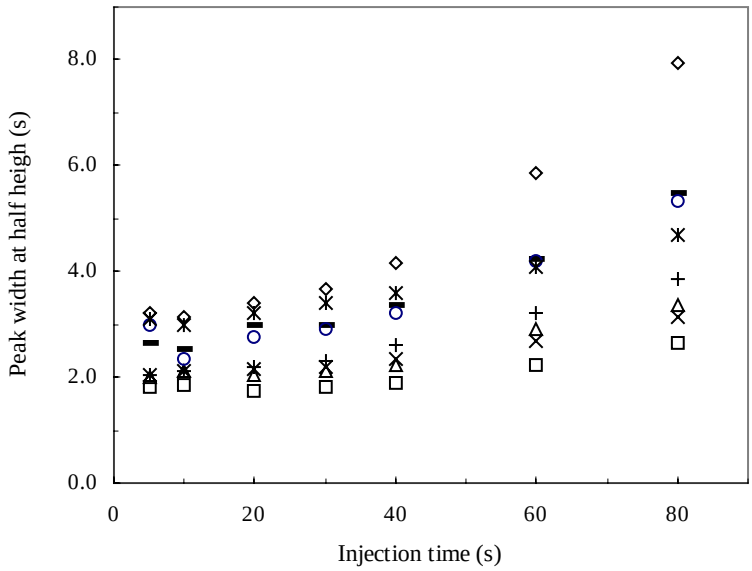

Figure 4.10. Peak widths at half height with various injection time.

The mixture of eight analytes was dissolved in 20 mM NaOH solution, with a concentration of 50 μM for each Analytes: PH (◊), EPO (∗), SB (o), EPS (–), MB (+), PB (×), EPH (Δ), and AB (□).

Stacking efficiency in terms of peak height (SE_{height}) is defined as Eq. 4-2.

$$SE_{height} = H_{stack}/H_{normal} \quad (4\text{-}2)$$

H_{stack} and H_{normal} are the peak heights obtained from the same sample solution but different injection time: long-time injection for stacking conditions, and 2 s-injection for normal conditions, respectively. Fig. 4.11 shows the SE_{height} varying with injection time. The sacking efficiency of most of the analytes increases linearly with longer injection time up to 40 s. With 40 s-injection time, the stacking efficiency for the eight analytes is from 11 to 17. Longer injection time than 40 s only causes slight increase of the stacking efficiency of EPS, PH, and EPH.

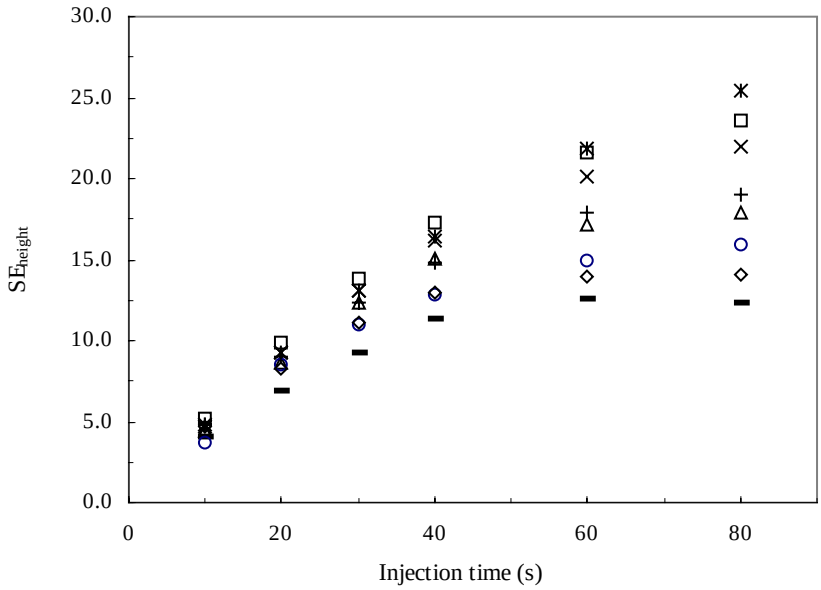

Figure 4.11. Stacking efficiency versus injection time.

The CE conditions were the same as in Fig. 4.10. Analytes: PH (◊), EPO (∗), SB (o), EPS (−), MB (+), PB (×), EPH (Δ), and AB (□).

The limits of detection (LOD) were greatly improved by sample stacking. The limits of detection (S/N=3) using 30 s-injection are listed in Table 4.3. By application of sample stacking, we could analyze samples containing less than one micromolar drugs.

Table 4.3. The limits of detection using 30 s-injection in stacking MEKC

Analyte	AB	EPH	MB	PB	EPS	SB	EPO	PH
LOD (μM)	0.65	0.77	0.37	0.38	0.80	0.70	0.41	0.43

4.3.7 Determination of drugs in bovine serum

To apply the established method to serum samples, pretreatment was found to be necessary. A solid phase microextraction-CE (SPME-CE) procedure has been developed in our lab.[37, 47] In SPME, plasticizers function as nonvolatile solvents doped in PVC polymer support. The forward extraction was carried out in an acidic buffer (pH 4.50), and the back extraction was carried out in a basic solution (20 mM NaOH). Various PVC plasticizers: tributylphosphate (TBP), dioctyl sebacate (DOS), and Santicizer 141 (90% octyl diphenyl phosphate) have been investigated. Santicizer 141-doped PVC films were stable in the experimental conditions and produced satisfactory extraction of all the eight compounds. Fig. 4.12 shows the electropherograms of a direct injection of a serum sample and an injection of serum sample treated by SPME. The SPME procedures are very effective for removing the background from the serum matrix. Compared to the SPME treatment of aqueous standard solutions, the spiked serum samples had lower preconcentration factors for all the eight compounds. This is likely caused by the binding of these compounds to the serum proteins.[37] The preconcentration factor of EPO is so low that it becomes difficult to analyze EPO quantitatively, therefore EPO was excluded in SPME-MEKC analysis.

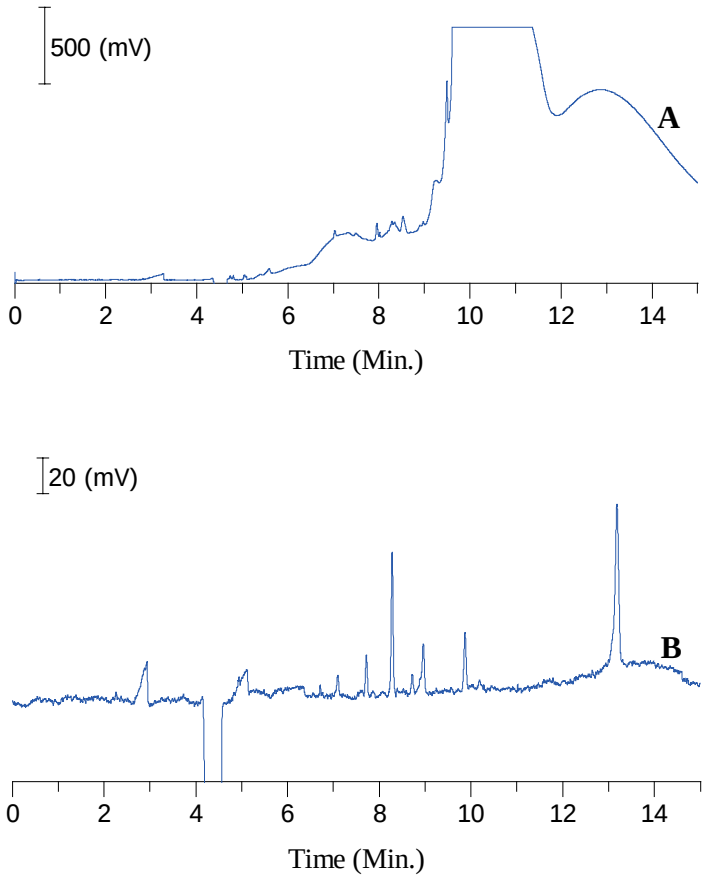

Figure 4.12. Determination of anticonvulsants in serum with (B) and without (A) solid phase pretreatment.

A, direct injection of a serum sample spiked with 50 μM drug standards. B, injection of a serum sample pretreated with SPME: extraction with a SPME rod coated with a PVC-santicizer film for 15 minutes, back-extraction with 10 μL 20 mM NaOH solution for 30 minutes. CE injection: 30 s.

Calibration curves of serum samples with concentration range from 15 μM to 100 μM gave good linearity for the seven investigated compounds, with correlation coefficients from 0.990 to 0.997. Figure 4.13 shows the calibration curves for four anticonvulsants

prescribed for patients: 5,5-diphenylhydantoin (PH), phenobarbital (PB), secobarbital (SB), and mephobarbital (MB).

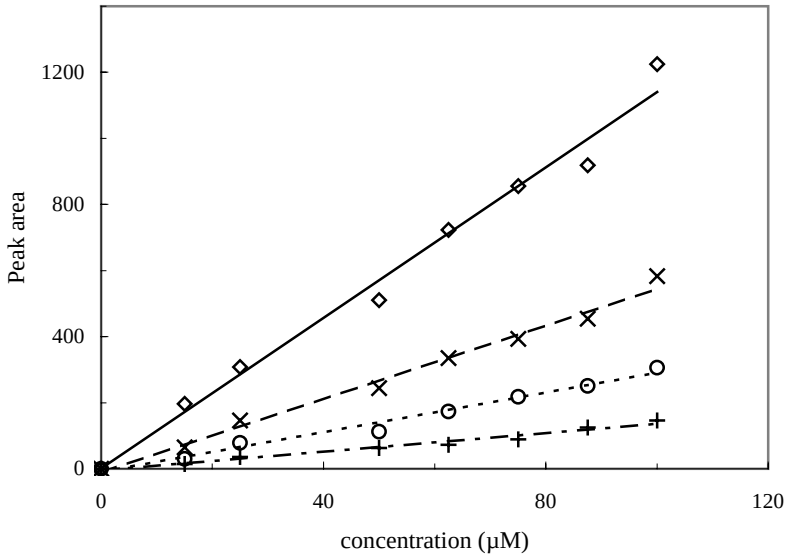

Figure 4.13. Standard curves for analytes spiked in bovine serum.

The analysis procedures were the same as in Figure 2.12B. Analytes: PH (◊), SB (o), MB (+), and PB (×).

4.4 CONCLUSIONS

Four barbitals were separated by CZE with normal sample stacking for increased sensitivity. For a more complex mixture that contains eight barbiturate drugs and drug analogs, MEKC with pH 8.00 Tris-TAPSO separation buffer containing 24 mM SDS results in good separation. The very different affinity of these analytes for SDS micelles brings challenges to sample stacking. It is much easier to achieve efficient sample stacking for analytes with small retention factors when the sample matrix has a lower

conductivity than the separation buffer (normal stacking mode) or the sample matrix contains a leading ion (transient ITP stacking mode). However, it is difficult to obtain stacking for the analytes with larger retention factors under these conditions. High pH sample solutions have been demonstrated to solve the problem through complete ionization of the analytes, thus decreasing their affinity for the SDS micelles. A stacking mechanism similar to CZE (normal stacking mode and transient ITP) can be achieved with this method, without adverse effects on the MEKC separation. The limits of detection have been improved to 0.37 - 0.80 μM for the eight analytes in aqueous solutions. Seven compounds spiked in serum can be measured quantitatively with the developed MEKC method after a SPME pretreatment which efficiently removes the serum background.

4.5 REFERENCES

(1) Boone, C. M.; Franke, J. P.; de Zeeuw, R. A.; Ensing, K. *Journal of Chromatography. A* **1999**, *838*, 259-272.

(2) Couderc, F.; Causse, E.; Bayle, C. *Electrophoresis* **1998**, *19*, 2777-2790.

(3) Jiang, J.; Lucy, C. A. *Journal of Chromatography, A* **2002**, *966*, 239-244.

(4) Rada, P.; Tucci, S.; Perez, J.; Teneud, L.; Chuecos, S.; Hernandez, L. *Electrophoresis* **1998**, *19*, 2976-2980.

(5) Qian, J.; Wu, Y.; Yang, H.; Michael, A. C. *Analytical Chemistry* **1999**, *71*, 4486-4492.

(6) Baldwin, R. P. *Electrophoresis* **2000**, *21*, 4017-4028.

(7) Chen, Y.-R.; Tseng, M.-C.; Chang, Y.-Z.; Her, G.-R. *Analytical Chemistry* **2003**, *75*, 503-508.

(8) Schmitt-kopplin, P.; Frommberger, M. *Electrophoresis* **2003**, *24*, 3837-3867.

(9) Baker, D. R. *Capillary Electrophoresis*; Wiley, New York, N. Y., 1995.

(10) Terabe, S.; Otsuka, K.; Ichikawa, K.; Tsuchiya, A.; Ando, T. *Analytical Chemistry* **1984**, *56*, 111-113.

(11) Molina, M.; Silva, M. *Electrophoresis* **2002**, *23*, 3907-3921.

(12) Pyell, U. *Fresenius' Journal of Analytical Chemistry* **2001**, *371*, 691-703.

(13) Mitchelson, K. R.; Cheng, J. E. *Capillary electrophoresis of natural products*; Humana Press: Totowa, NJ, 2001.

(14) Issaq, H. J. *Electrophoresis* **1999**, *20*, 3190-3202.

(15) Quirino, J. P.; Terabe, S. *Journal of Capillary Electrophoresis* **1997**, *4*, 233-245.

(16) Kim, J.-B.; Terabe, S. *Journal of Pharmaceutical and Biomedical Analysis* **2003**, *30*, 1625-1643.

(17) Chien, R.-L. *Electrophoresis* **2003**, *24*, 486-497.

(18) Urbanek, M.; Krivankova, L.; Bocek, P. *Electrophoresis* **2003**, *24*, 466-485.

(19) Liu, Z.; Sam, P.; Sirimanne, S. R.; McClure, P. C.; Grainger, J.; Patterson, D. G., Jr. *Journal of Chromatography, A* **1994**, *673*, 125-132.

(20) Kruaysawat, J.; Marriott, P. J.; Hughes, J.; Trenerry, C. *Electrophoresis* **2003**, *24*, 2180-2187.

(21) Quirino, J. P.; Terabe, S. *Journal of Chromatography, A* **1997**, *781*, 119-128.

(22) Aguete, E. C.; Gago-Martinez, A.; Leao, J. M.; Rodriguez-Vazquez, J. A.; Menard, C.; Lawrence, J. F. *Talanta* **2003**, *59*, 697-705.

(23) Palmer, J.; Munro, N. J.; Landers, J. P. *Analytical Chemistry* **1999**, *71*, 1679-1687.

(24) Carabias-Martinez, R.; Rodriguez-Gonzalo, E.; Revilla-Ruiz, P.; Dominguez-Alvarez, J. *Journal of Chromatography, A* **2003**, *990*, 291-302.

(25) Choy, T. M. H.; Chan, W.-H.; Lee, A. W. M.; Huie, C. W. *Electrophoresis* **2003**, *24*, 3116-3123.

(26) Quirino, J. P.; Terabe, S.; Bocek, P. *Analytical Chemistry* **2000**, *72*, 1934-1940.

(27) Quirino, J. P.; Terabe, S. *Science* **1998**, *282*, 465-468.

(28) Quirino, J. P.; Terabe, S. *Analytical Chemistry* **2000**, *72*, 1023-1030.

(29) Eadie, M. J.; Vajda, F. J. E.; (Editors) *Antiepileptic Drugs: Pharmacology and Therapeutics*; Springer, Berlin, Germany, 1999.

(30) Delinsky, D. C.; Srinivasan, K.; Solomon, H. M.; Bartlett, M. G. *Journal of Liquid Chromatography & Related Technologies* **2002**, *25*, 113-123.

(31) Lucarelli, C.; Villa, P.; Lombaradi, E.; Prandini, P.; Brega, A. *Chromatographia* **1992**, *CHRGB733*, 37-40.

(32) Valenta, J. N.; Weber, S. G. *Journal of Chromatography, A* **1996**, *722*, 47-57.

(33) Martinavarro-Dominguez, A.; Capella-Peiro, M.-E.; Gil-Agusti, M.; Marcos-Tomas, J. V.; Esteve-Romero, J. *Clinical Chemistry (Washington, DC, United States)* **2002**, *48*, 1696-1702.

(34) Wilson, J. F.; Watson, I. D.; Williams, J.; Toseland, P. A.; Thomson, A. H.; Sweeney, G.; Smith, B. L.; Sandle, L. N.; Ramsey, J. D.; Capps, N. E. *Clinical Chemistry* **2002**, *48*, 1963-1969.

(35) Tellez, S.; Forges, N.; Roussin, A.; Hernandez, L. *Journal of Chromatography* **1992**, *581*, 257-266.

(36) Hiraoka, A.; Miura, I.; Akai, J.; Tominaga, I.; Hattori, M.; Machida, S.; Arato, T. *Seibutsu Shiryo Bunseki* **1994**, *17*, 274-279.

(37) Li, S.; Weber, S. G. *Analytical Chemistry* **1997**, *69*, 1217-1222.

(38) Luis, M. L.; Blanco, D.; Arias, J. J.; Jimenez, F.; Jimenez, A. I.; Fraga, J. M. G. *Journal of Liquid Chromatography & Related Technologies* **2001**, *24*, 1921-1928.

(39) Haque, A.; Xu, X.; Stewart, J. T. *Journal of Pharmaceutical and Biomedical Analysis* **1999**, *21*, 1063-1067.

(40) Shihabi, Z. K. *Methods in Molecular Medicine* **1999**, *27*, 157-163.

(41) Zaugg, S.; Caslavska, J.; Theurillat, R.; Thormann, W. *Journal of Chromatography. A* **1999**, *838*, 237-249.

(42) Meier, P.; Thormann, W. *Journal of Chromatography* **1991**, *559*, 505-513.

(43) Thormann, W.; Meier, P.; Marcolli, C.; Binder, F. *Journal of Chromatography* **1991**, *545*, 445-460.

(44) Kataoka, Y.; Makino, K.; Oishi, R. *Electrophoresis* **1998**, *19*, 2856-2860.

(45) Schmutz, A.; Thormann, W. *Electrophoresis* **1994**, *15*, 51-61.

(46) Srinivasan, K.; Bartlett, M. G. *Rapid Communications in Mass Spectrometry* **2000**, *14*, 624-632.

(47) Zhang, X.; Zhao, H.; Chen, Z.; Nims, R.; Weber, S. G. *Analytical Chemistry* **2003**, *75*, 4257-4264.

(48) SciFinder, 2004 ed.; Chemical Abstract Service, Columbus OH, 2004; Vol. 2004.

(49) Turiel, E.; Fernandez, P.; Perez-Conde, C.; Camara, C. *Analyst (Cambridge, United Kingdom)* **2000**, *125*, 1725-1731.

(50) Shihabi, Z. K. *Electrophoresis* **2002**, *23*, 1612-1617.